Version of Record: https://www.sciencedirect.com/science/article/pii/S0142961222001715
Manuscript_7bad4051e78439623af0fde63a4e6cd5

Brain-on-a-chip: Recent Advances in Design, Biomaterials, and Cell Culture Techniques for Microfluidic Models of the Brain in Health and Disease

Leyla Amirifar, Amir Shamloo, Rohollah Nasiri, Natan Roberto de Barros, Ze Zhong Wang, Bige Deniz Unluturk, Alberto Libanori, Oleksandr Ievglevskyi, Sibel Emir Diltemiz, Samuel Sances, Ilangko Balasingham, Stephanie K. Seidlits, Nureddin Ashammakhi**

L. Amirifar, A. Shamloo, R. Nasiri
Department of Mechanical engineering, Sharif University of Technology, Tehran, Iran

R. Nasiri, Z. Z. Wang, A. Libanori, S. K. Seidlits, N. Ashammakhi
Department of Bioengineering, University of California, Los Angeles, California, USA

N. R. de Barros
Bioprocess and Biotechnology Department, São Paulo State University (Unesp), School of Pharmaceutical Sciences, Araraquara, Brazil

S. E. Diltemiz
Department of Chemistry, Eskisehir Technical University, Eskisehir, Turkey

S. Sances
Regenerative Medicine Institute, Cedars-Sinai Medical Center, Los Angeles, California, USA

B. D. Unluturk, N. Ashammakhi
Department of Biomedical Engineering, Michigan State University, East Lansing, USA

I. Balasingham
Department of Electronic Systems, Norwegian University of Science and Technology (NTNU), Trondheim, Norway

I. Balasingham, O. Ievglevskyi
Intervention Center, Oslo University Hospital, Oslo, Norway
Department of Basic Medical Sciences, University of Oslo, Oslo, Norway

*Department of Bioengineering, Henry Samueli School of Engineering, University of California, Los Angeles, 420 Westwood Plaza, Engineering V, Los Angeles, CA 90095-1600, Los Angeles CA 90095, USA, Tel. +1 310 794 5845. E-mail: n.ashammakhi@ucla.edu, n.ashammakhi@gmail.com, seidlits@g.ucla.edu

Brain-on-a-chip: Recent Advances in Design and Techniques for Microfluidic Models of the Brain in Health and Disease

Abstract

Recent advances in biomaterials, microfabrication, microfluidics, and cell biology have led to the development of organ-on-a-chip devices that can reproduce key functions of various organs. Such platforms promise to provide novel insights into various physiological events, including mechanisms of disease, and evaluate the effects of external interventions, such as drug administration. The neuroscience field is expected to benefit greatly from these innovative tools. Conventional *ex vivo* studies of the nervous system have been limited by the inability of cell culture to adequately mimic *in vivo* physiology. While animal models can be used, their relevance to human physiology is uncertain and their use is laborious and associated with ethical issues. To date, organ-on-a-chip systems have been developed to model different tissue components of the brain, including brain regions with specific functions and the blood brain barrier, both in normal and pathophysiological conditions. While the field is still in its infancy, it is expected to have major impact on studies of neurophysiology, pathology and neuropharmacology in future. Here, we review advances made and limitations faced in an effort to stimulate development of the next generation of brain-on-a-chip devices.

Keywords: Biomaterials, organ-on-a-chip, microfluidics, brain, neuroscience

1. Introduction

Pathologies such as trauma, neurovascular events, addiction, and neurodegenerative diseases, such as Alzheimer's disease (AD), represent major health concerns with limited clinical options for which effective therapies are under extensive investigation.[1] According to the World Health Organization (WHO), approximately one billion people around the world suffer from neurological disorders.[2] Due to increasing age of the population,[3] numbers of diagnosed neurodegenerative disease cases are rising[4] and so, is their medical and socioeconomic impact.[5] An improved understanding of the brain's development and physiology is required to bridge our current knowledge gaps and develop new strategies for the prevention, treatment, and eradication of diseases affecting the brain.[6] Model platforms of brain tissues represent an exciting tool for bridging these knowledge gaps. To date, attempts to use biomaterials for three-dimensional (3D) culture have been limited, in particular with respect to their ability to model dynamic changes.[7] Organoids have also been developed as cell-based, 3D models in the absence of biomaterials;[8] however, they are not a perfect model as they lack a controlled, extracellular microenvironment and have a small size scale relative to the human organs. As organoids typically lack a stable vasculature, large organoids (millimeter-scale) have compromised survival due to limited nutrient diffusion.[9] In addition, thick tissues, including cells cultured in 3D biomaterials and organoids, are more challenging to image using a typical microscope due to short working distances of objectives and interference from out-of-plane light.[10] In animal experiments, although drugs can prove successful and effective, over 80% have failed when in clinical trials.[11] Moreover, neurodegenerative diseases, such as AD, are almost never found in other animal species,[12] further highlighting the limitations of utilizing animal models for studying such diseases.

Brain-on-a-chip (BoC) models have been developed in an attempt to address many of the limitations found in other models. BoCs have been used with human cells and dynamic

systems to create microphysiological models exhibiting specific functions and unique brain tissue regions. BoC designs may incorporate compartmentalized neuronal chambers, static or dynamic fluid conditions, non-neuronal cells (e.g., glia and vasculature), and/or biomaterial scaffolds. Compared to organoids, typical BoC models have thinner, micrometer-scale cell layers that retain some dimensionality beyond two-dimensional (2D) monolayers, yet have ample access to nutrients and metabolite exchange with the flowing media.[13] Using a BoC, more robust and complex neural networks in 3D culture could be established.[14] A limited number of studies have been able to capture the complexity of key elements, such as the blood brain barrier (BBB)[15] and its neurovascular units,[16] neurons[17] and their axodendritic synapses,[18, 19] and the supporting roles of oligodendrocytes,[20] astrocytes,[21] and microglia.[22] The advent of microfluidics and its adaptation to produce organ-on-a-chip (OoC) constructs represents a major milestone on the way of modeling various key functions and structure of major organs;[23] for example, lung,[24] gut,[25] liver,[26] kidney,[27] and more recently brain.[28] In this review, we discuss the latest developments in and applications of BoC models (**Figure 1**). First, we discuss technical considerations in the design BoCs and introduce the most commonly used layouts. Physiological BoC models focusing on neurite outgrowth, axon formation and synaptogenesis, glial cell support and cell-cell communication and development, immune function, and neurovascular units of the BBB are then reviewed in the following Section 3. Section 4 provides an overview of brain injury, neurodegenerative diseases, brain tumors, inflammatory conditions, and infectious conditions as pathological BoC models. Application of BoCs for pharmaceutical studies and personalized medicine are summarized in section 5, followed by discussing neuromorphic chips in section 6. Section 7 includes studies performed on integrating BoCs with other organs to develop practical multi-organ-on-chips. Finally, current challenges and future directions of the field are highlighted in section 8.

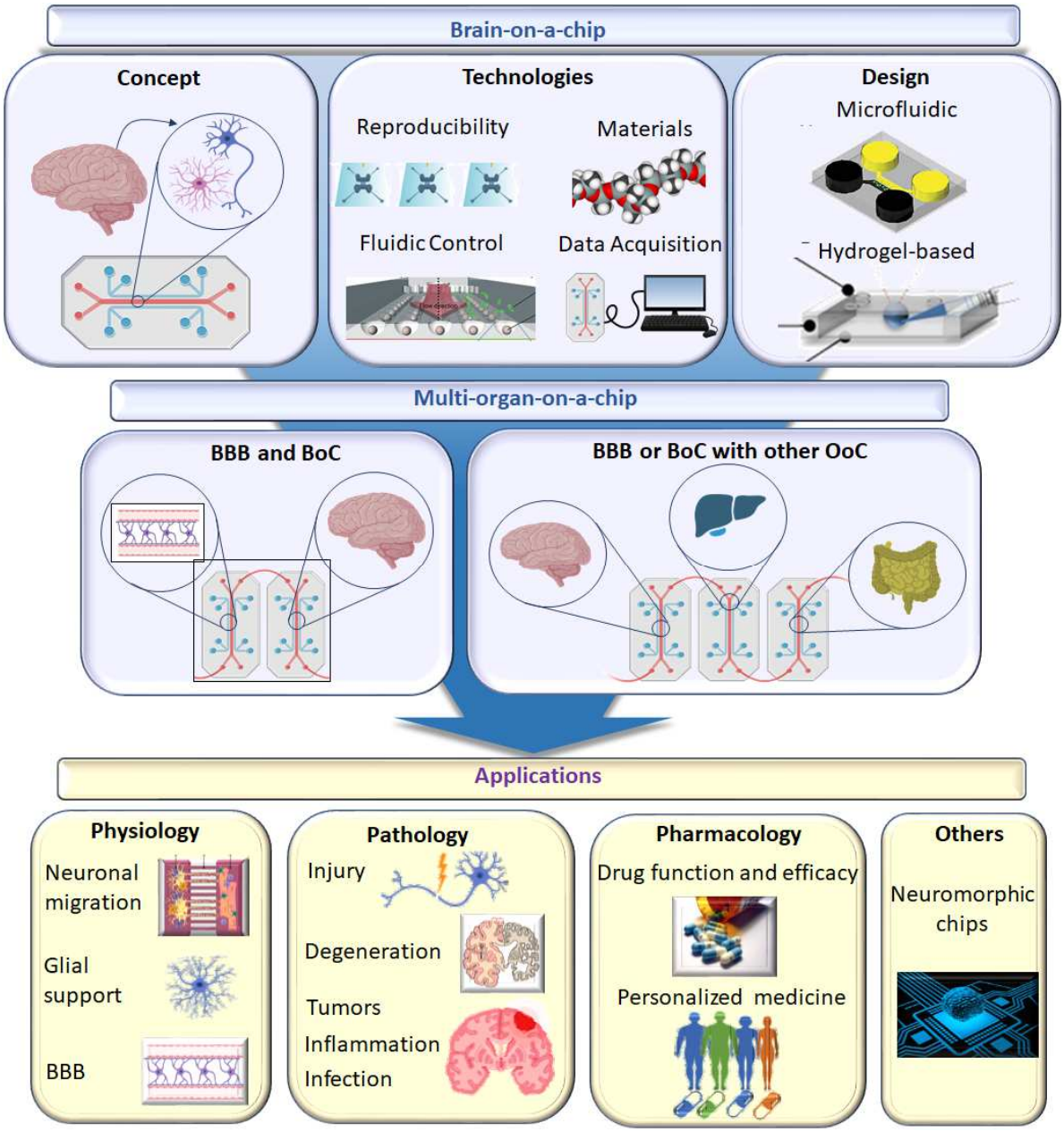

Figure 1. Overview of brain-on-a-chip models and their applications discussed in this review.

2. Brain-On-A-Chip (BoC): General Design Features

BoC devices can facilitate the study of neural cells and circuitry in a spatially and temporally controlled environment. BoCs can be produced across a range of size scales, from the sub-micron, tens of micron (cell scale), and larger multi-tissue organ scale, to enable *in vitro* studies targeting the molecular level, cellular level, tissue level, and organism level. On the molecular level, compartmentalized neural models are often used to examine the effects of

biological molecules on neural cell populations.[29] Similarly, BoC devices enable researchers to investigate the impact of mechanical and electrical stimuli on neural cells.[30, 31] Interactions among neurons, such as within synaptic networks, and between neurons and glia, such as astrocyte-neuron junctions or myelinating oligodendrocytes, can both be modeled using BoC constructs.[32, 33] In particular, formation of functional neuronal networks is critical for developing behavioral and pathological models.[34] In this section, technical considerations, including reproducibility, fluidic control, material properties, and data acquisition, are discussed. In addition, commonly used device designs and their applications are introduced.

2.1. Technical Considerations

2.1.1. Reproducibility

Robust reproducibility is crucial for BoC models. In principle, BoC devices are designed to mimic the microenvironment of the brain. However, small variations in the material, fabrication process, and microenvironment may significantly affect study variables at the cellular and subcellular levels.[35] To achieve high reproducibility, especially for large-scale device production, the impact of different fabrication processes must be considered. A common approach for highly reproducible production of BoC devices is replica molding followed by soft lithography. Using this method, a large number of fluidic devices can be derived from a single master mold. On the other hand, a single-step method employing 3D printing can be more accurate[36] and can also be used for chip mass production.[37] However, printing resolution to produce delicate microsystems has not been overcome yet and further advances in 3D printing technologies are required to achieve high resolution in fabricating chips.

2.1.2. Fluidic Control

Physical parameters, such as shear stress, need to be compatible with cultured cells. Fluid flow through microchannels can expose cells to shear forces, introducing stresses that could

bias, for better or worse, neuronal development and function.[38] In particular, higher strain rates (>1 sec^{-1}) can cause neuronal cell detachment and death.[39] However, a completely static culture condition with no fluid exchange, such as in a standard well plate, is undesirable because of infrequent chemical exchange. Use of flow rates similar to the interstitial flow rate in the brain, about 0.1-0.3 μL/min, has been shown to accelerate differentiation of neural progenitor cells into neurons seeded in microfluidic devices, highlighting a potential benefit of dynamic cultures.[14] To recapitulate selective permeability of the BBB, fluidic control in BBB models must incorporate both 1) a higher flow rate mimicking physiological blood flow experienced in the vessel lumen (0.5 mL/g/min)[40] and 2) a lower flow rate mimicking cerebrospinal fluid (CSF) circulation (295 ± 53 mL in 24 h).[41]

2.1.3. Material Properties

Solubility and permeability of gases, in particular oxygen (O_2) and carbon dioxide (CO_2), are key properties to be considered when selecting a material for chip fabrication, as living cells depend on efficient exchange of these gases. Polydimethylsiloxane (PDMS) is used most commonly for its low cost, accessibility, ease of preparation and rapid, high-fidelity curing. Furthermore, PDMS is biologically inert, gas-permeable, and forms a non-toxic surface that resists cell adhesion in its unmodified form. While measuring the specific gas levels at various regions of a microfluidic device is challenging, numerical simulation of O_2 transport in a rectangular channel comprised of O_2-permeable polymer bonded to a glass substrate suggested that PDMS up to 1.9 mm thick does not reduce O_2 concentration substantially.[42] However, increasing channel height further led to reduced O_2 concentration, indicating limited O_2 diffusion.

A major drawback of PDMS is its tendency to adsorb hydrophobic molecules,[43] including serum components, many pharmacological compounds, and neurotransmitters. Adsorption of

components in culture media and sera to walls of a BoC device can deplete components in the media required for cell function. Efforts to reduce adsorption have included modifying the surface of PDMS microchannels.[44] A convenient method has been to saturate the PDMS surface with bovine serum albumin (BSA), which effectively reduces non-specific adsorption of large hydrophobic compounds, such as proteins.[45] However, albumin treatment of PDMS did not adequately prevent adsorption of small hydrophobic molecules and adsorption of small molecule drugs or other potential therapeutics can significantly affect experimental outcomes.[43] Lastly, evaporation through porous materials, including PDMS, can cause shifts in media osmolarity. Increased osmolarity can cause osmotic stress, which can compromise cell function; for example, osmotic shifts were found to delay growth of mouse embryos *in vitro*.[46]

Alternative materials to PDMS for creating microfluidic devices include polymethylmethacrylate (PMMA), cyclic olefin copolymer (COC), polycarbonate, and polystyrene.[47] While O_2 solubility in COC and PMMA is found to be similar to that of PDMS, O_2 diffusivity of COC and PMMA was significantly lower than that of PDMS, indicating that convection-dominant flow should be used when employing COC and PMMA.[42] A recent study investigated tetrafluoroethylene propylene (TFEP) for constructing microfluidic devices.[48] When directly compared to PDMS, TFEP minimally absorbed small hydrophobic compounds, including rhodamine B, nifedipine, coumarin, and Bay K8644. However, fabrication of TFEP chips involves molding with a 200-ton vacuum compression machine, which is not likely to be an option in most laboratory settings.

2.1.4. Data Acquisition

The ease of data acquisition plays an important role in determining experimental feasibility and practical utility of BoC devices. Conventional methods for data acquisition from BoCs

include microscopy and characterization of the effluent. However, typically only minimal quantities can be accessed from on-chip effluents (on the order of microliters), which limits detailed analysis. To address these issues, several recent efforts have focused on developing "on-chip" sensors, including those fabricated from carbon-based nanomaterials, for physical, chemical, and biochemical features to enable real-time data collection.[49]

Transendothelial electrical resistance (TEER) electrodes have been commonly used to quantify the formation, stability, and function of *in vitro* models of the BBB.[50] Resistance across the barrier is measured to evaluate coverage and the presence of tight junctions between cultured brain microvascular endothelial cells.[51] Fabrication of guidance channels for electrode insertion into a chip can provide precise control over electrode position, and computationally calculated coordinates can be utilized to optimize the positioning of TEER electrodes.[52] Similarly, microelectrode arrays (MEAs) can be used for real-time measurement and electrical stimulation of neuronal activity; for example, to detect effects of drugs being screened in an AD model.[53] One approach has been to integrate a MEA within a BoC featuring mouse brain slices, in which an aperture layer provided electrode access.[54] An alternative approach has been demonstrated in which sensory neurons were seeded into a microfluidic device. A polycarbonate sheet with a gasket having adhesive edges was pressed on top of the MEA layer, enabling detection of single-unit action potentials.[55]

Combining microfluidic and optogenetic techniques with computer automation has led to consistent data collection and image processing in synaptic transmission studies.[56] For example, in a microfluidic design of a synapse-on-a-chip, chemical stimulation of neurons in one lateral compartment induced a neuronal response in the opposing compartment, indicating functional synaptic connection between the two populations of neurons.[57] Integration of

MEAs into BoC devices creates a powerful tool for measuring electrophysiological activity of neural networks.[58]

Monitoring neurotransmitters release will be crucial for understanding synaptic connectivity and the activity in BoC models. While conventional analytical methods, such as high-performance liquid chromatography (HPLC), can provide offline analysis of the effluent from a BoC, sensors compatible with inline, real-time detection of neurotransmitters are still being developed. For example, a large-scale, homogeneous, nanocup-electrode array (LHONA) has been reported to detect dopamine release from stem cell-derived neurons.[59] A more recent study developed an integrated microfluidic-MEA system that can monitor extracellular dopamine uptake and release.[60] Another method for monitoring the neurotransmitter release is the use of molecular optical sensors, which include chemical probes, genetically modified proteins, nanoparticles and quantum dots. Calcium ion (Ca^{2+}) indicator dyes are widely used chemical probes that are commercially available.[61] The major advantage of chemical Ca^{2+} probes is the ease of introducing these liquid dyes to cells in a BOC device. However, such chemical indicators tend to be compartmentalized by, and eventually extruded from, cells, making them incompatible with long-term experiments (e.g., hours or days).[61] Commonly used Ca^{2+} indicators, such as G-CaMP, have been used to study neuronal activities of *C. elegans* in microfluidic devices.[62] A major advantage of using genetically modified protein indicators for dynamic monitoring of chemical species is their ability to monitor specific cell populations through target-specific expression. For example, a genetically encoded transmitter indicator, FLIPE, comprising CFP and YFP fused to the glutamate binding domain, was used to visualize glutamate, the primary excitatory neurotransmitter in the mammalian central nervous system (CNS).[63] Nanoparticle-based sensors have gained recent attention because they offer flexibility and modularity for the modification of their physicochemical properties.[64] For example, Luo *et al.* developed a nanoparticle-based sensor with

acetylcholine-catalyzing enzymes and pH-sensitive gadolinium contrast agents that could detect changes in acetylcholine concentration *in vivo*.[65] The integration of such sensors into BoC devices is an important next step in developing real-time methods to detect and quantify neurotransmitter release.

2.2. Model Designs

2.2.1. Microfluidic-integrated Models

Microfluidic-based models can be categorized into two models of dynamic culture models and static culture models. Microfluidic compartmentalized neuronal models, generally consist of at least two chambers (**Figure 2**).[66] Typical compartmentalized models are either static or provide only slow fluid flow (up to 100 μL/hr[67, 68]), which facilitates creation of controlled concentration gradients of molecular species. The dimensions of the microchannels connecting each chamber are usually restrictive to prevent the mixing of different neural populations from different culture chambers. At the same time, microchannels can accommodate formation of neuronal extensions. For example, Fantuzzo *et al.* used human iPSC-derived-neurons in a circular device that consisted of a large central chamber connected to twelve surrounding smaller chambers, to study synapse formation.[69] This study demonstrated that the use of compartmentalized devices is promising for understanding neurocircuitry formation.

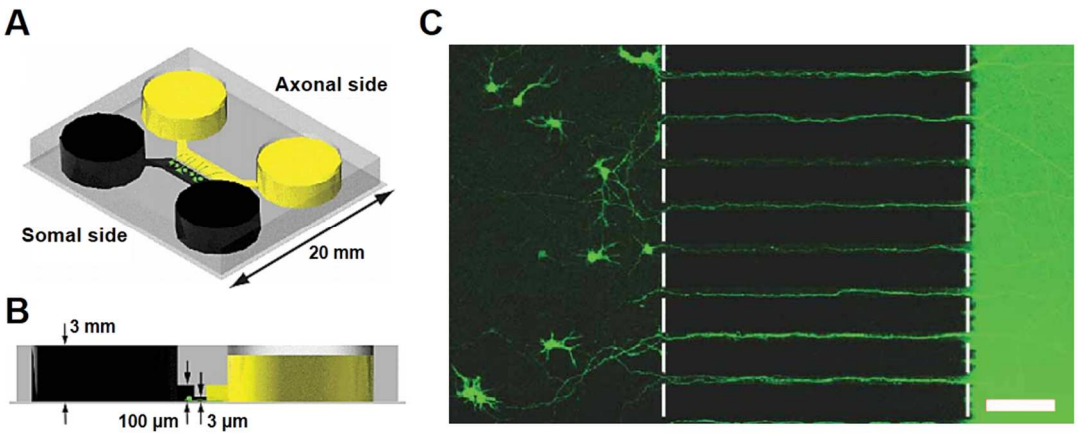

Figure 2. (A) Schematic representation of a microfluidic device consisting of somal and axonal compartments that are connected by microgrooves.[66] Neurons were initially cultured within the somal compartment. After 3-4 days, axons began to extend into the axonal side via the microgrooves, while cell bodies stayed within the somal side. (B) Side view of the microfluidic platform illustrating the height of the reservoirs and microgrooves. Generating a volume difference between somal and axonal sides provided fluidic isolation of the axonal compartment. (C) Axonal guidance via the microgrooves into the axonal side was observed. Neurons and their isolated axons were detected by application of CellTracker Green. Scale bar=100 µm. Reproduced with permission,[66] 2005, Springer Nature.

Active perfusion, albeit at a slow rate, is important for many physiological functions of the brain. Controlled perfusion can influence several intracellular activities; for example, phosphorylation of cyclic-AMP response element-binding protein (CREB), which is involved in a number of brain functions including neuronal survival and formation of long-term memory.[68] In this study, pulsed perfusion (1 minute of flow, followed by 5 minutes of no flow) of glutamate across dendrites of rat hippocampal neurons increased activated CREB levels, when compared to dendrites exposed to steady perfusion for an equivalent total time.

Microfluidics-based models of the BBB generally consist of 1) a lumen lined by brain microvascular endothelial cells (BMVECs) through which fluid is actively perfused and 2) an opposing compartment seeded with astrocytes (and often pericytes) which experiences a relatively static flow. Shear stress should mimic typical stresses found in brain capillaries (i.e., 3—20 dyne/cm^2).[70] Active fluid flow is necessary to develop an endothelial barrier with tight junctions[71] onto which astrocytes can form complexes characteristic of the BBB.[72] Likewise, dynamic flow is necessary to have an efficient barrier function in microfluidic BBB-on-chip.[50, 73, 74]

Brain organoid-on-a-chip models represent one of the advanced 3D cell culture models that can provide self-organization of brain organoid and *in situ* neural differentiation under dynamic and continuous culture conditions[75]. As brain models including recent brain organoids are getting bigger, brain-on-a-chip designs also seem to evolve into the macroscale devices. Therefore, chip designs for organoids can be called millifluidics or bioreactors[76] [77] [78]. For instance, Qian *et al.* [76] proposed a spinning bioreactor to create and cultivate forebrain-specific organoids derived from human iPSCs. These organoids mimic essential aspects of human cortex development, such as progenitor zone structure, neurogenesis, gene expression, and, most notably, a unique layer of human-specific outer radial glia cells. To model Zika virus (ZIKV) exposure, they used the forebrain organoid platform. Quantitative analyses demonstrated that either African or Asian ZIKV strains infect brain progenitors preferentially and productively. In another study on organoid culture, Park *et al.* [77] presented a biochip containing 3D neurospheroids housed in concave microwells located within a chip that was used for Alzheimer disease studies. One of the goals of using this chip was recapitulating the *in vivo* brain microenvironment more closely by supplying a constant flow of fluid normally observed in the interstitium of the brain. They studied the effect of the fluid flow on the size of the neurospheroids, neural differentiation, and neural network formation.

Neurospheroids cultivated in flow generated more robust and sophisticated neural networks than those cultured in static conditions, implying that the interstitial level of slow and diffusion-dominant flow affects continuous supply of nutrients and oxygen, cytokine transit and metabolic waste removal. Moreover, Che *et al.* [78] showed that the use of microfluidic device with brain extracellular matrix for brain organoid cultivation encourages and improves functional and structural maturation of human brain organoids.

2.2.2.. Hydrogel-Based Models

Hydrogel-based models offer the advantage of mimicking the extracellular matrix (ECM) of tissues using a biocompatible material. Hydrogel-based models can be classified according to their dimensions such as 2D, 2.5D, and 3D models. In addition to providing a scaffolding for cell adhesion, hydrogels can be designed with varying elastic moduli, ranging from in order of magnitude from Pascals (Pa) to megapascals (MPa).[79] A landmark study demonstrated that human mesenchymal stem cells differentiated into neurons on soft polyacrylamide gels having elastic moduli ranging from 0.1 to 1 kPa, but differentiated toward muscle- and bone-like lineages on stiffer gels corresponding to 8-17 kPa and 35-40 kPa, respectively.[80] Subsequently, several studies have found that neural stem/progenitor cells prefer to differentiate and extend neurites when seeded on softer hydrogels with a shear modulus in the range of 100-500 Pa.[81] In contrast, glial cell types have been found preferentially to differentiate on relatively stiffer substrates that have generally exhibit a linear elastic modulus above 1 kPa.[81]

Hydrogel degradation also influences neural cell behavior. Mouse embryonic stem cell-derived motor neurons encapsulated in a matrix metalloproteinase (MMP)-degradable gel supported more extensive neurite outgrowth than those encapsulated in a non-degradable gel.[82] In a separate study, neural progenitor cells obtained from rat embryonic day 14

forebrain encapsulated in a degradable polyethylene glycol-polylactide (PEG-PLA) hydrogel showed increased expression of proteins associated with mature neurons and astrocytes over time.[83] In a hydrogel-based BoC, rat primary cortical neurons seeded onto the outer, silk-based layer of a multi-layer scaffold were found to extend neurites into the collagen-based inner layer, forming neural networks.[84]

Although all technical considerations are significant and must be taken into account for BoC models, each one of them has different level of importance depending on availability and application. Reproducibility of BoCs can be achieved at a lower cost by the use of replica molding followed by soft lithography. However, when more accuracy is required, 3D printing can be a better choice.[36] While dynamic cultures are essential in BoC models,[14] fluid flow should be handled carefully. When the BoC platform includes only neural cells, shear stress needs to be maintained at lower levels.[39] In BoCs with BBB structures, a higher shear stress is needed for endothelial cell side for their normal function.[71] Thus, fluid flow within each compartment of the BoC platform must be adjusted separately, based on the cell type used. PDMS is the most commonly used material for BoC fabrication, yet it has major drawbacks as discussed earlier.[43] In BoC applications which are sensitive to adsorption of hydrophilic molecules [43] such as pharmaceutical studies, alternative materials must be sought. In addition, for chip fabrication process (such as 200-ton vacuum compression machine for TFEP chips[48]) and special requirements in the design of the OoC device (such as convention-dominant flow for COC and PMMA chips[85] must be considered. For data collection, on-chip sensors are inseparable components of BoCs,[49] however, integration of sensors into BoC platforms and collecting their data must be managed carefully. Due to electrical activity of neural cells, MEAs are essential to evaluate the function of BoCs both in physiological and pathological models. Electrodes are becoming increasingly important in BoCs with BBB components for measuring TEER.[50] Chemical probes[61] and nanoparticle-based[64] sensors

are also of interest to monitor uptake and release of neurotransmitters. Finally, choosing the best model design should be based on technical considerations as well as distinct characteristics of each study. Even though the compartmentalized model is the most popular design, dealing with BBB places emphasis on the necessity of active fluid flow and working with stem cells highlights the vital role of cellular interaction with ECM. Hence, using microfluidic-integrated models for the first and hydrogel-based models for the latter is advantageous. A summary of materials used for chip fabrication and ECM along with their benefits and drawbacks is presented in **Table 1**.

3. Physiological Models

Microfluidic OoC models are being developed to study normal neural cell and tissue physiology.[86] In this section, we will discuss examples of recently developed models for studying neurite outgrowth, axon formation and synaptogenesis, glial cell support and cell-cell communication and development, immune function, and neurovascular units of the BBB. Chip materials and design, along with cell types and culture duration used in the BoC studies discussed in this section, are summarized in **Table 2**.

3.1. Neuronal Migration, Neurite Outgrowth, Axon Formation, and Synaptogenesis

3.1.1. Neuronal Migration and Neurite Outgrowth

Neuronal and synaptic development are regulated by spatial concentration gradients of various chemo-attractive and chemo-repulsive factors. For example, to better understand how chemical gradients generated within a biomaterial matrix induce neurite outgrowth, Zhen Xu *et al*. used microfluidics to create a large-scale array of Matrigel hydrogels in which chemotaxis could be interrogated in a 3D culture environment.[87] Specifically, this study found that neurite outgrowth from E18 rat hippocampal neurons was repelled down concentration gradients of semaphorin3A (Sema3A), in a manner dependent on gradient

steepness. Furthermore, they demonstrated that this chemo-repellent effect was governed by both serine/threonine kinase-11 (STK11) and glycogen synthase kinase-3 (GSK-3).[87] In addition to this example, many previous reports have demonstrated similar BoC devices for modeling neurite migration in response to concentration gradients of various biological factors.[88]

3.1.2. Guided Axon Formation

Understanding guided formation of axons and dendrites, which then form synapses, is a key process in neural development and regeneration, and microfluidic models have been commonly used for this purpose.[89] To study longer term (10 hours) chemotactic responses of axons, a microfluidic platform composed of a 16×64 array of gradient chambers, in which stable linear concentration gradients of netrin-1 were generated, was developed.[90] Results revealed a directional, gradient-dependent response of growth cone turning, where increasing concentrations of netrin-1 acted as a chemoattractant while decreasing concentrations led to repulsion. The authors suggest that actions of protein kinase C-α (PKC-α) were responsible for this biphasic response. This study highlights the need for defining the spatio-temporal landscape of microenvironment features in BoC models.[91] Beyond concentration gradients, geometric characteristics, such as the size and shape of microfluidic channels, can impact axon growth and function. [92]

3.1.3. Synaptogenesis

To create a synapse-on-a-chip model,[57] axons and dendrites were guided to connect within microchannels and form a synaptic connection while neuronal soma were constrained to two parallel, lateral compartments. Chemical stimulation of neurons in one lateral compartment induced neuronal response in the opposing compartment, indicating that the two populations of neurons were connected via functional synapses (**Figure 3**).[57] Improved spatial and

temporal resolution was achieved by incorporating a local microchannel, which could provide fluid flow directly in the region of synapse formation.[68] Synapse-to-nucleus signaling was verified in this BoC platform by injecting glutamate into the perfusion microchannels, which sat between pre- and post-synaptic compartments, and monitoring calcium dynamics and transcriptional responses of cell bodies and dendrites. In another study, synaptic competition was modeled using two lateral channels containing neurons[93]. This study demonstrated that changes in neuronal activity within one population affects axon growth and synapse formation of a competing neuronal population and that a BoC system can be used to study activity-dependent synaptic plasticity.

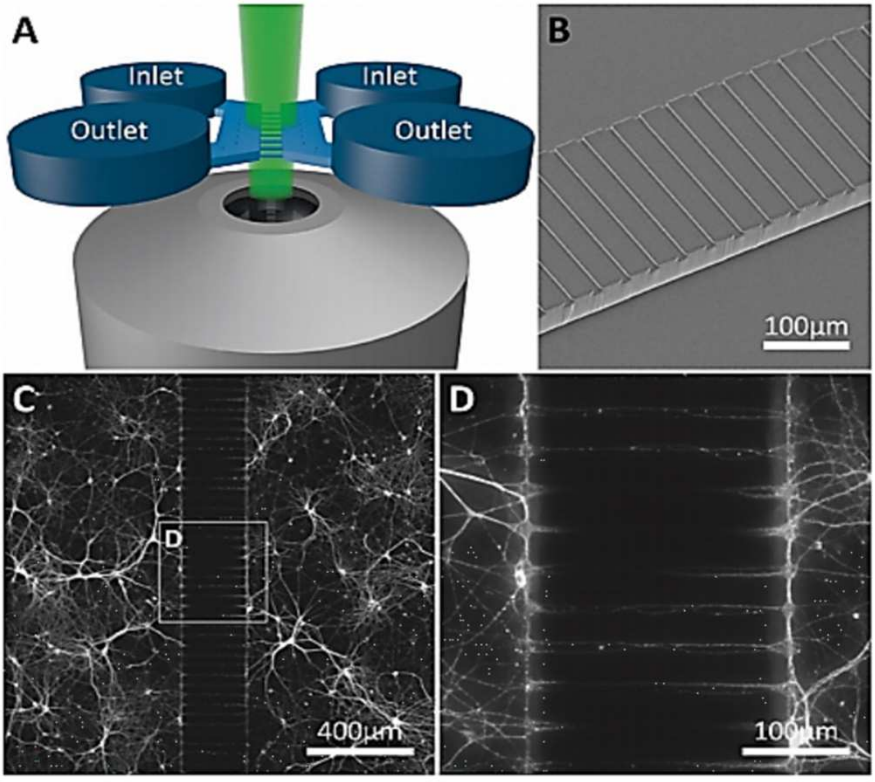

Figure 3. (A) Schematic setup of the compartmentalized microfluidic device with fluorescent microscopy. Open inlets and outlets fed two parallel compartments connected by an array of 200 microchannels. By introducing a chemical compound to the inlets, the population within one compartment was stimulated, leading to a change in neuronal activity in the opposing

population. (B) SEM image of the connecting microchannels (250 µm long, 10 µm wide and 7 µm deep). (C) Neuronal networks were formed within each compartment and physically connected with synaptic communication via the microchannels. (D) Magnification of indicated area in (C). Reproduced with permission,[57] 2014, Oxford University Press.

The studies mentioned above were limited to a single neuronal subtype analysis and did not account for the complex connectivity of multiple subtypes of neurons that make up functional circuitry in the CNS. To study a simplified version of human brain circuitry which could enable studies of higher level functions, a model with neurons capable of receiving multiple inputs was developed.[69] A compartmentalized microfluidic device that can allow for spatial separation of cell bodies of induced pluripotent stem cells (iPSC)-derived excitatory, inhibitory, and dopaminergic neurons was demonstrated.[94] The device comprised a large central chamber with four outer chambers connected by an array of microchannels. By seeding excitatory and dopaminergic neurons in the outer and central chambers, respectively, extension of excitatory neuronal processes toward the dopaminergic cells through the connecting microchannels was observed, with synapse-like structures formed within the central compartment.

As glia and other non-neuronal cells have important functions in the CNS and significant effects on synaptic formation, it is necessary to introduce non-neuronal cells into synapse-on-a-chip platforms. Co-culture of neurons with glia in a microfluidic system can lead to increased numbers of synapses formed and improved stability of the synaptic contact.[95] In this model, neurons were cultured on the bottom and glial cells on the top of chip chamber, separating the two cell types by 50-100 µm, thus the exchange of secreted molecules was maintained (**Figure 4**). In another study, iPSC-derived neurons and astrocytes were mixed

with Matrigel and transferred into the channels of an OrganoPlate® microfluidic platform, which is a microtiter plate with 96 tissue chips that can be used for 3D cell culture, co-culture, and non-invasive media change[96]. Cellular networks were rapidly formed within this plate, and spontaneous neuronal activity was detected.[97]

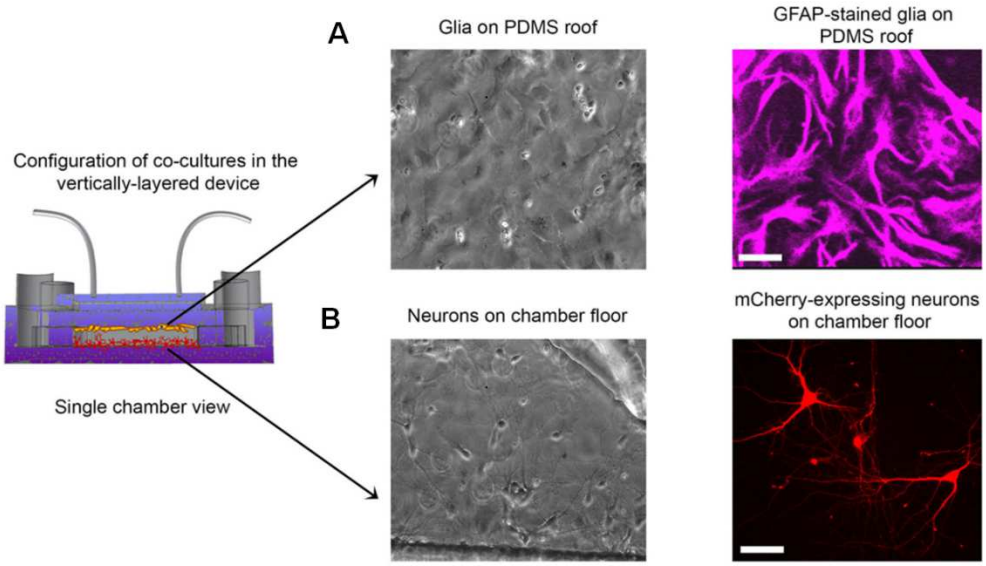

Figure 4. Schematic illustration of neuron-glia co-culture, seeded on bottom and top of the microfluidic chamber, respectively. (A) Phase-contrast (left panel) and immunostained with glial fibrillary acidic protein (GFAP) (right panel) images of glial cells cultured on the PDMS roof after 20 days of culture. Normal morphology of glial monolayer was observed after loading of neurons. (B) Phase-contrast (left panel) and fluorescent (right panel) images of neurons in co-culture with glia, indicating their normal morphology with branches. Scale bars are 25 µm. Reproduced with permission,[95] 2013. This work is licensed under a Creative Commons Attribution 3.0 Unported License.

3.2. Glial Cell Support, Cell-Cell Communication, and Development

3.2.1. Myelination-On-A-Chip

Glial cells provide support to neuronal functions[98] and include oligodendrocytes, astrocytes, ependymal cells, and microglia.[99] Oligodendrocytes are responsible for producing myelinated sheaths around axons, which insulates axons enabling long-range conduction.[100] In addition, oligodendrocytes couple morphologically and metabolically with axons via cytoplasmic-rich myelinic channels.[101] BoC systems could be used to study myelin formation in normal development, neurodegenerative disease (e.g., in multiple sclerosis, a hallmark of which is oligodendrocyte death), and both mechanical and chemical injuries.

Microfluidic-based devices for oligodendrocyte-axon co-culture have most commonly used a compartmentalized model in which myelination events are restricted to a defined area, making it easier to monitor these events.[20, 32] For example, a microfluidic chip comprising a single compartment for neuronal soma and six satellite axon/glia compartments was developed in which oligodendrocyte progenitor cell (OPC)-axon, astrocyte-axon, and OPC-astrocyte-axon co-cultures could be compared.[33] While robust myelin formation was not established in this device, OPCs differentiated into mature oligodendrocytes and extended processes which aligned with axons, a precursor event to myelination, after two weeks in culture.

Application of an electric field across cultures by microfluidic chips using integrated electrodes can increase myelination. For example, oligodendrocytes co-cultured with neurons from dorsal root ganglia (DRG) within a microfluidic device showed improved myelination when exposed to seven 1 hour/day sessions of electrical stimulation.[102] The effect of electrode location on myelin formation was investigated in a compartmentalized microfluidic chip for oligodendrocyte-axon co-culture.[103] In this study, electrical stimulation was applied to the neuronal compartment, myelination compartment or both compartments. Interestingly,

OPC differentiation and axonal myelination were reported to be similar in all three electrical stimulation scenarios (**Figure 5**).[104]

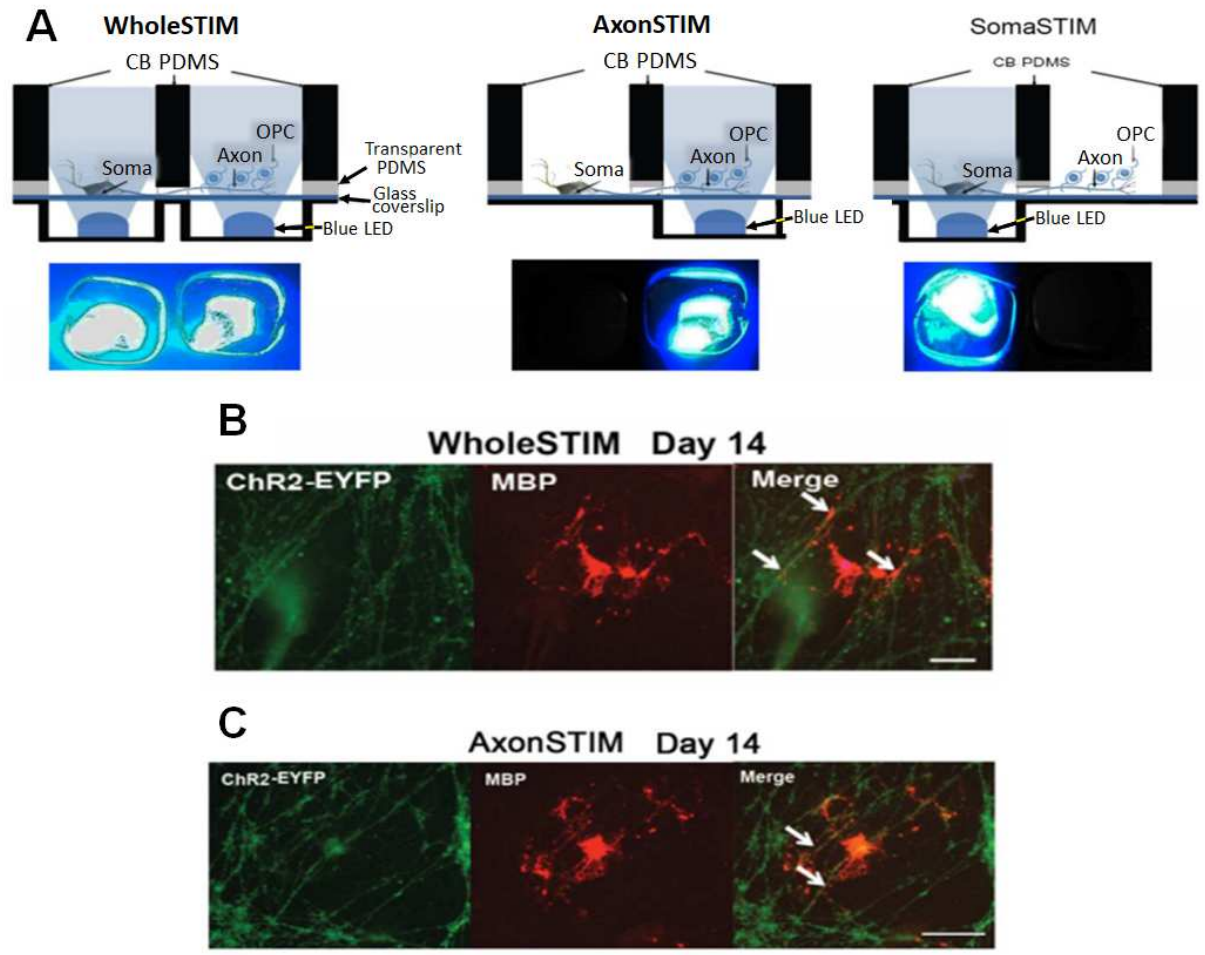

Figure 5. Optogenetic stimulation (OSTIM) platform to evaluate OPC differentiation and myelination in co-culture with axons. (A) Simultaneous optogenetic stimulations of soma and axon compartments called WholeSTIM as well as individual stimulations named AxonSTIM and SomaSTIM were attained using a controllable array of blue LEDs. After 14 days of WholeSTIM (B) and AxonSTIM (C), myelin sheaths indicated by arrows were formed in co-culture of myelin basic protein (MBP)-expressing oligodendrocytes (red) and channel rhodopsin 2 (ChR2)-expressing axons (green). Scale bars are 50 µm. Reproduced with permission,[104] 2016, American Chemical Society.

3.2.2. Immune Function

Microglia are the smallest neuroglia and act as immune cells of the CNS.[105] They are extremely plastic in their transition from a resting to an active state and exhibit diverse functions.[106] Even a small change in the microenvironment can lead to microglia activation and structural remodeling.[107] Infection, ischemia, trauma, and neurodegenerative diseases all trigger microglia activation.[108] Activated microglia migrate to the inflamed site, proliferate, phagocytose foreign material and dead cells, release proinflammatory and immunoregulatory factors, and signal endangered neurons.[109] Microglia have been widely studied for their diagnostic value in various CNS disorders.[109, 110]

However, much is still unknown about microglial states and functions. The first step towards improving our understanding of microglia is to characterize their morphology, which indicates their functional state in different microenvironments. In general, microglia in their resting state assume a multipolar morphology with round, stationary cell bodies and button-shaped pseudopodia that extend to explore the microenvironment. Conversely, activated microglia have elongated bipolar flattened shapes. Primary microglia in culture can undergo selective plasticity in response to various microstructures.[111] For example, microglia adopted a resting state morphology when cultured on microstructured pillars and an activated state when cultured on line-gratings.[111, 112] When seeded into microfluidic devices with a single culture channel attached to multiple microchannels, ~50% of primary and immortalized microglia entered adjacent microchannels, traveling up to 500 µm in about 12 hours.[111] While primary microglia attained stretched morphology and moved individually within the microchannels, immortalized cells had quadrangular shapes and formed compacted clumps (**Figure 6**). This study highlights challenges finding physiologically appropriate cells for use in BoCs, given that CNS-derived, immortalized cell lines are often not able to recapitulate functions of their primary counterparts.

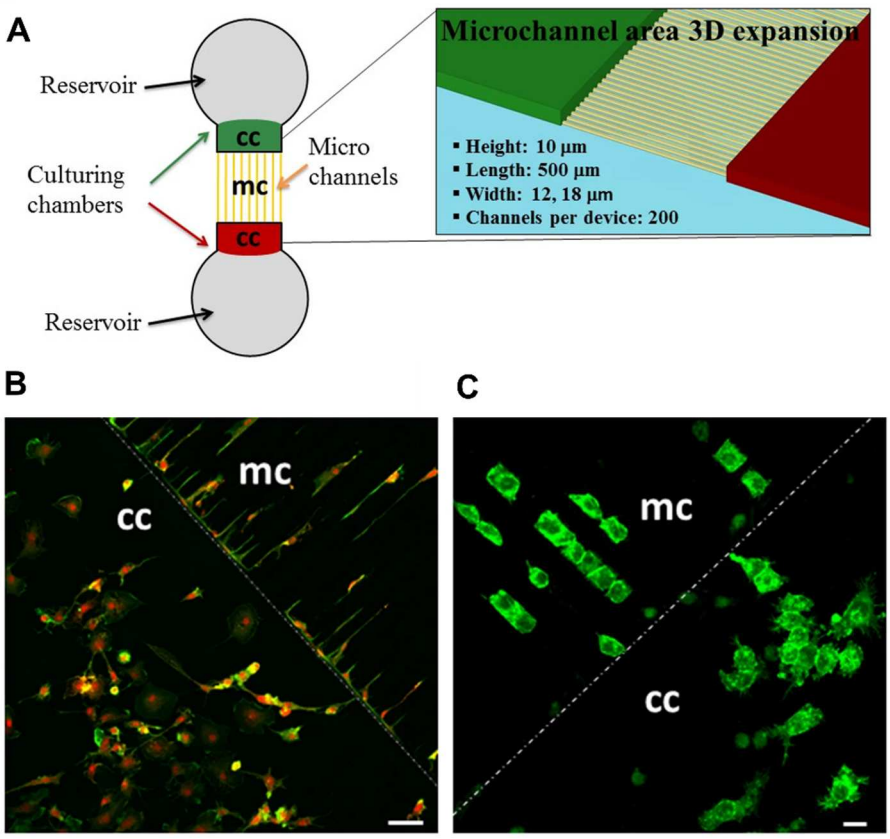

Figure 6. (A) Schematic representation of the microfluidic device used to explore morphological behavior of microglia migrating within a microchannel. Cells were seeded within the culturing chambers (cc) and moved through a set of microchannels (mc) with the presented dimensions. Immunofluorescence images of primary rat microglia (B) and N9 cell line (C) within the microfluidic platform. Primary microglia took elongated shapes and traveled individually, whereas quadrangle-shaped N9 cells advanced in groups. Scale bars = 20 µm. Reproduced with permission,[111] 2013, Springer Nature.

3.3. Blood-Brain-Barrier-On-A-Chip

The BBB is a complex structure, which acts a gate-keeper separating the CNS from the systemic circulation. The BBB is formed by junctions between endothelial cells, glial cells, and pericytes. The BBB selectively filters blood across the microvessel endothelium to control the CSF composition by facilitating passing of nutrients and preventing passing of harmful compounds. Chronic BBB malfunction has been associated with development of

neurodegenerative disorders.[113] While selective permeability of the BBB maintains homeostasis in the brain, entry of many therapeutic drugs into the CNS is blocked. BBB-on-a-chip models in which cells can be studied in real time within a dynamic microenvironment will be instrumental for studying pathological changes in the BBB, such those that occur with stroke, AD, cancer, and multiple sclerosis.[114, 115] The following sections discuss the three main BBB-on-a-chip designs that have been reported: 1) a sandwich design in which an upper and a lower microchannel are separated by a porous membrane, 2) a parallel design in which side-by-side microchannels are separated horizontally by an array of microstructures, and 3) a 3D tubular structure design with cylindrical microchannels.[116]

3.3.1. Sandwich Design: Upper and Lower Microchannels Separated by Porous Membrane

Ideally, a BBB-on-a-chip model should achieve TEER values close to those of the normal mammalian BBB, which range from 1500 to 2000 Ω cm^2.[117] Booth *et al.* demonstrated that exposure of BMVECs in a chip device to dynamic fluid stress lowers BBB permeability and increases TEER values, compared to monolayers cultured in a static, transwell format, suggesting that dynamic flow is important to induce formation of a BBB model with physiologically relevant functional resistance.[30] Booth and Kim created a BBB-on-a-chip using a 10 μm-thick porous polycarbonate membrane (pore size of 0.4 μm) to separate two perpendicularly crossing channels housing endothelial cells and astrocytes (**Figure 7A, I**).[73] The permeability coefficients for the BBB layer were comparable to those reported for previous BBB-on-a-chip models. However, a modified version of the original BBB-on-a-chip was developed in which higher values of shear stress (0.6-1.2 dyn/cm^2) were applied, leading to higher TEER values 280-420 Ω cm^2 (**Figure 7A, IV**).[118]

A more advanced BBB-on-a-chip, developed by Jeong *et al.* and based on the design of Booth and Kim,[118] included an array of 4×4 intersecting microchannels and porous membranes at

the intersections creating 16 BBB sites on a single chip.[119] Each BBB unit included a unique pair of electrodes for TEER measurement. Porous membranes coated with fibronectin or Matrigel were seeded with endothelial cells in one chamber and astrocytes in the other chamber. After four days of culture, devices with Matrigel coating had improved BBB integrity, exhibiting significantly higher TEER values than those for devices with fibronectin coating.

Although many microfluidic-based, BBB-on-a-chip models, including those described above, use pumps to establish fluid flow and exert shear stress on endothelial cells, pumpless strategies, where the flow is driven by gravity, have also been implemented.[15] Griep *et al.* developed a human cell-based BBB-on-a-chip composed of top and bottom channels separated by a polycarbonate filter and platinum electrodes for dynamic TEER measurements.[50] This device was used to demonstrate the positive effects of shear stress and negative effects of stimulation with tumor necrosis factor-alpha (TNF-α) on BBB function.

One of the first cultured neurovascular units to provide a 3D microenvironment incorporated collagen hydrogel-encapsulated astrocytes separated from endothelial cells by a hydrophilized polytetrafluoroethylene membrane with 0.4 μm pores.[120] When endothelial cells were exposed to 5 dyn/cm^2 shear stress, BBB permeability properties established were consistent with those reported by Booth and Kim[73] (Permeability coefficient of ~ 9 x 10^{-7} cm/s). Addition of co-cultured astrocytes and pericytes can enhance formation of a more efficient BBB.[121] For example, soluble factors secreted by astrocytes may be sufficient to induce these effects, as pericyte-conditioned medium has been shown to induce BBB in endothelial cells derived from human umbilical cord blood CD34$^+$ cells.[122]

3.3.2. Parallel Design: Side by Side Microchannels Separated by an Array of Microstructures

As an alternative to the porous membrane, one BBB-on-a-chip model took advantage of side-by-side apical and basolateral microchannels separated by micropillars with 3 μm gaps.[74] The unique design of these microchannels included convergence and divergence to mimic the bifurcations of *in vivo* microvascular networks (**Figure 7B**). Interestingly, this study showed that astrocyte-conditioned media, as opposed to co-culture with astrocytes, was sufficient to induce tight junction formation in a rat BMVEC line under the influence of fluid shear stress. Another microfluidics-based BBB-on-a-chip platform employed microposts as the interaction interface, positioned in a central vascular network channel, a vascular channel on one side for media supply, and a neural channel on the other side for astrocytes and neurons and another media supply (**Figure 7C**).[123] Vascular networks and neural cells could directly contact each other through the spaces between microposts, which is more representative of native BBB as compared to the sandwich design.

Adriani *et al.* designed four side by side microchannels separated by trapezoidal posts in their BBB-on-a-chip: the first one was for endothelial cell culture under shear stress, the second and third microchannels were for the 3D culture of astrocytes and neurons in collagen hydrogels, and the fourth one for media provision.[124]

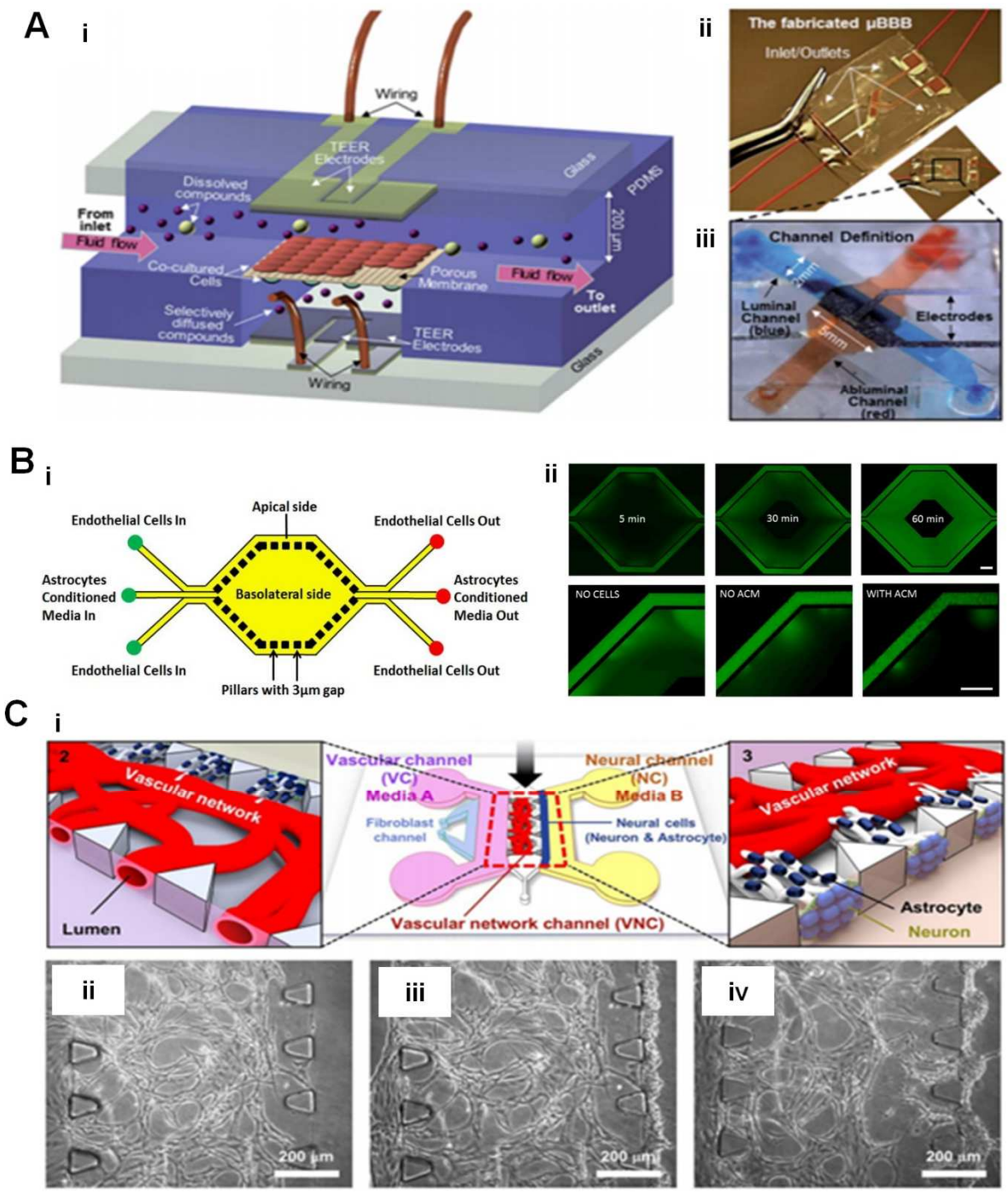

Figure 7. (A) Sandwich-designed microfluidic blood-brain barrier (µBBB) chip. (i) Endothelial cells were injected to the upper channel, where they are exposed to flow shear stress, and astrocytes were cultured in perpendicular lower channel, which has minimal shear stress. The two cell types interacted via a thin, porous membrane at the intersection of microchannels. Two sets of two silver chloride (AgCl) transendothelial electrical resistance(TEER) electrodes were placed on opposite sides of the membrane. Fabricated µBBB

(ii) and its details (iii) are depicted. Reproduced with permission[73] 2012, Royal Society of Chemistry. (B) Parallel-designed synthetic microvasculature model of BBB (SyM-BBB). (i) Apical microchannels were used for endothelial cell culture and basolateral microchannel was for loading astrocyte-conditioned media (ACM). The interface of two sides was comprised of micropillars located at 3 μm gaps. (ii) Comparison of fluorescein isothiocyanate-dextran (FITC-dextran) permeability from apical to basolateral side without cells, with endothelial cells but without ACM, or with both endothelial cells and ACM. Minimal permeation was noticed when endothelial cells were cultured with ACM. Scale bars are 500 μm. Reproduced with permission,[74] 2013, Royal Society of Chemistry. (C) Parallel-designed neurovascular chip for direct contact between vascular network and neural cells through separator microposts. (i) Media were provided for vascular network channel (VNC) by vascular channel (VC) and neural cells were injected and cultured adjacent to VNC via neural channel (NC). (B, C, D) Platform generation process. (ii) Perfusable vascular network formed over three days (not yet open to VC). (iii) Neurons and astrocytes settled on the VNC border posts. (iv) BBB tissue formed in 5 to 7 days after VC and NC channels are supplied with media. Reproduced with permission,[123] 2017, Springer Nature.

3.3.3. Three-Dimensional Tubular Structure Design with Cylindrical Microchannels

The tubular structure BBB-on-a-chip design, in which material science plays a key role, was inspired by brain capillaries and can be used to provide a more uniform flow and shear stress profile.[116] For example, Partyka *et al.* fabricated a mechanically compliant BBB-on-a-chip with vessel-like microchannels surrounded by astrocytes encapsulated in 3D hydrogels and

applied pulsatile flow to the *in situ* vessels.[125] This study found that shear stress and cyclic stretch were essential regulators of the barrier function of the BBB. In another tubular-based design, microtubes with average diameters of 10 μm and circular 1 μm diameter pores patterned on their surfaces were fabricated to produce capillaries matched in size to native capillaries.[126] In the aforementioned study, two-photon lithography was needed as a high-resolution 3D microfabrication technique to polymerize photoresists and obtain porous microcapillaries.

In a BBB-on-chip model employing only human iPSC-derived endothelial cells, it was possible to study barrier function of the BBB using p-glycoprotein inhibitor tariquidar and mannitol.[127] In this model, an 150 μm diameter microvessel was fabricated by removal of a suspended super-elastic nitinol wire embedded in a collagen and agarose hydrogel formed within a PDMS microchannel. The resultant hole was then seeded with BMVECs which were exposed to ~4 dyn/cm^2 shear stress. Addition of tariquidar, an inhibitor of the drug efflux mediator p-glycoprotein, increased transcellular permeability, while the hyperosmolar agent mannitol increased paracellular permeability.

In summary, for 2D BBB-chips, sandwich or parallel designs, accurate representations of the BBB environment are often limited by microfabrication challenges. For example, readily available porous membranes have pores with diameters of 3-50 μm, a few orders of magnitude larger than the *in vivo* BBB.[128] Other membrane properties, including porosity, hydrophilicity, thickness, and diffusive and hydraulic permeabilities, can impact cell-cell interactions across a membrane on which cells are cultured. In 3D BBB models, designs including microchannels surrounded by a hydrogel encapsulating astrocytes have been developed. This 3D design better mimics native tissues. In the future, advanced BoCs can be

designed to mimic the dynamics of nervous system activity and function, from early stages of neural cell development to complex nature of neural signaling and communication.

4. Pathological Models

4.1. Injury

Traumatic injury to the brain can be physical or chemical in nature. The former results from direct physical trauma to the brain that can be accidental, incidental or inflicted trauma.[129] Chemical brain injury may result from causes such as intoxication[130], neurodegenerative disease,[131] ischemic insult,[132] or O_2 free radicals[133] as an indirect consequence of head injury. Development of appropriate biomimetic models of different mechanisms of traumatic brain injury would enable profound studies of injury pathology and help to identify effective therapeutics. Specific BoC devices modeling brain injury are discussed below.

4.1.1. Axonal Injury

About half of patients with traumatic brain injury experience events associated with diffuse axonal injury, resulting in significant neuronal degeneration. In one BoC model of axonal injury, a small region of hundreds of aligned axons crossing axotomy microchannels were cut by introducing air to the channel and accelerating the flow.[134] This mechanical axotomy was found to be very similar to physical injuries occurring *in vivo*. In another study, a BoC model was developed to investigate response of hippocampal axons to increasing degrees of uniaxial strain injury with respect to axonal bead formation, delayed structural recovery and microtubule degeneration.[135] Axonal diameter was found to play a significant role in strain injury, with results indicating a positive correlation between axonal diameter and resistance to axonal injury. Using a similar microfluidic device in which rat embryonic hippocampal neurons were cultured, mechanical axotomy induced *Netrin-1* downregulation and subsequent

loss of dendritic spines and presynaptic hyper-excitability, which are both hallmarks of injury *in vivo*.[136]

While drugs, such as benzodiazepines and diuretics, are used to reduce damaging edema after traumatic brain injury, they have marked side effects and do not actually heal the injury.[137] BoCs representing the injured brain can be used to screen pharmacologics for their ability to effectively treat injury. Dauth *et al.* created a multi-modal BoC, recapitulating various brain regions, as a platform for drug screening.[138] This BoC contained separate compartments integrated with MEA representing amygdala, hippocampus, and prefrontal cortex, with each compartment connected through neurites crossing adjoining channels. This study found that injury to one brain region compartment resulted in sustained, decreased electrical activity of neurons in the other two compartmental regions.

Overall, BoC models of traumatic brain injury will likely be useful for understanding the biochemical consequences of diffuse axonal injury and screening potential therapeutic agents. However, desired improvements to such BoC platforms include the capability to model injuries that happen across intact tissues, rather than individual axons, such as occurs during blast-induced injuries.

4.1.2. Astrocytes

Local astrocytes transform into a reactive state in response to a traumatic injury[139] and help mediate the wound healing response in the CNS.[140] However, reactive astrocytes can have neurotoxic effects on neurons and oligodendrocytes and investigations of these effects would benefit from BoC models including glia and customized to study brain trauma.[141] One study investigated the effects of simulated blast traumatic brain injury (through shock waves that create microbubbles) on astrocytes using a controlled electrical discharge system to produce a

direct, physical injury as well as an indirect, chemical injury caused by reactive O_2 species (ROS) generated by localized electrolysis.[142] In another study, astrocytes were cultured on the top and the bottom of microfluidic chamber, and exposed to repetitive microbubbles (20-30 µm diameter) created by applied shock waves of ~10 MPa pressure.[143] Although equal propagation of shock waves was achieved in the top and bottom regions of the chamber, astrocytes seeded on the top had more interactions with microbubbles, which rose to the top of the chamber, leading to reduced adhesion, fewer microfilament stress fibers, compromised membrane permeability, and increased death of astrocytes seeded on the top of the chamber (**Figure 8**).[143] Using this setup, the authors demonstrated that Poloxamer P188, a linear, non-ionic polymer known for its ability to reseal cell membranes,[144] enabled the repair of damaged astrocyte membrane and maintained cell viability.

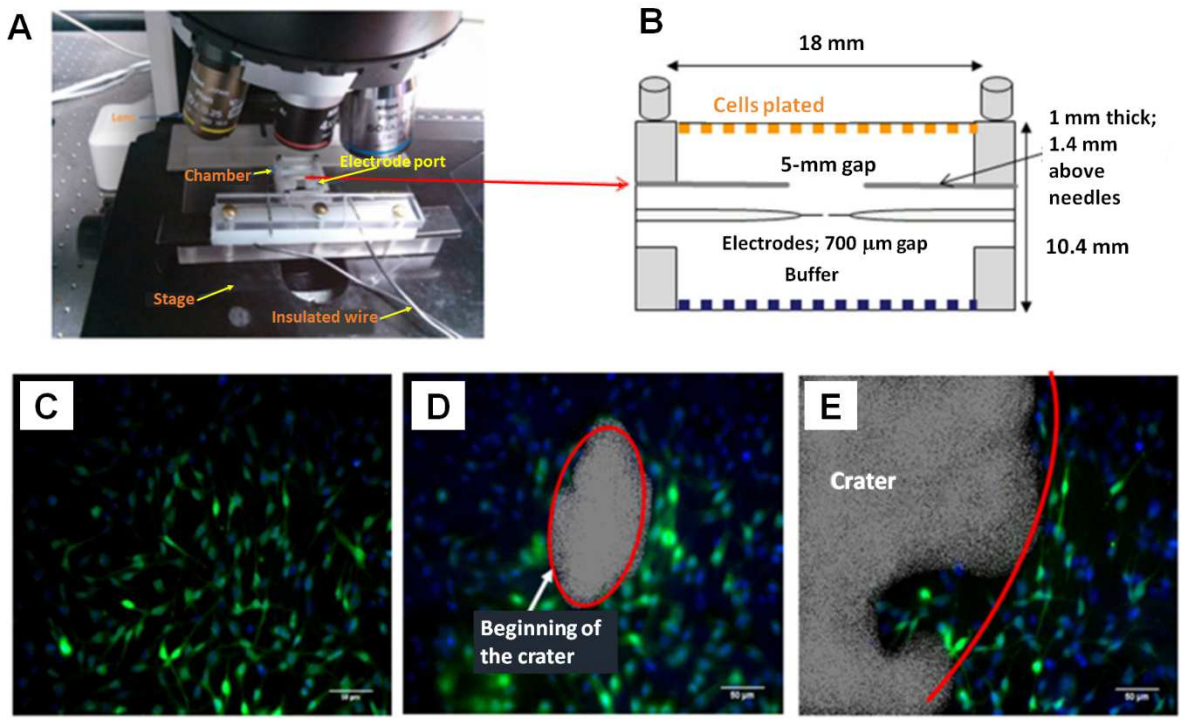

Figure 8. (A) Experimental setup for real-time imaging of the exposure chamber mounted on a microscope stage. (B) Schematic illustration of the exposure chamber with a controlled electrical discharge system to stimulate astrocytes with shock waves and microbubbles. Dimensions of the chamber and locations of electrodes are presented. (C) Confluent layer of

astrocytes before the collapse of microbubbles. (D) A crater indicating cell detachment began to form while microbubble collapsing. (E) Crater at the end of collapsing microbubble. Astrocytes were colored with Flou-4 AM (green) and NucBlue (blue) to visualize calcium activity and nuclei, respectively. Reproduced with permission,[143] 2017, Springer Nature.

To study the effect of external mechanical forces on astrocytes, a precisely controlled, fast fluidic flow, which exerts a shear force on cells seeded in the a microfluidic device, was produced using a servo motor-based pump.[145] Intracellular Ca^{2+} levels, which depends on booth applied forces and the viscoelastic properties of the cells themselves,[146] in response to applied fluidic shear stress were measured. Aside from the magnitude of the shear force, shear loading rate and repeated shear pulses significantly affected Ca^{2+} dynamics. Applying a narrow pulse (short duration), as opposed to a wide pulse, also enhanced Ca^{2+} influx.

4.1.3. Microglia Accumulation

Microglia are key to the inflammatory response in the brain and are thought to mediate synaptic plasticity in repair.[106, 147] Migration of microglia to the site of an ischemic injury was studied using microfluidic chips simulating the soluble microenvironment seen following stroke *in vivo*.[148] Alternatively, a BoC in which neurons and microglia were co-cultured was used to mimic the accumulation of microglial cells near injured axons in the CNS.[149] The circular configuration of this chip made it suitable for centrifugation, a step which enhanced axonal outgrowth into microchannels and improved microglia-axon interactions. Oxidative stress was induced by adding hydrogen peroxide selectively to neuronal soma, which provided a model of microglia encountering injured or inflamed CNS axons.

4.2. Neurodegenerative Diseases

Neurodegenerative diseases such as AD, motor neuron disease and Parkinson's disease (PD) represent growing global health problems [150] and have few treatment options available.[151] New and biomimetic human brain *in vitro* models are; therefore, needed to improve our understanding of disease mechanisms and accelerate the development of effective and personalized therapeutics.[152]

4.2.1. Alzheimer's Disease

AD is characterized by the accumulation of amyloid peptide and phosphorylated Tau microtubule protein in the brain. Chemotaxis and the accumulation of microglia in response to amyloid-β plaque signatures of AD have been modeled with the aid of a microfluidic chemotaxis device, in which stable long-lasting concentration gradients of soluble β-amyloid 42 ($A\beta_{42}$) were generated and migration of human microglia in response to these chemical gradients was monitored.[153] This platform was composed of a central compartment in which surface-bound $A\beta_{42}$ ($bA\beta_{42}$) and soluble $A\beta_{42}$ ($sA\beta_{42}$) were loaded, and an annular compartment in which microglia were seeded (**Figure 9A**). Successful modeling of microglia chemotaxis and accumulation characteristics in a BoC model of AD was established.

In another study, using a BoC seeded with cortical neurospheres derived from rat embryos, it was found that dynamic flow, which simulated flow rates of CSF, increased expression of Aβ (**Figure 9B**).[14] This BoC included a concave microwell array to facilitate generation of homogeneous neuronal spheroids and an osmotic micropump system to provide continuous medium flow. The concave meniscus in each microwell was formed through surface tension of PDMS pre-polymer. An osmotic gradient was maintained via concentration differences between two solutions separated by semipermeable, cellophane film. While it was found that Aβ expression in the neurospheres increased with dynamic flow, increased Aβ in the culture was associated with fewer viable cells, highlighting its neurotoxic and apoptotic effects.[154]

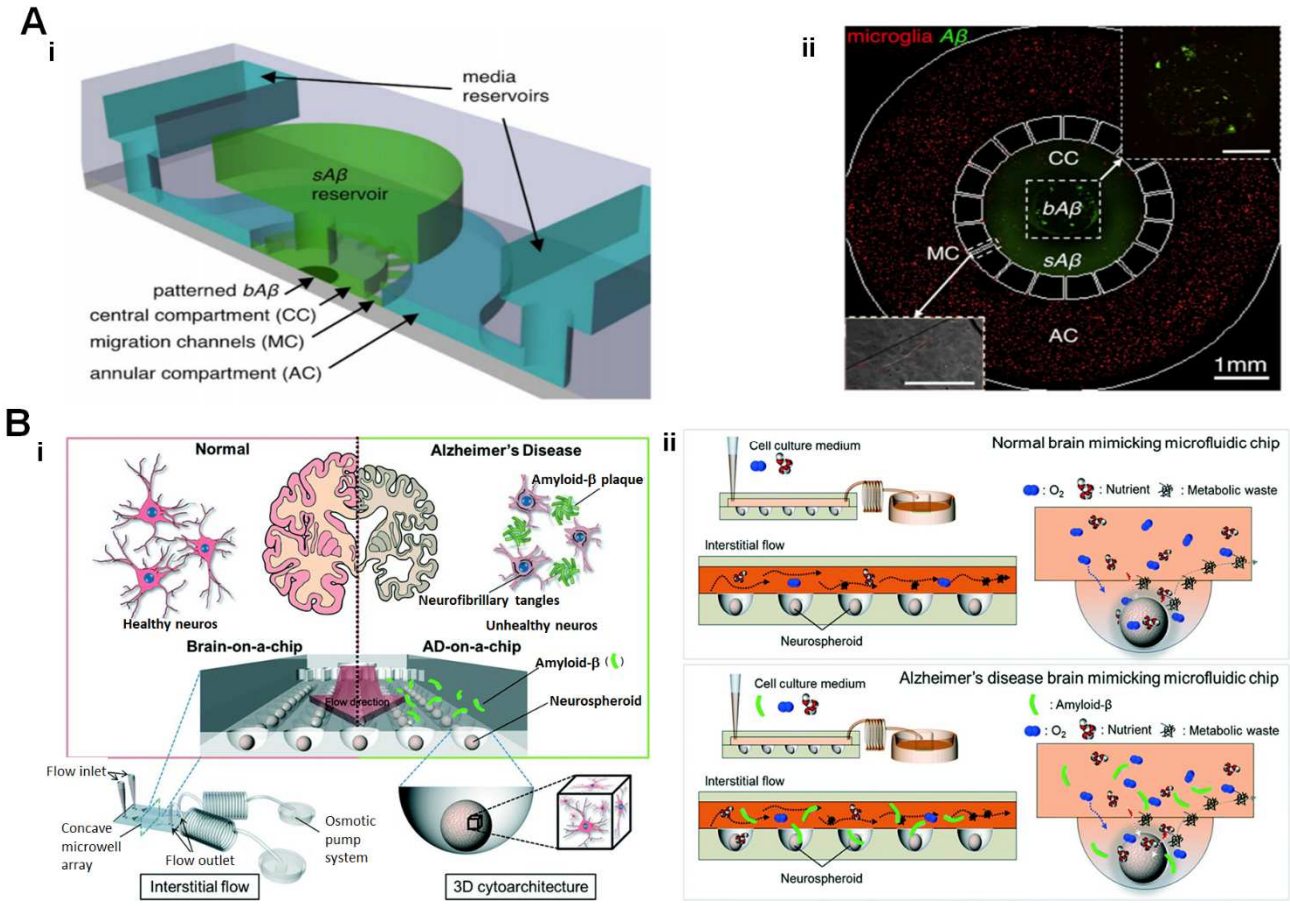

Figure 9. Alzheimer's disease (AD)-on-chips. (A) Microfluidic platform for modelling chemotaxis and accumulation of microglia in AD. (i) Due to the presence of $sA\beta_{42}$ and $bA\beta_{42}$, microglia cultured within the annular component (AC) traveled towards the central compartment (CC) via migration channels (MC). (ii) Fluorescent images indicating the migration process of microglia along the MC (left-lower panel) towards the $bA\beta_{42}$ at the center of CC (right-upper panel). Microglia, $sA\beta_{42}$, and $bA\beta_{42}$ are shown in red, light green, and dark green respectively. Scale bars = 200 µm. Reproduced with permission,[153] 2013, Springer Nature. (B) Schematic diagram of the brain-on-a-chip vs AD-on-a-chip. (i) The device is connected to an osmotic micropump which provides an interstitial flow. The chip is based on 3D neurospheres. Amyloid-β was added to model AD. (ii) Schematic representation of both a microfluidic chip mimicking a normal brain and a microfluidic chip mimicking a brain with AD. In normal conditions, neurospheres were cultured for 10 days with oxygen and nutrients. In AD conditions, cells were cultured for only 7 days with oxygen and nutrients and then with

a medium containing amyloid-β for three days. Reproduced with permission,[14] 2015, Royal Society of Chemistry.

The neurodegenerative process in AD was simulated in another compartmentalized microfluidic platform by exposing mouse primary cortical neuronal cell bodies and/or axons to Aβ peptides.[19] While application of Aβ to a chamber containing neuronal soma and extending dendrites resulted in a rapid loss of pre-synaptic activity in the neural network and triggered axonal degeneration, application of Aβ into the region of extended axons had minimal effects. This BoC holds the potential to detect early changes in AD pathology independently of local Aβ production.

To study AD-associated BBB dysfunction, Shin *et al*. developed a BoC with neurons and a BBB by constructing a tube-shape structure made of human BMVECs interacting with neurons differentiated from immortalized human neural progenitor ReN cells and exhibiting familial AD mutations.[155] These neural progenitor cells were encapsulated in Matrigel in one compartment of the microfluidic device, while endothelial cells were cultured on the walls a separate chamber. Once seeded endothelial cells had established a BBB function, a collagen gel was injected into a chamber separating neural progenitor cells and the BBB, creating a bridging interface. This model developed key indicators of BBB impairment seen in AD, such as high expression of MMP-2 and ROS, and aggregation of Aβ peptides on the vascular side of the BBB. However, Linville *et al.* found that TEER measurements obtained from BBB-on-a-chip models built using BMVECs, derived from MS or AD patients, were comparable to those obtained by using normal cell lines.[127] The reported TEER values for patients and non-diseased individuals were considered physiologically relevant.

4.2.2. Parkinson's Disease

PD is a degenerative disease leading to movement disorders, including both tremor and bradykinesia. Symptoms of PD are caused by loss and impairment of dopaminergic neurons in substantia nigra. A PD-on-a-chip model, named Pelican, was developed to investigate the differentiation of human neuroepithelial stem cells, derived from a PD patient, into dopaminergic neurons.[156] Ca^{2+} imaging and immunostaining assay confirmed that after 24 days, a homogeneously connected 3D network of dopaminergic neurons was achieved. This automated chip was integrated with a software for continuous long-term monitoring of an array of experiments. This automated system enabled longitudinal analysis of patient-specific cellular models exposed to different perturbations over time and could be valuable for personalized disease modeling.

Fernandes, *et al*. developed a microfluidic device in which soluble factor communication between two distinct cell types could be assessed.[157] Specifically, they modeled the spread of α-synuclein, a hallmark of PD pathology, by co-culturing naïve H4 neuroglioma cells with cells over-expressing GFP-tagged α-synuclein. Furthermore, H4 cells were co-cultured with N9 microglial cells in the chip device and demonstrated the utility of this platform to study cross-talk between neural and microglial cells in PD pathogenesis.

In addition to α-synuclein toxicity, astrocyte dysfunction has been associated with PD.[158] Intercellular transport of α-synuclein aggregates from astrocytes to neurons was investigated using primary cortical rat astrocytes and neurons co-cultured in a microfluidic platform.[21] Addition of exogenous, patient-derived α-synuclein aggregates from astrocytes to neurons induced neuronal death. The uptake of α-synuclein was greater and faster in astrocytes, which had minimal apoptosis, than in neurons. However, the level of endogenous α-synuclein was

higher in neurons, presumably because astrocytes, and not neurons, are able to degrade α-synuclein aggregates.[159]

Another microfluidic study provided evidence that the progression of PD could be caused by neuron-to-neuron transport of α-synuclein aggregates.[160] Using live-cell imaging and immunofluorescence, transport of fluorescent α-synuclein fibrils to second-order neurons were characterized (**Figure 10**). It was found that neuronal soma internalized fibrillar α-synuclein and transported in axons. A high-throughput PD model was established by Seidi *et al*. in which a concentration gradient of 6-hydroxydopamine (6-OHDA) was generated by the fluid flow, which in turn induced apoptosis of dopaminergic PC12 cells in an attempt to mimic the death of cells in substantia nigra, which leads to dopamine deficiency in PD.[161] It was found that for concentrations lower than 260 μM of 6-OHDA along the gradient, neurons died primarily by apoptosis, while at concentrations higher than 260 μM, neuronal death occurred mainly through necrosis. As apoptosis is the typical route for loss of dopaminergic neurons in PD pathology, this lower concentration gradient provides a better clinical representation of PD.[162]

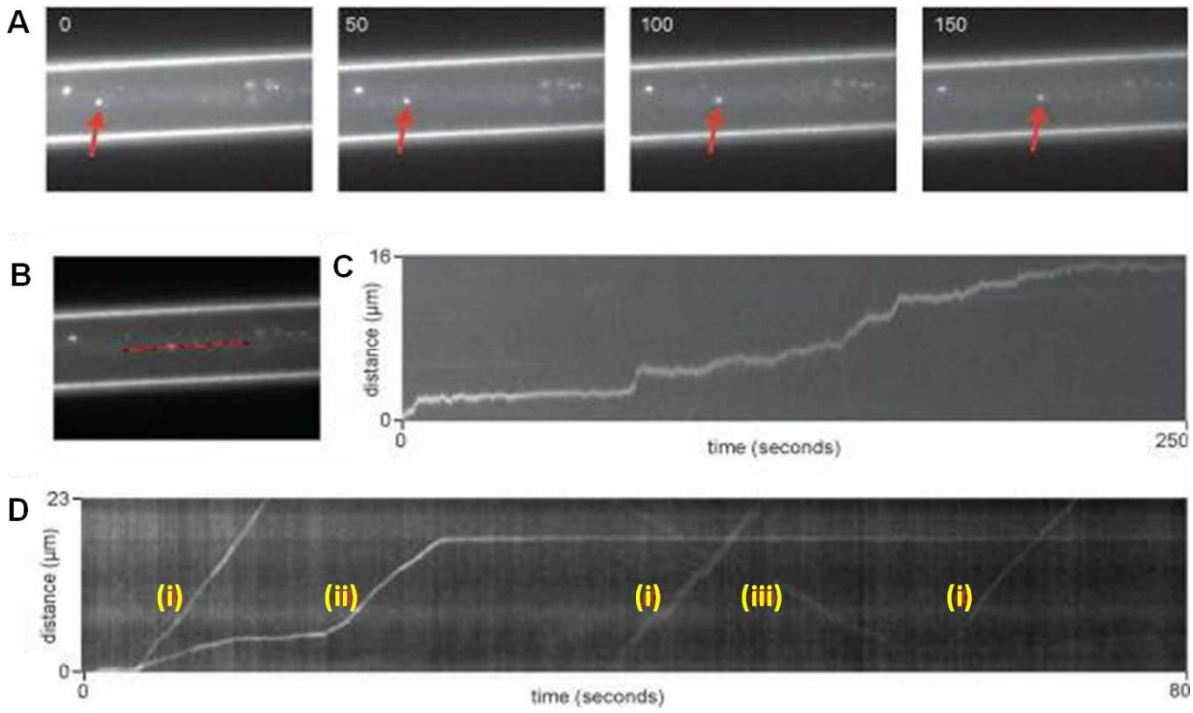

Figure 10. (A) Images showing time-lapse analysis for an axon in a microgroove (borders of the microgroove appear as white lines). The movement of a punctum through axon is shown (red arrow). Note that neuronal soma is located to the left. Time is indicated in seconds. (B) Red line indicates axonal segment selected for the measurement of velocity and flux. (C) Kymograph of the punctum shown in (A), which traveled through the segment of the axon indicated in (B) over a 250s period of time. (D) A kymograph showing different punctum movements, including fast-anterograde movement of three punctae (i), saltatory movement with a long pause of one punctum (ii), and a retrograde movement of one punctum (iii). Reproduced with permission,[160] 2012, John Wiley and Sons, Inc.

4.2.3. Huntington's Disease

HD is a genetic neurodegenerative disease that could benefit from microfluidic BoC models. A cortico-striatal network on-a-chip compatible with high-resolution video microscopy was developed to explore the effect of pre-synaptic alteration on synapse regulation and post-synaptic signaling during the initial phases of HD.[163] This microfluidic platform, in which HD networks were constructed using multiple, fluidically isolated neuronal compartments

(presynaptic, synaptic, and postsynaptic neurons from mice with HD-like pathology). Using this platform, it was possible to study how alterations in presynaptic dynamics, synaptic morphology and transmission, and postsynaptic trafficking and signaling, affect global neuronal network dynamics in HD. It was found that in an HD neural circuit, changes in synaptic dynamics and function of the post-synaptic cortical compartment depended on the status of the pre-synaptic striatal compartment, suggesting that manipulation of only cortical neurons may be sufficient to achieve therapeutic effects.

A common trans-synaptic dysfunction present in many brain pathologies, including HD, is known as diaschisis, defined as a change in the function of a defined brain area due to damage in a distant connected brain area. Diaschisis was modeled *in vitro* by generating an oriented cortico-striatal network from primary mouse neurons within a microfluidic chip, which was subjected to cortical insults.[164] In this work, viability of striatal neurons connected distally to cortical neurons via projected axons increased from 35% to 60%, when synapses were established. When chemical axotomy was performed on cortical axons, tetrodotoxin treatment, which blocks Na^+-channeled mediated conduction, did not protect from axotomy-induced fragmentation, but fully protected striatal dendrites from blebbing and pruning. This result suggests that hyperactivity of cortical neurons, rather than axonal degeneration or loss of neuronal activity, triggers trans-synaptic degeneration. Furthermore, a role for glutamate signaling dysfunction in neuronal pathways of a diaschisis-like process was observed, which might be useful to study neurodegenerative conditions in which diaschisis occurs, such as HD and PD.

Despite these efforts, there is no model which can recapitulate HD, in large part because the underlying pathology is not well-known. One tool to study HD, a strongly genetic disease, is culture of iPSC-derived GABAergic spiny neurons (which are the neurons that die off in HD)

in vitro. However, due to large variability across differentiation protocols, it has been difficult to achieve a consistent, iPSC model of HD *in vitro*. Microfluidic platforms may enable parallel differentiation of iPSCs exposed to several conditions in parallel to identify protocols yielding the neuronal phenotypes most representative of HD.[165]

4.2.4. Amyotrophic Lateral Sclerosis

ALS is a typically fatal neurodegenerative motor neuron disease for there is relatively limited understanding and few treatment options. An ALS-on-a-chip model was developed to explore the interplay of neurons and two lines of genetically modified astrocytes through indirect metabolic contact.[166] Activated primary mouse astrocytes and neurons were co-cultured in a compartmentalized configuration with cell-cell contact area and no-contact area. When astrocytes overexpressing superoxide dismutase enzyme 1 (SOD1), for which genetic mutations have been associated ALS,[167] were co-cultured in the BoCs, neuronal survival dropped by 45% in the cell-cell contact area compared to survival in the no-contact area. In contrast, no differences were seen between in neuronal survival in the contact and no-contact areas when co-cultured with wild-type astrocytes. Furthermore, when glutamate treatment was applied to SOD-mutant astrocyte co-culture, increased cytotoxicity and loss of synapsin protein expression were observed in neurons.

4.3. Brain Tumors

4.3.1. Primary Brain Tumors

Primary brain tumors are less common than those tumors which metastasize from other organ sites to the brain.[168] Using biomaterial science to study gliomas, various tumor-on-a-chip models have been developed, such as the one by Fan *et al*. who used a polyethylene glycol diacrylate (PEGDA) hydrogel as a cell culture scaffold for drug screening.[169] PEGDA offers a quicker and less expensive option to PDMS for fabrication of physiologically relevant, 3D

microenvironment with high spatiotemporal precision. Cultured glioblastoma cells from U87 cell line formed 3D brain cancer tissues on the chip and were assayed for their responses to combinatorial treatment with Pitavastatin and Irinotecan.[169] Such tumor-on-a-chip models could be used in the future for high-throughput, parallel screening of drug responses in glioblastoma multiforme (GBM) spheroids.

A microfluidic chip, in which microglia and glioma cells from immortalized mouse microglia cell lines were co-cultured, was used to explore the roles of microglial behaviors in tumors, including chemotactic migration, activation, and phagocytotic activity.[170] The chemotactic response of microglia migrating within device channels was bidirectional, followed by microglial activation upon encountering glioma cells. Phagocytosis-related markers were expressed in 2D assays in accordance with early stages of glioma, but were absent in 3D models. This indicates that the immune response of microglia changes during tumor progression.

It is known that brain tumors lead to serious dysfunction of the surrounding brain tissue and BBB. To study the blood-tumor barrier (BTB), a microfluidic chip model with apical and basolateral compartments and an array of 3 μm pores was developed by Terrell-Hall *et al*.[171] Human umbilical vein endothelial cells (HUVECs) were cultured in the apical side and exposed to fluid flow in both BBB and BTB models. BBB models were established with CTX-TNA2 rat astrocytes seeded in the basolateral compartment. To create BTB models, astrocytic cells were replaced with Met-1 metastatic murine breast cancer cells. Passive permeabilities of several model compounds were assessed and reported to be similar to *in vivo* permeabilities. Brown *et al.* improved this apical and basolateral design by coating the apical side with human fibronectin before culturing confluent monolayers of a human BMVEC cell line (hCMEC/D3) on every surface of the apical microchannel, which yielded a lumen-like

structure when subjected to the shear stress of 2.73 dyne/cm^2.[172] Primary human astrocytes were seeded on the basolateral side. Spatio-temporal permeability of model dextrans with varying molecular weights were monitored in real time. Separately, a purely mathematical model was developed to characterize the design of BBB-on-a-chip that employed a co-culture of endothelial-like and glioblastoma cells.[126]

4.3.2. Metastatic Tumors in the Brain

Brain metastases arise from cancers originating at other sites, such as lung, breast, bowel, kidney, and skin, and where circulating tumor cells enter the brain through the bloodstream.[173, 174] Lung cancer metastasis to distant organs, including brain, was modeled using a multi-organ-on-a-chip (MoC) platform by connecting an upstream lung-on-a-chip, comprising human bronchial epithelial, microvascular endothelial, lung fibroblast, mononuclear, and lung cancer cells, with three individual downstream units containing either astrocytes, osteocytes, or hepatocytes as proxys for brain, bone, and liver metastatic sites, respectively.[175] Lung cancer cells showed metastatic behavior after four days in culture, traveling to the various tissue compartments. When tumor cells traveled to the cultured astrocytes, astrocytes upregulated CXCR4, indicating an inflammatory response. Another study developed an MoC specifically to model brain metastasis from primary lung tumors. This MoC consisted of a lung compartment upstream of a brain compartment with functional BBB structure.[176] Upregulation of MMP-2 and MMP-9 in metastatic subpopulations was found using this MoC, which may indicate an increased ability to disrupt tight junctions to penetrate the BBB structure.[177]

4.4. Inflammatory Conditions

Neuroinflammation, characterized by cellular and molecular changes in the CNS, occurs as a response to an inflammatory challenge like injury, infection, or degenerative disease and

involves complex interactions among various types of cells.[178] Unraveling the complexity of cell–cell interactions in neuroinflammation will be crucial for understanding the molecular mechanisms involved and increasing the efficacy of drug development.[179] Toward this end, Bianco *et al*. developed an overflow microfluidic network in which neuroinflammation could be simultaneously monitored by microscopy and electrophysiological recordings.[180] Silicon lids were fabricated using lithography and etching processes and attached to the overflow microfluidic network with an aluminum holder to enable studies in closed or open chambers. Using rat primary brain cortical and hippocampal astrocytes and neurons cultured in a microfluidic device and a multiparametric readout approach (**Figure 11**), an analytical method for investigating cell-cell communication was described. Cortical astrocytes were more sensitive to metabolic stress, as compared to hippocampal astrocytes, which were more sensitive to Aβ fibril exposure. The comparative method represents a promising tool for addressing a wide range of biological and biochemical phenomena characterized by complex interactions among multiple cell types.

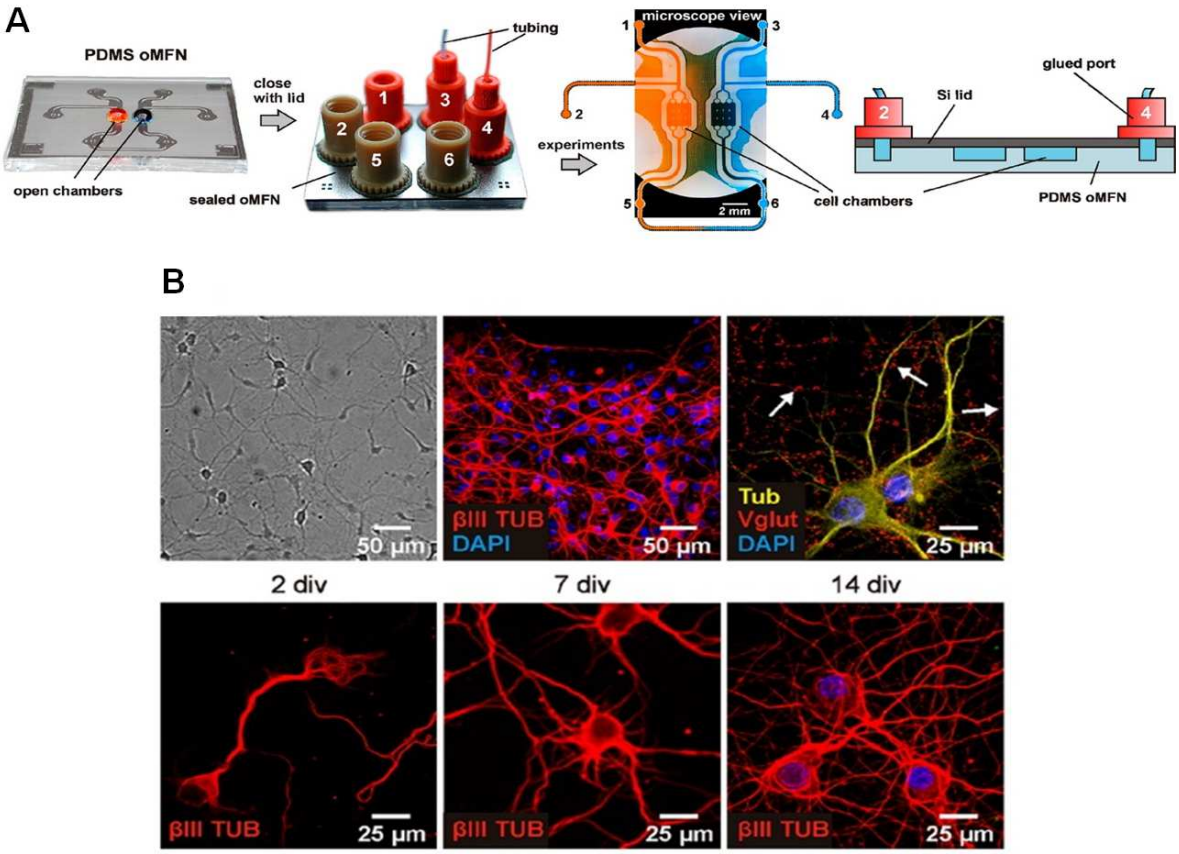

Figure 11. (A) Fabricated overflow microfluidic networks (oMFN) and its principle of operation. Cell chambers could be open or closed with Si lids during the experiment. The ports glued on the lids controlled the microchannels feeding the chambers and they maintained three modes: open, closed with a threaded plug, or connected to a computer-controlled syringe. (B) Development of the neuronal network showed by expressing late-stage specific markers and staining with βIII tubulin. Reproduced with permission,[180] 2012, American Chemical Society.

Blood vessels in the brain have a major importance in the local regulation of immune response.[181] Neurovascular dysfunction has been linked to a wide spectrum of neurological disorders.[115, 182] To investigate the inflammatory response in the neurovascular unit, Herland, *et al*. developed a 3D BBB-on-a-chip device with a hollow human brain microvessel of closely apposed, primary BMVECs, pericytes, and astrocytes, each isolated from human

brain.[183] This BBB-on-a-chip model was used to study neurovascular inflammation. Cytokine release induced by inflammatory stimulants, such as TNF-α, were measured. In addition, independent contributions of astrocytes and pericytes to the inflammatory response were assessed.

There is increasing evidence indicating that inflammation and the BBB are involved in the pathogenesis of neurological diseases.[184] To gain insights into how to modulate pathological immune responses and enhance host protective mechanisms in neuroinflammatory diseases, Cucullo *et al*. investigated the transendothelial trafficking of peripheral immune cells across the BBB by designing a humanized dynamic *in vitro* model based on the use of polypropylene hollow microfibers, patterned with transmural microholes (with diameters of 2–4 μm), seeded with commercially available, cryopreserved human BMVECs and astrocytes, and infused with pulsatile flow.[185] When monocytes (human monocytic leukemia cell line) were circulated through this model vessel, flow cessation followed by reperfusion, which could mimic an injury, caused a biphasic BBB opening (similar to what occurs *in vivo*)[186] with a significant increase in the production of proinflammatory cytokines and activated MMPs. When the BBB was breached, abluminal extravasation of monocytes was also observed.

4.5. Infectious Conditions

Infections of the brain can be caused by viruses, bacteria, fungi, or parasites and are typically clinically serious.[187] BoCs have potential to facilitate the study of various aspects of infectious brain diseases that include pathogen–host interactions, pathogenesis, evolution of therapeutic resistance, and development of new therapeutics.[188] A potential application of such BoC models is study of infection by the Zika virus, a pathogen of worldwide concern as it has been associated with microcephaly and other neurological disorders in newborn infants of infected mothers.[189] Qian, *et al*. developed a miniaturized spinning bioreactor to generate

human forebrain-specific iPSC-derived organoids, which were then utilized to model Zika virus exposure during cortical neurogenesis.[190] Quantitative analyses revealed preferential, productive infection of neural progenitors with either African or Asian Zika virus strains. Furthermore, Zika virus infection led to increased cell death and reduced proliferation, resulting in reduced neuronal cell-layer volume resembling microcephaly. Although this did not employ a BoC model, methodologies and insights described can assist in the development of new on-chip platforms for modeling human brain infection and the development of anti-infective therapeutics. Compared to organoids, a BoC can offer advantages like the ability to image live cultures and better control and reproducibility, which are particularly critical for applications such as high-throughput screening of anti-infectious agents.[191] Ultimately, organoids can be used within a BoC to gain advantages of both experimental platforms.[75, 192]

Recent pandemic of the severe acute respiratory syndrome coronavirus 2 (SARS-CoV-2) stimulated different research groups to employ OoC systems,[191, 193] brain organoids[194] and microfluidic systems[195] for investigating the disease. It was suggested that OoC systems can also be used for the study of possible therapeutics in conjunction with existing rapid cell-based screening.[196] Although SARS-CoV-2 causes respiratory symptoms, some patients have experienced neurological symptoms. Therefore, brain organoids and microfluidic systems can be very useful to study the effect of SARS-CoV-2 virus on neurovascular unit (NVU). For example, Pellegrini *et al.* [194] investigated SARS-CoV-2 neurotropism using human pluripotent stem cell-derived brain organoids. They used SARS-CoV-2 spike pseudovirus and live virus to infect the organoids, which showed viral tropism for choroid plexus epithelial cells but little to no infection of neurons or glia. They discovered that infected cells of the choroid plexus epithelial barrier express apolipoprotein and ACE2. Infection of choroid plexus epithelium may lead to damage of the B-CSF-B barrier, and consequent leakage and proinflammatory changes resulting in neurological problems. Ramani *et al*. showed that

SARS-CoV-2 enters 3D human brain organoids within two days of exposure and targets neurons.[197] Imaging neurons within organoids demonstrated that SARS-CoV-2 exposure leads to enhanced distribution of Tau in neurons soma, hyperphosphorylation, and neuronal death. Studying human NVU with a functional BBB-on-a-chip and co-culture of human neural stem cells, brain microvascular endothelial cells and brain vascular pericytes can also be useful for studying other infections, e.g. of Cryptococcus neoformans. [198] The use of BBB-on-a-chip enabled discovering that the pathogen generates clusters of cells that enter the BBB without disrupting tight junctions, implying that transcytosis-mediated mechanism is involved.

In summary, pathological BoC models will help to improve our knowledge of the function of brain affected by injury, neurodegenerative disorders, brain tumors, neuroinflammation, and infection. Specific pathologies of neurodegenerative diseases are easier to simulate and investigate using BoCs. Successful pathological applications of BoCs comprise modeling propagation of amyloid peptide and phosphorylated Tau, chemotaxis and accumulation of microglia in AD,[153] α-synuclein spreading, aggregation and astrocyte dysfunction in PD,[158] genetic and cellular mechanisms of disease progression[199] and diaschisis in HD,[164] and mutation of SOD1 in ALS.[167] In brain tumor studies, diagnostic and therapeutic applications of BoCs[170] are undeniable. Circulating tumor cells can be isolated and drug pharmacokinetics can be recapitulated with the aid of BoC platforms. Furthermore, BBB has been shown to play a key role in multiple brain disorders such as AD, PD, brain cancer, and inflammation. Thus, developing MoC platforms with BBB compartments is essential. However, for genetic brain disorders, understanding the underlying pathology requires the development of novel approaches. Using patient-derived cells in BoCs has the potential to provide deeper insight since these cells express genotype and phenotype of specific diseases.

5. Pharmacology Studies and Therapeutic Development

Before the introduction of any drug to the market, its safety has to be ensured through extensive testing *in vitro*, *in vivo*, and in clinical trials.[200] Because of the physiological mismatch between humans and the animals used to estimate drug efficacy in humans, drug safety and efficacy is not clearly predictable before beginning clinical trials in humans. For a drug meant to treat the brain, translational efficacy is perhaps less reliable than for other organs given the stark evolutionary differences between humans and animals. Furthermore, while experimental groups in preclinical studies are homogenous, physiology and drug responses can vary greatly across the heterogeneous human population. Thus, only around 14% of clinical trials worldwide[201] are successful and serious complications during clinical trials are not entirely uncommon.[202] For example, although many drugs for AD have shown promise in animal studies, they have failed in clinical trials.[203]

Tissue-on-a-chip models can address these limitations. BoC models using human cells can be used to approximate toxicity, function, and efficacy of administered drugs in the human brain. For personalized medicine, BoC devices have the potential to be made from a patient's own cells to capture their unique behaviors.[204] Finally, BoC models can include dynamic control of the microenvironment to mimic both normal and pathological conditions (e.g., by changing flow rate) and real-time monitoring of drug-induced changes.[205, 206] The widespread adoption of tissue chips as preclinical models will require the development of precise control over multiple aspects of the microenvironment to better approximate that of the human body.

5.1. Studies to Investigate Drug Function and Efficacy

Microfluidic-based models of the BBB have been used to test the permeability of a variety of drugs (e.g., caffeine, cimetidine, and doxorubicin) and drug conjugates (e.g., Angiopep2-functionalized nanoparticles).[15, 207] For example, a parallel design was used in a BBB-on-a-

chip in which a monolayer of HUVECs were exposed to astrocyte-conditioned medium to induce tight junction formation.[208] This BBB-on-a-chip was used to estimate permeability of common neurological drugs. A separate study used a similar BBB-on-a-chip, employing neural progenitor cells and BMVECs, to model the breakdown of the BBB under oxidative stress after introducing hydrogen peroxide into the system.[155] A high concentration of hydrogen peroxide (100 μM) instantly disrupted the integrity of BBB, marked by reduced expression of tight junction proteins and enhanced permeability across the endothelium. When introduced to the vascular compartment of the BBB, neurotoxic blood thrombin could easily cross the endothelium and damage neural progenitor cells. Furthermore, etodolac, a potential therapeutic agent for treating AD, was tested using this disrupted BBB-on-a-chip and found that etodolac substantially improved BBB integrity.

However, high-throughput platforms capable of screening many drugs in parallel are needed for rapid drug discovery. Therefore, Lee *et al.* fabricated a chip integrating microwells and micropillars for high-throughput drug testing, in which 432 microwells enabled parallel testing of 72 conditions, including different compounds or concentrations.[209] Another high-throughput parallel platform consisted of 96 chips with artificial membranes, each a surface for building an artificial BBB (**Figure 12**).[210] This platform was capable of detecting differences in levels of antibody which crossed the BBB structure, demonstrating its potential for use in large-scale studies to discover BBB-crossing therapeutics. Another BBB-on-a-chip has been developed with 16 semi-independent compartments.[119] This technology enables four different concentrations of a specific drug to be evaluated for BBB permeability at four different locations of a microchannel acting as a blood vessel. This system can be used to predict more precisely the BBB permeability and potential toxicity of specific drug candidates, as compared to previously investigated BBB models.

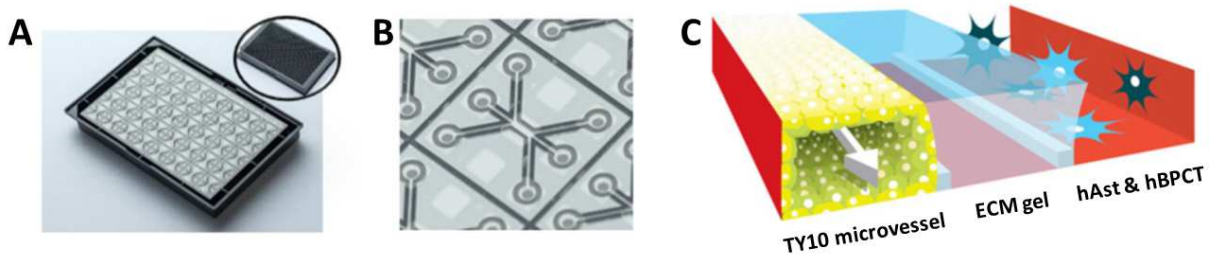

Figure 12. (A) Forty three-lane microfluidic channels were combined in parallel to culture endothelium, astrocytes, and pericytes.[210] (B) Enlarged view of a single tissue culture chip, showing the three adjacent microchannels. (C) Extracellular matrix (ECM) gel was injected to the middle lane, while it was restricted by two phase-guides (white rims) to avoid flowing into the other lanes. After gelation, TY10 endothelial cell line was cultured within one of the side lanes in a three-dimensional manner, forming a vessel-like structure. Astrocytes (hAst cells) and pericytes (hBPCT cells) were then seeded within the other side lane. Hence, a blood-brain barrier co-culture system was obtained. Reproduced with permission,[210] 2018, Springer Nature.

Xu *et al.* developed a high-throughput microfluidic platform to model interactions between the BBB and various tumor cells and to study their response to chemotherapeutic agents.[173] The platform included an array of 16 parallel independent units connected by a microchannel network. In each unit, four BBB structures were generated by directly co-culturing primary rat BMVECs and cerebral astrocytes on a 3D collagen hydrogel. The integrity of the 64 (16x4) BBB structures was ensured (e.g., using TEER measurements). In some experiments, glioma cells (U87 cell line) were seeded in the collagen hydrogel to investigate whether brain tumor cells could cross the BBB. To study metastasis to the brain, liver, lung, breast, and skin melanoma cancer cells were introduced into the vascular compartments. In agreement with clinical findings, breast cancer, lung cancer, and melanoma cells were capable of crossing BBB, with lung cancer cells having the highest invasion distance in 72 hours, whereas liver

cancer and glioma cells did not cross the BBB. Furthermore, eight therapeutic agents (temozolomide, Carboplatin, Cisplatin, 5-Fluorouracil, Nedaplatin, Gemcitabine, Tegafur and Ifosfamide) were tested in this BBB-on-a-chip to evaluate their potential to treat brain tumors. Only temozolomide, which is the current clinical standard for GBM chemotherapy, was found to pass through the BBB and induce apoptosis in tumor cells. This BBB-on-a-chip provides a new testing model that can be used in preclinical studies to identify compounds most likely to be successful in clinical trials.

In the embryonic brain, the BBB is formed prior to the circulatory system and thus, develops under hypoxic conditions (1-8% O_2). To model this physiological state, Park *et al.* described hypoxia-induced, human iPSC-derived BMVECs using Matrigel culture before transferring BMVECs into a sandwich-designed BBB-on-a-chip in which hypoxia was continued for one day, after which normoxic conditions were used.[211] Characterization of molecular trafficking across the BBB and efflux of the cancer drug doxorubicin from BMVECs revealed that this method produced a BBB-on-a-chip with a drug-specific, selective barrier. Furthermore, reversible osmotic opening of the BBB was demonstrated in this chip by injecting mannitol solution to the system, leading to decrease of TEER by 50% and enhanced permeation of 10 kDa dextran and anti-cancer antibody cetuximab.[211] Hyperosmolar agents, which include mannitol, have been used to increase the delivery of drugs across the BBB.[212] In separate publications, the effect of molecules shown to facilitate drug delivery to the brain via receptor-mediated transcytosis, such as Angiopep-2 peptide[213] and anti-TfR antibody[214], were successfully recapitulated in this device.

Potentially, BoCs can be used to study pathologies specific to brain regions. For example, a multiregional BoC was used to approximate a phencyclidine-induced, schizophrenia-like state.[138] This *in vitro* model was used to evaluate differences among cultured rat cells

originating from different brain regions in terms of cell composition, protein expression levels, metabolism, and electrophysiology. The advantages of this model include the presence of functionally interconnected brain areas and the ability to treat one brain region specifically with a drug and assess the effects on parameters, such as electrophysiology, on all interconnected brain areas.[138]

For high-throughput studies, an OoC can be produced using one-step UV photolithography (e.g., using a photo-polymerizable PEGDA hydrogel), which requires no silicon wafer, replica molding, or plasma bonding.[169] This leads to rapid and cost-effective production of chips. In this chip, the U87 GBM cell line was in 3D culture and the hypoxic gradient produced a model with hypoxia-related features representative of an *in vivo* tumor. The chip was used for simultaneous administration of multiple drugs (Pitavastatin and Iriontecan) and a high-throughput, parallel testing of drug responses.. Another GBM-on-chip model was developed using 3D bioprinting to create a cancer--on-a-chip that combines a compartmentalized cancer-stroma structure, an oxygen-gradient-generating system and brain decellularized ECM (**Figure 13**).[215] Since *ex vivo* cultures of patient-derived cells are used in this chip, it can help identify patient-specific drug sensitivity, which will guide clinicians to choose the most efficient treatment for individual patients.

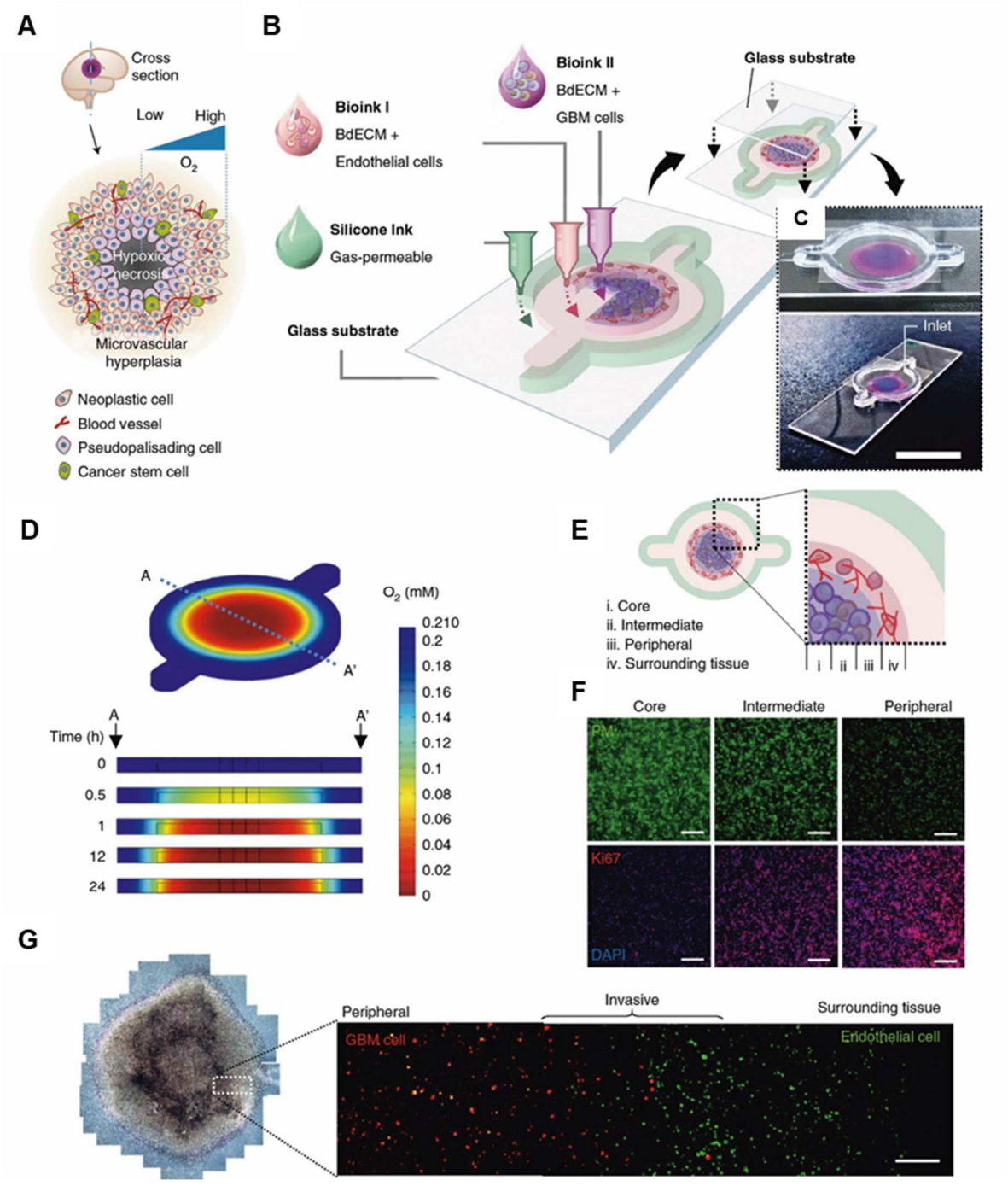

Figure 13. (A) Schematic showing a cross-section of glioblastoma multiforme (GBM). (B) Schematic of the 3D bioprinting of GBM to produce GBM-on-a-chip using various bioinks and materials. (C) Images of a mock GBM-on-a-chip employing human umbilical vein endothelial cells (HUVECs) (magenta) or GBM cells (blue) laden brain decellularized extracellular matrix (BdECM)-based. Scale bar, 2 cm. (D) Time-lapse jet colourmap images of oxygen concentrations along the cross-section A–A' calculated by using computer

simulation. (E) Schematic showing: (i) core, (ii) intermediate and (iii) peripheral regions in the 3D bioprinted GBM and (iv) the surrounding HUVECs containing 3D bioprinted region. (F) Immunostaining images of the different regions using pimonidazole (PM) for the hypoxic cells, Ki67 for the proliferating cells and DAPI for the cell nuclei. Scale bar, 200 μm. (G) Images of the GBM-on-a-chip observed using phase-contrast optical (left) and fluorescence microscopy (right) with the GBM cells labelled with DiI and HUVECs labelled with DiO (n= 3). Scale bar, 500 μm. Reproduced with permission,[215] 2019, Springer Nature.

5.2. Studies for Development of Personalized Medicine

BoC systems have the enormous potential to personalized medicine by providing more physiological *in vitro* models, where patient's own cells can be used to populate the BoC platform in which drug regiments are screened for treatment efficacy. Isolated non-invasively from the skin, skin cells can be reprogrammed into iPSCs, which can then be differentiated into all the cell types needed to recapitulate brain tissue in a chip device.[216] Using dynamic chip-based in vitro models may provide advantages over other culture methods used for iPSC differentiation and organization into functional tissue assemblies, as the device architecture and biochemical functionalization can guide these processes *in situ*.[217] Using patient-derived primary cells or iPSCs in OoC systems can help in developing more accurate models for personalized medicine, which is one of the key goals of using OoC technology.

An iPSC-based, BBB-on-a-chip with potential use for personalized medicine and prediction of drug penetrability into human CNS was produced using human iPSC-derived BMVECs and neural cells seeded on either side of a porous membrane in a microfluidic device.[218, 219] To evaluate potential changes in BBB function in AD, cells generated from iPSCs obtained from healthy donors were compared to those from AD donors. It was found that the permeability of BBB formed from AD donor cells was significantly higher than when formed

from healthy donor cells. Penetration of three drugs (colchicine, levetiracetam, and retigabine) were tested in this BBB-on-a-chip, which had a moderate permeability to colchicine and efficient penetration of levetiracetam and retigabine. The use of iPSC-derived, human cells can create a BBB-on-a-chip that can potentially predict variations in BBB function among individual patients.

To summarize, a major concern in pharmacology and therapeutics is delivering drug to the diseased part of the brain. If the drug is incapable of reaching the target spot, its therapeutic effect will be lost. BBB plays a crucial role in controlling drug transport from the systemic circulation to brain tissue. Hence, integrating BBB compartments to BoC platforms is critical. Due to the fact that the majority of drug metabolism occurs in liver, integrating liver-on-a-chip with BoCs is important to understand pharmacokinetics and pharmacodynamics of the drugs. The use of patient's own cells in BoC will lead to the development of personalized drug screening platforms. Libraries of drugs can be examined on patient-derived iPSCs and the response to various drugs can be monitored. This approach will also enable the evaluation of patient's immune response to the drug. High-throughput parallel BoCs are the future of drug screening studies as they can rapidly test different drugs and precisely monitor drug safety and efficacy.

6. Other Applications

Inspired by the massively parallel communication and computation of the human neural network, neuromorphic chips, silicon-based[220] and microfluidic-based,[221] are being developed for robust information processing. Neuromorphic chips require an artificial neuronal network connected by functional synapses. However, reproducing artificial synapses with biomimetic ion transport has been particularly challenging. To address this issue,

engineers have designed a neuromorphic chip with precise control over the strength of electric current that passes through artificial synapses to simulate ion flow across synaptic connections.[222] A chip was successfully fabricated from silicon germanium with uniform performance that was capable of recognizing samples of handwriting with 95% accuracy. Artificial neural networks are promising tools in artificial intelligence, such as pattern recognition of spike-timing-dependent plasticity to adjust the efficacy of synaptic communication between neurons.[223] Although the ultimate biological application of neuromorphic chips is to construct a fully functional human brain *in vitro*, many commercial applications such as building power-efficient supercomputers, low-power sensors, and self-learning robots are also expected. There are examples of neuromorphic systems that have already been developed for the purpose of understanding the brain,[224] or for exploring potential for commercial applications such as the ones mentioned above.[225]

7. Integrating Chips: Multi-Organ-On-A-Chip (MoC) Platforms

With the use of single OoC units, it is not possible to pick up secondary toxicity that results from the metabolism of drugs or the systemic toxicity which may result from the circulation of drugs to other organs.[226] Thus, for proper drug screening and development, a MoC is required.[227] Different components of one specific organ or multiple individual OoC systems have been integrated into a single device to build MoC platforms with the goal of developing reliable models for predicting drug toxicity and efficacy in the human body. The arrangement of organ chips is also important. For example, the liver, which performs metabolism, should precede a kidney unit where a kidney disease-related metabolite is being investigated.[228] In addition, the relative volume of different organs and their representation in MoC should be considered. Currently, this is typically done using allometric scaling.[229] MoC platforms also enable investigation of crosstalk between multiple organs in response to various biochemical

stimulations. Hence, the drug metabolic processes through the human body are simulated in a more *in vivo*-like *in vitro* system.

In the remainder of this section, MoCs including brain components will be reviewed, a summary of which is presented in **Table 3**.

7.1. MoCs Comprising a BBB and a BoC

To create more advanced on-chip systems which contain more than one functional tissue, neurons were combined in 3D BBB-on-a-chip to provide insight into interactions between neural tissue and the BBB have been combined into a MoC.[236] To create a BBB structure, endothelial cells were cultured on one side, while astrocytes and pericytes were seeded on the opposite side, of a membrane dividing the vascular and neural chambers.[236] Neurons were then encapsulated within a collagen hydrogel loaded into the neural compartment. This device was found to provide the necessary structures for investigating the effects of drugs on neuronal function in the context of BBB permeability to drugs and effects on the BBB. Addition of ascorbate or glutamate to the vascular channel either enhanced the barrier function or disrupted barrier function, respectively, as expected based on their *in vivo* activities.

In another study, Kilic *et al.* modeled the interaction between the brain parenchyma and the BBB using cells differentiated into neurons and astrocytes from NTERA2 cells, a pluripotent human cell line derived from an embryonic carcinoma, over the course of four weeks in the bottom channel of the tissue chip device (**Figure 13A, I**).[237] Resulting mature axons and dendrites were surrounded by astrocytes, mimicking the microenvironment of the brain parenchyma (**Figure 13A, II**). Then, human BMVECs were introduced into the top

microchannel of the device to form a monolayer on the porous membrane. In this same study, chemotactic migration of human neural progenitor cells into surrounding tissue in response to concentration gradients of CXCL12 and SLIT2-N, factors well known to mediate chemotaxis after injury and during development, respectively. It was found that neural progenitor cell response time, as well as their directional and persistent migration, induced by gradients were enhanced in the presence of neuron-astrocyte network.

Maoz *et al.* combined two BBB chips with a BoC in the middle to investigate metabolic coupling of endothelial and neural cells by intravascular introduction of methamphetamine.[16] In the two BBB chips, primary human BMVECs were cultured on all four walls of a bottom vascular microchannel, which was perfused with artificial blood to mimic circulation. Primary human astrocytes and pericytes seeded on the other side of a membrane, from where they could interact with endothelial cells. A mixed population of human hippocampal neural stem cell derived neurons and human cortical origin glial cells were cultured on the bottom chamber of the brain chip (**Figure 14B, I**). These three chips were then connected by a perivascular microchannel through which artificial cerebral spinal fluid was flowed. This configuration provided precise control over the shear stress exerted on different cell types. As neurons and astrocytes in the brain experience virtually no shear stress, this chip mimics the *in vivo* environment better than conventional cultures. When methamphetamine, which is known to disrupt the BBB reversibly, was introduced into the vascular channel, barrier function was compromised for the first BBB-on-chip, but not the second as expected. (**Figure 14B, II**). Moreover, this neurovascular unit confirmed the metabolic effect of brain vasculature on neuronal synthesis and secretion of neurotransmitters.

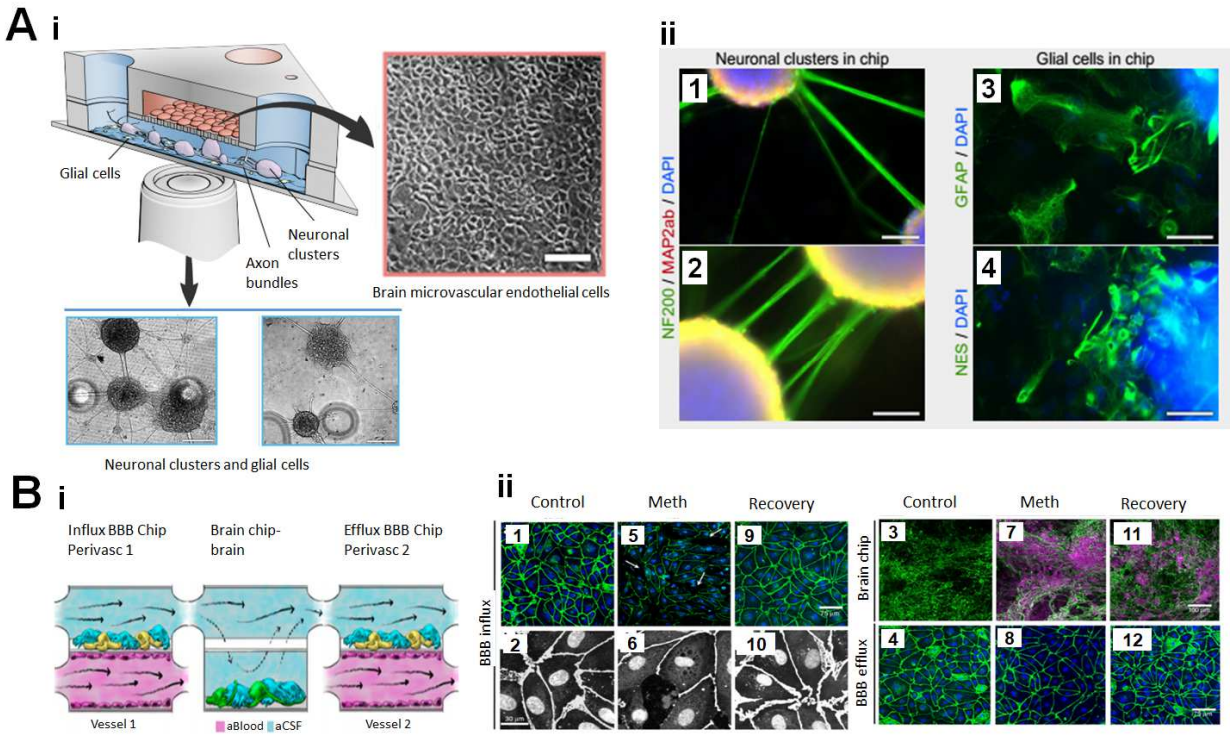

Figure 14. Multi-organ-on-chips (MoCs) with blood brain barrier (BBB) compartment. (A) Microfluidic chip designed for brain parenchyma and BBB interaction (I) Schematic cross-section illustration of the brain-on-chip that includes a bottom brain parenchyma microchannel and a top endothelial microchannel, separated by a porous membrane. Brightfield images of the endothelial monolayer formed on the membrane (scale bar=250 µm) and neuron-glia layer within the bottom compartment (scale bar=200 µm) are provided. (II) Mature axons (NF200 marker, 1, 2), mature dendrites (MAP2ab marker, 1, 2), astrocytes (GFAP marker, 3), and neuronal precursor/astrocytes (NES marker, 4) were distinguished after four weeks of culture. Nuclear staining was performed with DAPI. Scale bars are 100 µm. Reproduced with permission,[237] 2016, Royal Society of Chemistry. (B) Neurovascular unit composed of two blood-brain barrier (BBB) chips and a brain chip connected by a top microchannel containing artificial cerebral spinal fluid. (I) Endothelial cells (pink) cultured under the influence of artificial blood flow generated in the vascular compartment of two BBB chips, while astrocytes (blue) and pericytes (yellow) cultured on the other side of membranes on top of the vascular compartment formed perivascular compartments. Neurons (green) and glial cells were seeded

on the bottom of the brain chip in the middle. (II) Immunofluorescence images of different cell types exposed to methamphetamine (meth) injected from vascular microchannel of influx BBB chip. In control conditions, endothelial cell junctions stained for VE-cadherin in both influx and efflux BBB chips (green in (1) and (4), white in (2)) and neuronal networks stained for β-III-tubulin in the brain chip (green in 3) were exhibited. By 24-hour injection of Meth, endothelial junctions in BBB_{influx} were lost (white arrows in (5), (6)) and the compound penetrated the brain chip, affecting neural cells demonstrated by anti-GluR2 staining (magenta in (7)). However, due to the low concentration of meth, endothelial junctions in BBB_{efflux} were intact (8). 24 hours after meth withdrawal, recovery of BBB structure in the influx chip was observed (9, 10), while no change in neural cells (11) and BBB_{efflux} endothelial cells were detected. Reproduced with permission,[16] 2018, Springer Nature.

7.2. MoCs Including BBB and/or BoC Components

7.2.1. With One Other Organ

In the one study we identified, liver spheroids were co-cultured with neurospheres in an MoC with common media circulation.[238] Metabolic activity of both spheroid types, as measured by glucose consumption and lactate production, was stable after six days in culture for up to two weeks. Introducing 2,5-hexanedione, a known toxin, into the system caused metabolic stress, as indicated by increased activity of lactate dehydrogenase, in both single-tissue and multi-tissue cultures. However, co-cultures showed higher sensitivity, which the authors hypothesized might be caused by one spheroid type sensing necrotic signals released by the other spheroid type. In future studies, this MoC platform may be able to model effects of liver metabolites of an introduced substance on other organs, including neural tissues.

7.2.2. With Multiple Other Organs

A neurovascular unit with intact BBB was functionally coupled with intestinal, liver, and kidney OoCs to investigate absorption, distribution, metabolism, and excretion, respectively.[228] Individual OoCs were developed in different labs and media were derived from these modules were used for functional coupling of the OoCs. Transport of terfenadine, a drug for treatment of PD, trimethylamine, a compound produced by gut microbiota, and vitamin D3 across BBB models were assessed. The MoC was able to model terfenadine metabolized to fexofenadine in intestine and liver chips, shuttled through the kidney chip without begin excreted, and was unable to cross the BBB. Administered trimethylamine was transported across the epithelium in the intestine-on-a-chip and converted to trimethylamine-N-oxide in the liver-on-chip. Around half of the trimethylamine-N-oxide was excreted in the kidney-on-a-chip and around a quarter crossed the BBB-on-a-chip. No metabolism of vitamin D3 was seen in intestine-on-a-chip, but it was metabolized to 25-(OH) vitamin D3 by the liver-on-a-chip and 6% of its metabolite was found in the BoC. This comprehensive study provided organ-specific processing of multiple substances and the results were generally consistent with known human physiology.

In another work, brain, pancreas, liver, lung, heart, gut, and endometrium were integrated in a MoC system to obtain the metabolism of tolcapone, via mass spectrometry of the circulating medium.[239] Following the building of each OoC separately using their respective media, OoCs were integrated into a MoC platform, where basal and apical media were used. Flow partitioning from the mixer to each OoC was used to achieve scaling that corresponds to the distribution of cardiac output to different organs in the body. Twelve talcapone metabolites, including three that were previously unknown, were identified and changes in 18 key biomarkers associated with tryptophan and phenylalanine metabolism, glycerophospholipid metabolism, energy metabolism, and aspartate metabolism were detected using this robust approach.

Finally, Edington *et al.* developed MoC platforms with seven (brain, liver/immune, lung, gut/immune, endometrium, heart, and pancreas units) and ten (brain, liver/immune, lung, gut/immune, endometrium, heart, pancreas, kidney, skin, and skeletal muscle units) integrated OoCs integrated with a high degree-of-freedom on-board pumping system which provided precise control over intra- and inter-compartment flow rates and drug distributions.[240] Robust performance and long-term functionality of the interconnected units were maintained, and reliable diclofenac metabolic activity was achieved in this system.

In summary, single OoC models fail to fully reflect the communication of human tissues and predict response to stimuli and drugs. Hence, MoCs in which different organ representing chips are integrated to establish a unified system are attracting more attention. Scaling and arrangement of organs, media composition and circulation, and automation and stability are major challenges in MoCs. BBB-on-a-chip is the most common component to combine with BoCs since BBB is involved in physiological, pathological, and pharmaceutical studies of the brain. Numerous organ representing chips have also been coupled with BoCs such as liver, kidney, gut, pancreas, lung, and hearth. Although, the use of MoCs is being increasingly explored, it is still limited by cost and data acquisition challenges. Advanced imaging techniques and use of sensors are required for collecting large amounts of data without interfering with chip operation. Conducting long-term examination and real-life measurement will be ideal to capture inter-organ interaction and cross-organ communication.

8. Current Challenges and Future Perspectives

The development of *in vitro* BoC models is an important strategy to better understand the underlying pathologies in traumatic brain injury, degenerative disorders, brain tumors, inflammation, infection, and other conditions in the brain. BoC models can be used alone or

as part of an integrated MoC set-up to ask questions about the local and systemic features of a particular developmental process or pathology, for example. Such tissue-on-a-chip provide precise control over the dynamic physical and biochemical features that affect brain tissue development and function, offering unprecedented opportunities to investigate human brain physiology and pathophysiology.[235, 241] Furthermore, these microphysiological systems are expected to revolutionize how preclinical drug identification and development are performed, as they can provide a more accurate representation of the events that would occur in clinical patients, including liver metabolism and BBB penetration in MoC platforms. Finally, these platforms provide a promising avenue for personalized medicine, where a patient's own cells can be used to construct a tailored BoC. This capability is especially important for the brain-related pathological conditions, which tend to have high variability among patients and potentially complex underlying genetic drivers.

Despite recent strides, significant challenges still need to be overcome before the full potential of BoC-based systems can be realized. These obstacles revolve around few major issues: 1) the need to incorporate several cell types, potentially from iPSCs obtained from a single donor, into a single device, 2) scaling to best approximate the behavior of organs in a miniaturized device, 3) complications due to reliance on PDMS, 4) methods for efficient, reproducible microfluidic chip fabrication, and 5) including on-chip sensors. First, the multicellular architecture of brain tissue is essential to its function and thus, must be represented in BoC models. However, the majority of existing BoC systems were designed to include two or three cellular types.[242] It has been challenging to implement stable co-cultures of more than two or three cell types *in vitro*. In particular, an ideal universal cell culture medium suitable for supporting such multicellular networks has yet to be developed. Identifying a universal medium is an even greater challenge when integrating BoCs into larger MoC configurations, as cells of different organ origins may have vastly different nutritional demands. Moreover, to

model brain pathologies, it will be crucial to add both innate (microglia) and peripheral (e.g., neutrophils) immune cells into BoC-based platforms.

Scale-up of OoC models presents another important issue.[231] As much fewer cells are used in OoC systems, compared to the number of cells that form the models organ in the human body. This scaling discrepancy is especially important in drug testing and development, where drug availability and effective dosage may depend greatly on the size of the target tissue and other tissues the compound may encounter prior to acting on the target tissue such as the liver and BBB. Various models have developed to scale drug dosages from human organs to OoC platforms, but further analysis is needed to propel BoC models into widescale use for preclinical drug development.[231]

While PDMS is by far the most widely used material for the production of tissue chips because of its ease-of-use and flexibility, PDMS has the key disadvantage that it non-specifically adsorbs small hydrophobic molecules,[243] which include many drugs. Nonabsorbent elastomeric polymers such as styrene-ethylene/butylene-styrene polyurethane elastomers are developed to solve this problem.[244] While several materials, including PMMA, COC, and PEGDA, have been explored as alternatives to PDMS, each of these materials has its own downsides and none is ideal,[47, 169] and new materials need to be explored.[245] In compartmentalized devices, inert thermoplastic polymers such as polycarbonate, polystyrene, polyetheramide, polysulfone, PMMA, and COC are used to fabricate the porous membrane.[246] Another group of promising materials are 3D-printed ones, however they are often nontransparent and may release toxic compound that affect the experiment.[36]

For cellular support and enhanced attachment and function, natural ECM biomaterials such as collagen, hyaluronic acid, and gelatin and also synthetic matrices such as polyethylene glycol

and polylactide have been employed.[246] However, each one of these has its own advantages and limitations. Natural hydrogels are more biocompatible, on the other hand, the properties of synthetic hydrogels are more tunable. Matrix architecture, chemical composition, and mechanical strength can easily be controlled in synthetic hydrogels. Besides Matrigel, another engineered material called gelatin methacryloyl (GelMA) has been proven effective as to provide ECM support for cells.[247] Organ-specific decellularized matrices have also proved to act as effective ECMs.[246]

Integration of microfluidics with organoids and 3D bioprinting is expected to evolve more in the future, with each approach bringing its own advantages, and combined technology can solve several problems. By using 3D bioprinting, precise patterning of cells, ECMs, and other biomaterials as well complex designs for OoCs can be achieved. In addition, to mimic dynamic interaction and compatibility between different parts of OoCs, tissue-specific bioinks have been developed.[36] Sensors can also be printed into BoC platforms for data acquisition. Therefore, 3D printing and 3D bioprinting are promising technologies capable of taking BoC models to the next generation. Brain organoids are excellent candidate models to study CNS; and combined with microfluidics in OoCs, their oxygen supply and nutrient/waste exchange can be improved.[248] Hence, formation of necrotic region and apoptotic cell death in organoids will be reduced significantly. In brain organoids, diversity, maturity, and consistency are the main concerns which can be improved using BoCs. Similarly, improvements can be made to move towards fully automated biomanufacturing processes for BoC devices, which newer technologies such as 3D bioprinting will likely facilitate.[36, 249]

Generally, it will benefit future OoC systems to increase the numbers and types of integrated sensors; for example, to detect synaptic transmission in various device compartments.[250] Overall, much room for development remains and the next generation of BoC models are

expected to be achieved by leveraging recent advances in materials science, biofabrication, and sensor technology.[251]

Functional inputs and outputs of any BoC or MoC system will require physiological validation through animal studies and clinical data. Such validation will confirm what type of knowledge can be gained from a particular chip and whether it can be used as a preclinical model, potentially reducing the numbers of animals needed for future studies *in vivo* validation will also help to standardize BoC structures, functional outcomes, and testing procedures. The ultimate goal of MoCs is building a human-on-a-chip as an advanced predictive tool for drug development.[252] In the field of personalized medicine, constructing patient-on-a-chip is envisioned by combining iPSC technology and MoC systems.[253] As a result, personalized drug testing and disease modeling will be feasible.

Standard validation and experimental procedures will ensure that results obtained from different researchers can be compared and facilitate adoption of a BoC model as a reproducible platform for drug development in future. Quality control measures for individual BoCs will be particularly important for use in personalized medicine. While the use of iPSC-derived cells in OoC models has become more common, they remain limited.[218, 254] Cells derived from iPSCs can be highly variable between patients and cell lots from a single patient. Thus, robust characterization and validation is crucial for patient-tailored models.

In moving towards high-throughput, complex MoC systems, researchers will obtain large data sets to work with that likely will benefit from applications of machine learning and artificial intelligence; for example, to identify a particular functional or genetic feature common across patients with a particular disease.[255] With the aid of machine learning algorithms, gathered relevant and irrelevant information of high-throughput BoCs and MoCs can be separated,

which would help improving reproducibility and standardization. Artificial intelligence can also be used to control and modify various parameters of several experiments in an automatic and dynamic manner. This will enhance the use of BoCs and MoCs in drug discovery and development.

Multidisciplinary teams will be required to achieve the goals described above and create the next generation of BoC platforms. There is need to involve biomaterials scientists, biologists, biochemists, statisticians, electrical and computer engineers, pathologists, pharmacologists, and clinicians. In addition, early involvement regulatory bodies and funding agencies will help to foster such collaborations, bring together large teams, and identify areas where knowledge is missing and on which funding should be focused. Ultimately, we expect these large-scale efforts will be reflected in the development of BoC-based platforms as invaluable tools for investigations of brain pathologies, preclinical drug development, and personalized medicine.

9. Conclusion

Leveraging recent advances in the fields of biomaterials, microfabrication, microfluidics, and stem cell biomanufacturing, it is becoming possible to develop BoC platforms that can recapitulate key functions and complexity of various brain regions. These platforms are expected to greatly facilitate to study normal brain development and physiology, uncover mechanisms underlying various pathologies, and develop new and effective therapeutics. To date, BoC systems have been developed to model different tissue components of the brain, including region-specific tissues such as cortico-striatal networks and the BBB, both in normal and pathophysiological conditions. Despite immense promise, several challenges remain, including addressing scale-up to best model human tissues, establishing best practices for quality control and functional validation, and building complexity through dynamic, MoC

systems. Furthermore, adoption of advanced biofabrication techniques, automation hardware, and data analysis pipelines will be needed to create truly BoCs compatible with truly high-throughput assays, such as therapeutic compound screening. Integration of cost-effective sensors that can measure specific BoC functions, and changes in these functions in response to perturbation, will similarly be necessary for high-throughput applications. Finally, while early BoCs have relied on rodent sources or human immortalized cell lines, a future focus on iPSC-derived cells is expected to lead to development of BoCs that are more physiologically accurate and patient-specific.

Acknowledgements

The authors acknowledge funding from the National Institutes of Health (1UG3TR003148-01).

Table 1. Summary of materials used in the fabrication of brain-on-a-chip, showing their advantages and disadvantages. For chip fabrication, polydimethylsiloxane (PDMS), polymethylmethacrylate (PMMA), cyclic olefin copolymer (COC), polycarbonate (PC), polystyrene, and tetrafluoroethylene propylene (TFEP) are the most commonly used materials. Natural hydrogels such as Matrigel, gelatin methacryloyl (GelMA), collagen, and hyaluronic acid as well as synthetic hydrogels such as polylactic acid and polyethylene glycol are used to provide extracellular (ECM) like substrate for enhancing cell function.

Role	Material	Advantages	Disadvantages
Chip material	PDMS	• Biocompatibility • Gas permeability • Low cost • Optical transparency	• High hydrophobic molecule adsorption • Media evaporation
	PMMA	• Biocompatibility • Gas permeability • Low cost • Optical transparency • Low hydrophobicity • Ease of fabrication	• Low O_2 diffusivity • Low resistance to certain solvents
	COC	• Biocompatibility • Low cost • Ease of fabrication	• High hydrophobic molecule adsorption • Low O_2 diffusivity • Brittleness
	PC	• Biocompatibility • Gas permeability • Low cost • Optical transparency • High impact resistance • Good machining properties	• Low resistance to certain solvents • Relatively high intrinsic fluorescence
	Polystyrene	• Biocompatibility • Low hydrophobic molecule adsorption	• Expensive equipment for fabrication • Microchannel collapsing
	TEEP	• Biocompatibility • Low hydrophobic molecule adsorption	• Expensive equipment for fabrication
ECM substrate	Matrigel	• Biocompatibility • Bioactivity	• High batch-to-batch variability • Tumor originality • Uncontrolled quantities of growth factors
	GelMA	• Biocompatibility • Biodegradability • High reproducibility • Tailorable mechanical properties •	• Fast degradation rate • Poor mechanical properties
	Collagen	• Biocompatibility • Mechanical strength • Biodegradability	• High cost • Low reproducibility

		• Cell adhesion regulation • Cell migration support	
	Hyaluronic acid	• Hydrophilicity • Biodegradability • High compressive force resistance • Hydration and swelling • No immunogenicity • No inflammation	• Poor mechanical properties
	Polylactide	• Biodegradability • Simple processability • Adjustable chemical and mechanical properties	• Hydrophobicity • Uncontrolled drug release pattern
	Polyethylene glycol	• Hydrophilicity • Biodegradability • Controlled gelation response • Adjustable chemical and mechanical properties	• Low drug loading capacity • Sensitive to pH • Low cell proliferation and adhesion

Table 2. Summary of brain on chip studies showing type of cells used. These included cell lines such as hippocampal neurons from a tdTomato-expressing mouse line, human neuroepithelial stem cell line, murine N9 microglia cell line, mouse microglial cell line BV-2, human brain endothelial cell line (hCMEC), b.End3 endothelial cell line, C8D1A astrocyte cell line, mouse pericyte cell line, TY10 human BMEC line, human brain pericyte cell line (hBPCT), human astrocyte cell line hAst, BC1 and iPS12 cell lines from healthy human, KW01 cell line from patient with multiple sclerosis, AD6 cell line from patient with AD, hCMEC/D3 cell line, rat brain endothelial cell line RBE4, rat brain astrocyte cell line CTX-TNA2, and murine metastatic breast cancer cell line Met-1, primary cells [such as primary human dorsal root ganglion neurons (hDRGNs), primary rat dorsal root ganglion neurons (rDRGNs), hippocampal cells derived from embryonic mice (EM-HCC), Hippocampal cells from embryonic rat (ER-HCC), cortical neurons from mouse embryos (mECNs), cortical neurons from rat embryos (rECNs)] and stem cell [iPSC, such as human iPSC-derived neural stem cells (iPSC-NSCs), Human iPSC-derived OPCs (iPSC-OPCs), iPSC-derived mature neurons (iPSC-Ns) and ESCs such as Human embryonic stem cell line (hESCs), Mouse embryonic stem cells (mESCs), ESC derived such as], mouse, rat or human. PDMS was the material used for the fabrication of the chips in most of studies. In addition, materials such as polystyrene [17] or silicon-parylene hybrid [256] were used to build Compartmentalized (COMP) chips. The culture in chips extended from less than one day [142, 143], to 55 days.[257]

Brain-on-a-chip	Cell type	Chip material	Chip design	Integrated sensors/ electrodes	Culture duration	Ref.
Neuron-based	EM-HCC	PDMS	16×64 array of gradient chambers	-	34 hours	[90]
	hDRGNs	Polystyrene	Well	Microelectrode array	23 days	[17]
	rECNs	PDMS	COMP with presynaptic, postsynaptic, and synaptic chambers	Microelectrode array	14 days	[18]
	ER-HCC, glial cells from rat brain	PDMS	Vertically layered	-	20 days	[95]
	iPSC-NSCs, iPSC-Ns, iPSC-derived astrocytes	OrganoPlate (glass and hydrophilic transparent	Ninety-six parallel chips on a 384 well-plate with gel and medium microchannels separated by phase-guides	-	7 days	[97]

		polymer)				
	mECNs	PDMS	COMP with straight connecting microchannels intersected perpendicularly by an axotomy channels	-	7 days	[134]
	Human neuroepithelial stem cell lines from a healthy donor and a patient with PD	Pelican	Sterile automated enclosure with 2-lane OrganoPlate	-	24 days	[156]
Oligodendrocyte-based	mESCs	PDMS	Open COMP with connecting microgrooves	-	2 weeks	[32]
	rDRGNs, OPCs from P0-P2 rat brain	PDMS	Open COMP with connecting microtunnels	-	39 days	[20]
	Neurons from E16 embryonic Sprague-Dawley rat forebrain, Oligodendrocytes and astrocytes from P0-P2 Sprague-Dawley rat cerebral hemispheres	PDMS	Multi- COMP with one central and six lateral chambers connected by radial microchannels	-	29 days	[33]
	Cortical OPCs from P2-P4 Sprague-Dawley rat, dorsal root ganglion neurons from P4 Sprague-Dawley rat	PDMS	COMP with connecting microchannels	Microelectrode array	12 days	[102]
	Dorsal root ganglion neurons from E15 embryonic Sprague-Dawley rat or E13 embryonic ICR mouse, OPCs from P1 mouse brain	PDMS	COMP with connecting microchannels	Electrodes	24 days	[103]
	Dorsal root ganglion neurons from E13 embryonic ICR mouse, OPCs from P1 mouse brain	Carbon black-containing PDMS	COMP with connecting microchannels	Blue LED array	24 days	[104]
Astrocyte-based	Cortical neurons from E18 embryonic Sprague-Dawley rat cortical lobes, cerebral cortical astrocytes from P0-P2 Sprague-Dawley rat	PDMS	COMP with connecting microvessels	-	15 days	[21]
	mECNs, astrocytes from P1-P2 OF1 mouse cortical brain region	PDMS	COMP with connecting microchannels	-	4 weeks	[166]
	Astrocytes from adult Sprague-Dawley rat brain	PDMS	Cell culture chamber	High speed pressure servo	5 days	[145, 146]
	Mouse astrocytes	Not reported	Cell culture chamber	Electrical discharge system containing two electrodes placed in the middle of culture chamber	Less than a day	[142]
	Mouse astrocytes	Not reported	Cell culture chamber with an electrical discharge system containing two electrodes	-	Less than a	[143]

			placed in the middle of the chamber with aperture above the electrodes		day	
Microglia-based	Primary microglial cells from 1-2-day-old rat and mouse, murine N9 microglia cell line	PDMS	Micro-structured pillar-shaped and line-grating geometry, COMP with connecting microchannels	-	1 day	[111]
	Hippocampal neurons from E17 embryonic pups, microglial cells from postnatal rat pups	PDMS	Multi- COMP circular with connecting microchannels	-	14 days	[149]
	ER-HCC, microglial cells from P3-P6 Sprague-Dawley rat or mouse pup's cortex	PDMS bonded to poly-D-lysine-patterned glass	COMP with connecting microchannels	-	7 days	[22]
	Human microglial cells from fetal brain tissue	PDMS	COMP circular with radial connecting microchannels	–	9 days	[153]
	Mouse microglial cell line BV-2, C6 cells from rat brain glioma	PDMS	COMP with connecting microchannels coupled with hollow-well (2D) and concave array (3D) micro-patterned chips	-	2 days	[170]
	Adult male Sprague-Dawley rat	Silicon-parylene hybrid	Drug delivery microchannels	Open architecture electrode array	4 weeks	[256]
Synapse	Hippocampal cells from 1-2-day-old Sprague-Dawley rat pups	PDMS	COMP with connecting microchannels	-	17 days	[57]
	Primary rat cortical neurons and astrocytes	PDMS	Three-nodal COMP with connecting microchannels	Microelectrode array	27 days	[58]
	Hippocampal neurons from P0-P2 rat	PDMS	COMP with synaptic, presynaptic and postsynaptic chambers connected by microgrooves	-	42 days	[68]
	rECNs	PDMS	COMP with a central and two lateral chambers connected by microgrooves	-	28 days	[93]
	mECNs and EM-HCC	PDMS	COMP with connecting funnel-shaped microchannels	-	3 weeks	[19]
	ER-HCC	PDMS	COMP with connecting microgrooves	-	17 days	[258]
	mECNs and striatal neurons from E15.5 embryonic wild type (C57/BL6J or CD1 background), and $Hdh^{CAG140/+}$ or $Hdh^{Q111/+}$ mouse	PDMS	COMP with cortical, striatal, and synaptic chambers connected by microchannels	-	18 days	[163]
	mECNs and striatal cells from E14 Swiss mouse embryos	PDMS	COMP with asymmetrical connecting microchannels	-	15 days	[164]
	iPSCs from human primary lymphocytes	PDMS	Multi- COMP with one open central and four lateral chambers connected by radial microchannels	-	6 weeks	[94]

	hESCs	PDMS	Open and closed COMP with connecting microgrooves	-	55 days	[257]
BBB	Human brain endothelial cell line hCMEC/ D3	PDMS	Perpendicularly crossing top and bottom microchannels separated by a polycarbonate membrane at their intersection	Electrodes for TEER measurement	7 days	[50]
	b.End3 endothelial and C8D1A astrocyte cell lines	PDMS	Perpendicularly crossing top and bottom microchannels separated by a polycarbonate membrane at their intersection	Electrodes for TEER measurement	7 days	[73]
	b.End3 endothelial cell line	PDMS	Perpendicularly crossing top and bottom microchannels separated by a polycarbonate membrane at their intersection	Electrodes for TEER measurement	4 days	[259]
	b.End3 endothelial and C8D1A astrocyte cell lines	PDMS	Perpendicularly crossing top and bottom microchannels separated by a polycarbonate membrane at their intersection	Electrodes for TEER measurement	7 days	[118]
	b.End3 endothelial cell line	PDMS	S-shaped crossing top and bottom microchannels separated by a topographically patterned polycarbonate membrane with 1 μm wide pits	Electrodes for TEER measurement	6 days	[207]
	BMECs and astrocytes from 1–2-day-old C57BL/6 mouse pups	PDMS	An array of 4×4 perpendicularly crossing top and bottom microchannels separated by polycarbonate membranes at their intersections, creating 16 BBB sites	Electrodes for TEER measurement	4 days	[119]
	Br-Bend5 murine endothelial brain cells	PDMS	Perpendicularly crossing top and bottom microchannels separated by a polycarbonate membrane at their intersection, integrated with guiding channels for electrodes	Electrodes for TEER measurement	5 days	[52]
	b.End3 endothelial and C8D1A astrocyte cell lines	PDMS	Top and bottom microchannels separated by a polytetrafluoroethylene or polyester membrane at their intersection μm	-	14 days	[120]
	b.End3 endothelial, C8D1A astrocyte, and mouse pericyte cell lines	PDMS	Top and bottom microchannels separated by a polyester membrane at their intersection	Electrodes for TEER measurement	21 days	[121]
	$CD34^+$ cells from human umbilical cord blood, Human $CD4^+CD45RO^+$ T helper 1 (Th1) cells, pericyte-conditioned medium	PDMS	Perpendicularly crossing top and bottom microchannels separated by a silicon nitride membrane at their intersection	-	6 days	[122]
	iPSC-ECs, pericytes and astrocytes from human brain	PDMS	A central microchannels for vascularization and two lateral microchannels for generating iPSC-ECs monolayers, all connected by	-	7 days	[260]

			arrays of microposts			
	Human BMEC line TY10, human brain pericyte cell line hBPCT, human astrocyte cell line hAst	OrganoPlate (glass and hydrophilic transparent polymer)	Ninety-six or 40 parallel chips on a 384 well-plate with two-lane or three-lane microchannels, respectively, separated by phase-guides	-	9 days	[210]
	Human brain endothelial cell line hCMEC/ D3, human astrocytes	PDMS	Two separate microchannels with a common hydrogel (collagen-Matrigel-hyaluronan) reservoir and cylindrical voids as lumens	Electrodes for TEER measurement	4 days	[125]
	b.End3 endothelial cell line, U87 glioblastoma cells	IP- Dip-in Laser Lithography (IP-DiLL) photoresin	Porous tubular structures with average diameters of 10 µm and circular 1 µm-diameter pores patterned on their surfaces	Electrodes for TEER measurement	5 days	[126]
	dhBMECs (BC1 and iPS12 cell lines from healthy human, KW01 cell line from a patient with multiple sclerosis, and AD6 cell line from a patient with AD)	PDMS	A cylindrical microchannel with the diameter of 150 µm, constructed within collagen hydrogel	Electrodes for TEER measurement	6 days	[127]
	hCMEC/D3 cell line, ReNcell VM human NPCs with familial AD mutations (ReN-AD)	PDMS	Side by side microchannels including a middle barrier microchannel and lateral ReNcell and BBB chambers separated by arrays of microposts	-	16 days	[155]
	HUVECs, ACM	PDMS	Side by side microchannels separated by an array of microholes with an angle of 45°	-	5 days	[208]
	Rat brain endothelial cell line RBE4, ACM	PDMS	Side by side apical and basolateral microchannels separated by an array of micropillars with 3 µm gaps	-	4 days	[74]
	HUVECs, rat brain astrocyte cell line CTX-TNA2, murine metastatic breast cancer cell line Met-1	PDMS	Side by side apical and basolateral microchannels separated by an array of micropillars with 3 µm gaps	-	4 days	[171]
	Human brain endothelial cell line hCMEC/ D3, primary human astrocytes	PDMS	Side by side apical and basolateral microchannels separated by an array of micropillars with 3 µm gaps	-	4 days	[172]
	HUVECs, human brain endothelial cell line hCMEC/ D3, rECNs, astrocytes from P0-P2 brain cortices of pups	PDMS	Four side by side microchannels separated by trapezoidal posts	-	14 days	[124]
	HUVECs, rECNs, astrocytes	PDMS	Three side by side microchannels including a central VNC and two lateral VC and NC separated by arrays of microposts	-	10 days	[123]

Table 3. Summary of multi-organ-on-a-chip (MoC)-based studies which involved brain-on-a-chip (BoC) as one component to study various physiological events or to develop disease models such as cancer metastasis or screen drugs. These include blood-brain barrier (BBB)-on-a-chip-based studies and other MoC components combined with BoC component. Cell types used in the BoC units of these MoCs extend from primary cell (such as primary human brain microvascular endothelial cells (hBMVECs), primary human astrocytes and pericytes), to cell lines (such as hNT2 cell line, neural progenitor cells derived from human H1 ES line, and astrocyte cell line HA-1800), and stem cells (such as human fetal neural progenitor cells (hNPCs), human iPSC-derived cortical glutamatergic neurons, iPSC-derived astrocytes and neurons (glutamatergic, GABAergic, and dopaminergic)).

Linked organ(s)	Brain component	Goal	Ref.
BBB	Neuron-based BoC	Evaluating the integrity of BBB via ascorbate and glutamate exposure	[236]
BBB	Neuron-astrocyte brain parenchyma on-a-chip	Building BBB by interaction of hBMVECs and brain parenchyma (created by human pluripotent cell differentiation), evaluating the role of brain parenchyma on chemotactic behavior of hNPCs by CXCL12 and SLIT2-N stimulation	[237]
BBB	Neuron-astrocyte BoC	Intravascular injection of Meth and identifying metabolic coupling between BBB and brain units	[16]
Liver	Neurospheres	Metabolic profiling of 2,5-hexanedione	[238]
Liver, gut and kidney	BBB	Metabolic profiling and evaluating BBB permeability of terfenadine, TMA, and vitamin D3	[228]
Liver, gut, pancreas, lung, heart and endometrium	Neuron-astrocyte BoC	Metabolic profiling of talcapone	[239]
Liver/immune, gut/immune, pancreas, lung, heart and endometrium	Neuron-astrocyte BoC	Maintaining long-term continuous interaction between multiple microtissues and metabolic profiling of diclofenac	[240]
Liver/immune, gut/immune, pancreas, lung, heart, endometrium, kidney, skin, and	Neuron-astrocyte BoC	Maintaining long-term continuous interaction between multiple microtissues and metabolic profiling of diclofenac	[240]

skeletal muscle			
Lung cancer	Astrocyte-based BoC	Monitoring metastasis of lung cancer cells to the brain and their invasion effect on neural cells	[175]
Lung cancer	BBB	Evaluating expressions of MMP-2, MMP-9, and AKR1B10 and characterizing the migratory capability of metastatic cancer cells to cross BBB	[176]

References

[1] K. G. Yiannopoulou, S. G. Papageorgiou, Therapeutic Advances in Neurological Disorders 2012, 6, 19; J. Wang, W.-W. Hu, Z. Jiang, M.-J. Feng, World journal of stem cells 2020, 12, 323; A. Nasrolahi, F. Safari, M. Farhoudi, A. Khosravi, F. Farajdokht, S. Bastaminejad, S. S. Shotorbani, J. Mahmoudi, Reviews in the Neurosciences 2019, 30, 709; M. Kiaei, Basic and clinical neuroscience 2013, 4, 3.

[2] World Health Organization, 2006.

[3] W. He, D. Goodkind, P. R. Kowal, 2016.

[4] K. Gammon, Nature 2014, 515, 299.

[5] D. G. Munoz, G. R. Ganapathy, M. Eliasziw, V. Hachinski, Archives of Neurology 2000, 57, 85; F. Christidi, R. Migliaccio, H. Santamaría-García, G. Santangelo, F. Trojsi, Behavioural neurology 2018; C. Strafella, V. Caputo, M. R. Galota, S. Zampatti, G. Marella, S. Mauriello, R. Cascella, E. Giardina, Frontiers in neurology 2018, 9, 701.

[6] E. Grandfils, M. Metzger, 2019.

[7] D. Antoni, H. Burckel, E. Josset, G. Noel, International journal of molecular sciences 2015, 16, 5517.

[8] A. Fatehullah, S. H. Tan, N. Barker, Nature cell biology 2016, 18, 246.

[9] H. Shen, Proceedings of the National Academy of Sciences 2018, 115, 3507.

[10] A. C. Rios, H. Clevers, Nature methods 2018, 15, 24.

[11] G. A. Van Norman, JACC: Basic to Translational Science 2019, 4, 845.

[12] A. Gołaszewska, W. Bik, T. Motyl, A. Orzechowski, International journal of molecular sciences 2019, 20, 1664; T. M. Dawson, T. E. Golde, C. Lagier-Tourenne, Nature neuroscience 2018, 21, 1370; S. Eaton, T. Wishart, Mammalian Genome 2017, 28, 324.

[13] E. Karzbrun, A. Kshirsagar, S. R. Cohen, J. H. Hanna, O. Reiner, Nature physics 2018, 14, 515; R. F. Mandelbaum, 2018.

[14] J. Park, B. K. Lee, G. S. Jeong, J. K. Hyun, C. J. Lee, S.-H. Lee, Lab on a Chip 2015, 15, 141.

[15] Y. I. Wang, H. E. Abaci, M. L. Shuler, Biotechnology and bioengineering 2017, 114, 184.

[16] B. M. Maoz, A. Herland, E. A. FitzGerald, T. Grevesse, C. Vidoudez, A. R. Pacheco, S. P. Sheehy, T.-E. Park, S. Dauth, R. Mannix, Nature biotechnology 2018, 36, 865.

[17] H. Enright, S. Felix, N. O. Fischer, E. Mukerjee, D. Soscia, M. Mcnerney, K. Kulp, J. Zhang, G. Page, P. Miller, Analyst 2016, 141, 5346.

[18] E. Moutaux, B. Charlot, A. Genoux, F. Saudou, M. Cazorla, Lab on a Chip 2018, 18, 3425.

[19] B. Deleglise, S. Magnifico, E. Duplus, P. Vaur, V. Soubeyre, M. Belle, M. Vignes, J.-L. Viovy, E. Jacotot, J.-M. Peyrin, Acta neuropathologica communications 2014, 2, 145.

[20] M. Ristola, L. Sukki, M. M. Azevedo, A. I. Seixas, J. B. Relvas, S. Narkilahti, P. Kallio, Journal of Micromechanics and Microengineering 2019, 29, 065009.

[21] F. Cavaliere, L. Cerf, B. Dehay, P. Ramos-Gonzalez, F. De Giorgi, M. Bourdenx, A. Bessede, J. A. Obeso, C. Matute, F. Ichas, Neurobiology of disease 2017, 103, 101.

[22] L. Rajbhandari, M. A. Tegenge, S. Shrestha, N. Ganesh Kumar, A. Malik, A. Mithal, S. Hosmane, A. Venkatesan, Glia 2014, 62, 1982.

[23] N. Ashammakhi, E. Elkhammas, A. Hasan, Journal of Biomedical Materials Research Part B: Applied Biomaterials 2018; M. Rothbauer, J. M. Rosser, H. Zirath, P. Ertl, Current opinion in biotechnology 2019, 55, 81; C. Tian, Q. Tu, W. Liu, J. Wang, TrAC Trends in Analytical Chemistry 2019, 117, 146; S. A. Hacking, N. Ashammakhi, A. Khademhosseini, in *Biomaterials Science*, Elsevier, 2020, 661; Q. Wu, J. Liu, X. Wang, L. Feng, J. Wu, X. Zhu, W. Wen, X. Gong, BioMedical Engineering OnLine 2020, 19, 9.

[24] D. Huh, B. D. Matthews, A. Mammoto, M. Montoya-Zavala, H. Y. Hsin, D. E. Ingber, Science 2010, 328, 1662; D. Huh, Annals of the American Thoracic Society 2015, 12, S42.
[25] H. J. Kim, D. Huh, G. Hamilton, D. E. Ingber, Lab on a Chip 2012, 12, 2165; H. J. Kim, H. Li, J. J. Collins, D. E. Ingber, Proceedings of the National Academy of Sciences 2016, 113, E7.
[26] C. H. Beckwitt, A. M. Clark, S. Wheeler, D. L. Taylor, D. B. Stolz, L. Griffith, A. Wells, Experimental cell research 2018, 363, 15.
[27] N. Ashammakhi, K. Wesseling-Perry, A. Hasan, E. Elkhammas, Y. S. Zhang, Kidney International 2018, 94, 1073.
[28] A. P. Haring, H. Sontheimer, B. N. Johnson, Stem cell reviews and reports 2017, 13, 381; M. I. Teixeira, M. H. Amaral, P. C. Costa, C. M. Lopes, D. A. Lamprou, Pharmaceutics 2020, 12, 542.
[29] P. Ramamurthy, J. B. White, J. Y. Park, R. I. Hume, F. Ebisu, F. Mendez, S. Takayama, K. F. Barald, 2017, 7.
[30] R. Booth, H. Kim, 2014, 42, 2379.
[31] S. Y. Park, J. Park, S. H. Sim, M. G. Sung, K. S. Kim, 2011, 263.
[32] B. E. Kerman, H. J. Kim, K. Padmanabhan, A. Mei, S. Georges, M. S. Joens, J. A. Fitzpatrick, R. Jappelli, K. J. Chandross, P. August, Development 2015, 142, 2213.
[33] J. Park, H. Koito, J. Li, A. Han, Lab on a Chip 2012, 12, 3296.
[34] J. Park, I. Wetzel, I. Marriott, D. Dréau, C. D. Avanzo, D. Y. Kim, R. E. Tanzi, H. Cho, Nature Neuroscience 2018, 21.
[35] A. J. Keung, P. Asuri, S. Kumar, D. V. Schaffer, Integrative Biology 2012, 4, 1049.
[36] H.-G. Yi, H. Lee, D.-W. Cho, Bioengineering 2017, 4, 10.
[37] H. Lee, D. W. Cho, Lab on a chip 2016, 16, 2618.
[38] A. D. V. D. Meer, A. A. Poot, J. Feijen, I. Vermes, 2010, 1; H. S. Shin, H. J. Kim, S. J. Sim, N. L. Jeon, 2009, 9.
[39] M. C. LaPlaca, L. E. Thibault, Annals of biomedical engineering 1997, 25, 665.
[40] S. Fantini, A. Sassaroli, K. T. Tgavalekos, J. Kornbluth, Neurophotonics 2016, 3, 031411.
[41] A. M. B. David Attwell , Serge Charpak , Martin Lauritzen , Brian A. MacVicar, Eric A. Newman, Nature 2010, 468, 232; E. S. Thomas Brinker, John Morrison and Petra Klinge, FLUIDS AND BARRIERS OF THE CNS 2014; B. V.Zlokovic, Trends in Neurosciences 2005, 28, 202.
[42] B. Zahorodny-Burke, B. Nearingburg, A. L. Elias, Chemical Engineering Science 2011, 66, 6244.
[43] K. J. Regehr, M. Domenech, J. T. Koepsel, K. C. Carver, S. J. Ellison-zelski, W. L. Murphy, L. A. Schuler, T. Alarid, D. J. Beebe, 2009, 2132.
[44] A. Gokaltun, M. L. Yarmush, A. Asatekin, O. B. Usta, 2017, 5, 1.
[45] E. Ostuni, R. Kane, C. S. Chen, D. E. Ingber, G. M. Whitesides, 2004, 7811.
[46] Y. S. Heo, L. M. Cabrera, J. W. Song, N. Futai, Y.-c. Tung, G. D. Smith, S. Takayama, A. Arbor, 2007, 79, 1589.
[47] N. Ashammakhi, R. Nasiri, N. R. d. Barros, P. Tebon, J. Thakor, M. Goudie, A. Shamloo, M. G. Martin, A. Khademhosseini, Biomaterials 2020, 255, 120196; K. Ren, J. Zhou, H. Wu, Accounts of chemical research 2013, 46, 2396; J. B. Nielsen, R. L. Hanson, H. M. Almughamsi, C. Pang, T. R. Fish, A. T. Woolley, Analytical Chemistry 2019, 92, 150.
[48] E. Sano, C. Mori, N. Matsuoka, Y. Ozaki, K. Yagi, A. Wada, Micromachines 2019, 10.
[49] T. Kilic, F. Navaee, F. Stradolini, P. Renaud, S. Carrara, Microphysiological Systems; Vol 2 (September 2018): Microphysiological Systems 2018; J. H. Sung, Y. I. Wang, N. Narasimhan Sriram, M. Jackson, C. Long, J. J. Hickman, M. L. Shuler, Analytical Chemistry 2019, 91, 330.

[50] L. Griep, F. Wolbers, B. De Wagenaar, P. M. ter Braak, B. Weksler, I. A. Romero, P. Couraud, I. Vermes, A. D. van der Meer, A. van den Berg, Biomedical microdevices 2013, 15, 145.
[51] D. Coronado‐Velázquez, A. Betanzos, J. Serrano‐Luna, M. Shibayama, Journal of Eukaryotic Microbiology 2018, 65, 804.
[52] G. S. Ugolini, P. Occhetta, A. Saccani, F. Re, S. Krol, M. Rasponi, A. Redaelli, Journal of Micromechanics and Microengineering 2018, 28, 044001.
[53] H. Charkhkar, S. Meyyappan, E. Matveeva, J. R. Moll, D. G. McHail, N. Peixoto, R. O. Cliff, J. J. Pancrazio, Brain Research 2015, 1629, 1.
[54] A. Scott, K. Weir, C. Easton, W. Huynh, W. J. Moody, A. Folch, 2013, 527.
[55] T. M. Pearce, J. A. Wilson, S. G. Oakes, S.-y. Chiu, J. C. Williams, 2005, 97.
[56] J. N. Stirman, M. Brauner, A. Gottschalk, H. Lu, Journal of neuroscience methods 2010, 191, 90.
[57] G. Robertson, T. J. Bushell, M. Zagnoni, Integrative Biology 2014, 6, 636.
[58] R. van de Wijdeven, O. H. Ramstad, V. D. Valderhaug, P. Köllensperger, A. Sandvig, I. Sandvig, Ø. Halaas, Biosensors and Bioelectronics 2019, 140, 111329.
[59] T.-h. Kim, C.-h. Yea, S.-t. D. Chueng, P. T.-t. Yin, B. Conley, K. Dardir, Y. Pak, G. Y. Jung, J.-w. Choi, K.-b. Lee, 2015, 6356.
[60] Y. Yu, R. P. S. D. Campos, A. R. Wheeler, Microsystems & Nanoengineering 2019.
[61] R. M. Paredes, J. C. Etzler, L. T. Watts, W. Zheng, J. D. Lechleiter, Methods 2008, 46, 143.
[62] N. Chronis, M. Zimmer, C. I. Bargmann, Nature methods 2007, 4, 727.
[63] S. Okumoto, L. L. Looger, K. D. Micheva, R. J. Reimer, S. J. Smith, W. B. Frommer, Proceedings of the National Academy of Sciences of the United States of America 2005, 102, 8740.
[64] B. R. Smith, S. S. Gambhir, Chem Rev 2017, 117, 901.
[65] Y. Luo, E. H. Kim, C. A. Flask, H. A. Clark, ACS Nano 2018, 12, 5761.
[66] A. M. Taylor, M. Blurton-Jones, S. W. Rhee, D. H. Cribbs, C. W. Cotman, N. L. Jeon, Nature methods 2005, 2, 599.
[67] Y. Gao, J. Broussard, A. Haque, A. Revzin, T. Lin, Microsystems & nanoengineering 2016, 2, 1.
[68] A. M. Taylor, D. C. Dieterich, H. T. Ito, S. A. Kim, E. M. Schuman, Neuron 2010, 66, 57.
[69] J. A. Fantuzzo, L. D. Filippis, H. McGowan, N. Yang, Y.-h. Ng, A. Halikere, J.-j. Liu, R. P. Hart, M. Wernig, J. D. Zahn, Z. P. Pang, 2017, 5, 87.
[70] S. Y. Desai, M. Marroni, L. Cucullo, L. Krizanac-bengez, M. R. Mayberg, M. T. Hossain, G. G. Grant, D. Janigro, S. Y. Desai, M. Marroni, L. Cucullo, L. Krizanac, M. R. Mayberg, M. T. Hossain, G. G. Grant, D. Janigro, S. Y. Desai, M. Marroni, L. Cucullo, L. Krizanac-bengez, M. R. Mayberg, M. T. Hossain, G. G. Grant, 2002, 3329; A. G. Koutsiaris, S. V. Tachmitzi, N. Batis, M. G. Kotoula, C. H. Karabatsas, E. Tsironi, D. Z. Chatzoulis, Biorheology 2007, 44, 375; C. F. Dewey, Jr., S. R. Bussolari, M. A. Gimbrone, Jr., P. F. Davies, Journal of Biomechanical Engineering 1981, 103, 177.
[71] A. D. van der Meer, A. A. Poot, J. Feijen, I. Vermes, Biomicrofluidics 2010, 4, 11103.
[72] N. J. Abbott, L. Rönnbäck, E. Hansson, Nat Rev Neurosci 2006, 7, 41.
[73] R. Booth, H. Kim, Lab on a Chip 2012, 12, 1784.
[74] B. Prabhakarpandian, M.-C. Shen, J. B. Nichols, I. R. Mills, M. Sidoryk-Wegrzynowicz, M. Aschner, K. Pant, Lab on a Chip 2013, 13, 1093.
[75] Y. Wang, L. Wang, Y. Zhu, J. Qin, Lab on a chip 2018, 18, 851.
[76] X. Qian, Ha N. Nguyen, Mingxi M. Song, C. Hadiono, Sarah C. Ogden, C. Hammack, B. Yao, Gregory R. Hamersky, F. Jacob, C. Zhong, K.-j. Yoon, W. Jeang, L. Lin, Y. Li, J.

Thakor, Daniel A. Berg, C. Zhang, E. Kang, M. Chickering, D. Nauen, C.-Y. Ho, Z. Wen, Kimberly M. Christian, P.-Y. Shi, Brady J. Maher, H. Wu, P. Jin, H. Tang, H. Song, G.-l. Ming, Cell 2016, 165, 1238.
[77] J. Park, B. K. Lee, G. S. Jeong, J. K. Hyun, C. J. Lee, S. H. Lee, Lab Chip 2015, 15, 141.
[78] A.-N. Cho, Y. Jin, Y. An, J. Kim, Y. S. Choi, J. S. Lee, J. Kim, W.-Y. Choi, D.-J. Koo, W. Yu, G.-E. Chang, D.-Y. Kim, S.-H. Jo, J. Kim, S.-Y. Kim, Y.-G. Kim, J. Y. Kim, N. Choi, E. Cheong, Y.-J. Kim, H. S. Je, H.-C. Kang, S.-W. Cho, Nature Communications 2021, 12, 4730.
[79] A. GhavamiNejad, N. Ashammakhi, X. Wu, A. Khademhosseini, Small 2020.
[80] A. J. Engler, S. Sen, H. L. Sweeney, D. E. Discher, Cell 2006, 126, 677.
[81] A. Banerjee, M. Arha, S. Choudhary, R. S. Ashton, S. R. Bhatia, D. V. Schaffer, R. S. Kane, Biomaterials 2009, 30, 4695; L. A. Flanagan, Y. Ca, B. Marg, M. Oster, P. A. Janmey, 2002, 13, 2411; P. C. Georges, W. J. Miller, D. F. Meaney, E. S. Sawyer, P. A. Janmey, Biophysical Journal 2006, 90, 3012; S. K. Seidlits, Z. Z. Khaing, R. R. Petersen, J. D. Nickels, J. E. Vanscoy, J. B. Shear, C. E. Schmidt, Biomaterials 2010, 31, 3930.
[82] D. D. McKinnon, A. M. Kloxin, K. S. Anseth, Biomaterials Science 2013, 1, 460.
[83] M. J. Mahoney, K. S. Anseth, Biomaterials 2006, 27, 2265.
[84] K. Chwalek, M. D. Tang-schomer, F. G. Omenetto, D. L. Kaplan, Nature Protocols 2015.
[85] J. B. Nielsen, R. L. Hanson, H. M. Almughamsi, C. Pang, T. R. Fish, A. T. Woolley, Analytical Chemistry 2020, 92, 150.
[86] J.-P. Frimat, R. Luttge, Frontiers in bioengineering and biotechnology 2019, 7, 100.
[87] Z. Xu, P. Fang, B. Xu, Y. Lu, J. Xiong, F. Gao, X. Wang, J. Fan, P. Shi, Nat Commun 2018, 9, 4745.
[88] J. S. Ji Hyeon Kim, Hyun-Jung Kim, Biomoleculess & Therapeutics 2018, 380; E. v. V. Chandrasekhar R. Kothapalli, Sarra de Valence, Seok Chung, Ioannis K. Zervantonakis, Frank B. Gertlerb, Roger D. Kamm, Lab on a Chip 2011, 497.
[89] D. Kilinc, A. Blasiak, G. U. Lee, Front Cell Neurosci 2015, 9, 282.
[90] N. Bhattacharjee, A. Folch, Microsystems & Nanoengineering 2017, 3, 17003.
[91] L. J. Millet, M. U. Gillette, Trends in neurosciences 2012, 35, 752.
[92] C. Forró, G. Thompson-Steckel, S. Weaver, S. Weydert, S. Ihle, H. Dermutz, M. J. Aebersold, R. Pilz, L. Demkó, J. Vörös, Biosensors and Bioelectronics 2018, 122, 75.
[93] A. Coquinco, L. Kojic, W. Wen, Y. T. Wang, N. L. Jeon, A. J. Milnerwood, M. Cynader, Molecular and Cellular Neuroscience 2014, 60, 43.
[94] J. A. Fantuzzo, L. De Filippis, H. McGowan, N. Yang, Y.-H. Ng, A. Halikere, J.-J. Liu, R. P. Hart, M. Wernig, J. D. Zahn, Technology 2017, 5, 87.
[95] M. Shi, D. Majumdar, Y. Gao, B. M. Brewer, C. R. Goodwin, J. A. McLean, D. Li, D. J. Webb, Lab on a Chip 2013, 13, 3008.
[96] Mimetas.
[97] N. R. Wevers, R. Van Vught, K. J. Wilschut, A. Nicolas, C. Chiang, H. L. Lanz, S. J. Trietsch, J. Joore, P. Vulto, Scientific reports 2016, 6, 38856.
[98] S. Jäkel, L. Dimou, Frontiers in Cellular Neuroscience 2017, 11.
[99] P. Rea, in *Essential Clinically Applied Anatomy of the Peripheral Nervous System in the Head and Neck*, (Ed: P. Rea), Academic Press, 2016, 1.
[100] K.-A. Nave, H. B. Werner, Annual review of cell and developmental biology 2014, 30, 503.
[101] M. Simons, K.-A. Nave, Cold Spring Harbor perspectives in biology 2016, 8, a020479.
[102] I. H. Yang, D. Gary, M. Malone, S. Dria, T. Houdayer, V. Belegu, J. W. Mcdonald, N. Thakor, Neuromolecular medicine 2012, 14, 112.

[103] H. U. Lee, A. Blasiak, D. R. Agrawal, D. T. B. Loong, N. V. Thakor, A. H. All, J. S. Ho, I. H. Yang, PloS one 2017, 12, e0179642.
[104] H. U. Lee, S. Nag, A. Blasiak, Y. Jin, N. Thakor, I. H. Yang, ACS chemical neuroscience 2016, 7, 1317.
[105] F. Aloisi, Glia 2001, 36, 165.
[106] A. Shemer, D. Erny, S. Jung, M. Prinz, Trends in immunology 2015, 36, 614.
[107] H. Kettenmann, U.-K. Hanisch, M. Noda, A. Verkhratsky, Physiological reviews 2011, 91, 461; Z. Chen, B. D. Trapp, Journal of Neurochemistry 2016, 136, 10.
[108] V. H. Perry, J. A. Nicoll, C. Holmes, Nature Reviews Neurology 2010, 6, 193; A. Lourbopoulos, A. Ertürk, F. Hellal, Frontiers in cellular neuroscience 2015, 9, 54.
[109] S. A. Wolf, H. Boddeke, H. Kettenmann, Annual review of physiology 2017, 79, 619.
[110] R. M. Ransohoff, J. El Khoury, Cold Spring Harbor perspectives in biology 2016, 8, a020560.
[111] S. Amadio, A. De Ninno, C. Montilli, L. Businaro, A. Gerardino, C. Volonté, BMC neuroscience 2013, 14, 121.
[112] C. Volonté, A. De Ninno, S. Amadio, in *Neurotrophic Factors*, Springer, 2018, 139.
[113] B. V. Zlokovic, Neuron 2008, 57, 178; K. Schoknecht, H. Shalev, Epilepsia 2012, 53, 7.
[114] M. W. van Der Helm, A. D. Van Der Meer, J. C. Eijkel, A. van den Berg, L. I. Segerink, Tissue barriers 2016, 4, e1142493; R. Daneman, Annals of Neurology 2012, 648; W. L. John F Deeken, Clinical Cancer Research 2007, 1663; A. A. Daniel Knowland, Kohei J Sekiguchi, Martin Hsu, Sarah E Lutz, John Perrino, Gary K Steinberg, Ben A Barres, Axel Nimmerjahn, Dritan Agalliu, neuron 2014, 603.
[115] A. Minagar, J. S. Alexander, Multiple Sclerosis Journal 2003, 9, 540.
[116] A. Oddo, B. Peng, Z. Tong, Y. Wei, W. Y. Tong, H. Thissen, N. H. Voelcker, Trends in biotechnology 2019.
[117] C. Crone, S. Olesen, Brain research 1982, 241, 49.
[118] R. H. Booth, H. Kim, "A parallel array microfluidic blood-brain barrier model for high-throughput quantitation of shear stress effects", presented at *16th International Conference on Miniaturized Systems for Chemistry and Life Sciences*, 2012.
[119] S. Jeong, S. Kim, J. Buonocore, J. Park, C. J. Welsh, J. Li, A. Han, IEEE Transactions on Biomedical Engineering 2017, 65, 431.
[120] K. L. Sellgren, B. T. Hawkins, S. Grego, Biomicrofluidics 2015, 9, 061102.
[121] J. D. Wang, E.-S. Khafagy, K. Khanafer, S. Takayama, M. E. ElSayed, Molecular pharmaceutics 2016, 13, 895.
[122] A. Mossu, M. Rosito, T. Khire, H. Li Chung, H. Nishihara, I. Gruber, E. Luke, L. Dehouck, F. Sallusto, F. Gosselet, Journal of Cerebral Blood Flow & Metabolism 2019, 39, 395.
[123] S. Bang, S.-R. Lee, J. Ko, K. Son, D. Tahk, J. Ahn, C. Im, N. L. Jeon, Scientific reports 2017, 7, 8083.
[124] G. Adriani, D. Ma, A. Pavesi, R. D. Kamm, E. L. Goh, Lab on a Chip 2017, 17, 448.
[125] P. P. Partyka, G. A. Godsey, J. R. Galie, M. C. Kosciuk, N. K. Acharya, R. G. Nagele, P. A. Galie, Biomaterials 2017, 115, 30.
[126] A. Marino, O. Tricinci, M. Battaglini, C. Filippeschi, V. Mattoli, E. Sinibaldi, G. Ciofani, Small 2018, 14, 1702959.
[127] R. M. Linville, J. G. DeStefano, M. B. Sklar, Z. Xu, A. M. Farrell, M. I. Bogorad, C. Chu, P. Walczak, L. Cheng, V. Mahairaki, Biomaterials 2019, 190, 24.
[128] P. J. Robinson, S. I. Rapoport, American Journal of Physiology-Regulatory, Integrative and Comparative Physiology 1987, 253, R459.
[129] T. Araki, H. Yokota, A. Morita, Neurologia medico-chirurgica 2016, ra. 2016.

[130] T. M. Marshall, K. L. Colvin, R. Nevin, J. Macrellis, G. P. Dardia, Alternative Therapies in Health & Medicine 2019, 25.
[131] R. A. Armstrong, P. L. Lantos, N. J. Cairns, Neuropathology 2008, 28, 351.
[132] J. Zhang, Z. Tan, N. D. Tran, Brain Res 2000, 877, 134.
[133] Y. Ikeda, D. M. Long, Neurosurgery 1990, 27, 1.
[134] Z. Tong, M. Segura-Feliu, O. Seira, A. Homs-Corbera, J. A. Del Río, J. Samitier, RSC Advances 2015, 5, 73457.
[135] J.-P. Dollé, B. Morrison, 3rd, R. S. Schloss, M. L. Yarmush, Technology (Singap World Sci) 2014, 2, 106.
[136] T. Nagendran, A. M. Taylor, Frontiers in Cellular Neuroscience 2019, 13.
[137] R. A. Stein, T. L. Strickland, Archives of Clinical Neuropsychology 1998, 13, 259.
[138] S. Dauth, B. M. Maoz, S. P. Sheehy, M. A. Hemphill, T. Murty, M. K. Macedonia, A. M. Greer, B. Budnik, K. K. Parker, Journal of neurophysiology 2017, 117, 1320.
[139] J. E. Burda, A. M. Bernstein, M. V. Sofroniew, Experimental neurology 2016, 275, 305; A. R. Filous, J. Silver, Progress in neurobiology 2016, 144, 173.
[140] M. V. Sofroniew, H. V. Vinters, Acta neuropathologica 2010, 119, 7.
[141] S. A. Liddelow, K. A. Guttenplan, L. E. Clarke, F. C. Bennett, C. J. Bohlen, L. Schirmer, M. L. Bennett, A. E. Münch, W.-S. Chung, T. C. Peterson, Nature 2017, 541, 481.
[142] S. Sun, J. Kanagaraj, L. Cho, D. Kang, S. Xiao, M. Cho, Journal of neurotrauma 2015, 32, 1441.
[143] J. Kanagaraj, B. Chen, S. Xiao, M. Cho, Annals of biomedical engineering 2018, 46, 354.
[144] J. G. Moloughney, N. Weisleder, Recent Pat Biotechnol 2012, 6, 200.
[145] M. M. Maneshi, F. Sachs, S. Z. Hua, Journal of neurotrauma 2015, 32, 1020.
[146] M. M. Maneshi, F. Sachs, S. Z. Hua, Frontiers in cellular neuroscience 2018, 12, 69.
[147] G. Sipe, R. Lowery, M.-È. Tremblay, E. Kelly, C. Lamantia, A. Majewska, Nature communications 2016, 7, 1; D. P. Schafer, B. Stevens, Cold Spring Harbor perspectives in biology 2015, 7, a020545.
[148] S. White, R. Plevin, M. Zagnoni, H. Carswell, Journal of Cerebral Blood Flow and Metabolism 2017, 37.
[149] S. Hosmane, I. H. Yang, A. Ruffin, N. Thakor, A. Venkatesan, Lab on a Chip 2010, 10, 741.
[150] A. D. Gitler, P. Dhillon, J. Shorter, The Company of Biologists Ltd, 2017.
[151] M. Van Bulck, A. Sierra-Magro, J. Alarcon-Gil, A. Perez-Castillo, J. A. Morales-Garcia, International journal of molecular sciences 2019, 20, 719.
[152] K. M. Kanninen, A. R. White, J Neurochem 2017, 141, 9; F. M. Menzies, A. Fleming, D. C. Rubinsztein, Nat Rev Neurosci 2015, 16, 345.
[153] H. Cho, T. Hashimoto, E. Wong, Y. Hori, L. B. Wood, L. Zhao, K. M. Haigis, B. T. Hyman, D. Irimia, Scientific reports 2013, 3, 1823.
[154] D. T. Loo, A. Copani, C. J. Pike, E. R. Whittemore, A. J. Walencewicz, C. W. Cotman, Proceedings of the National Academy of Sciences of the United States of America 1993, 90, 7951.
[155] Y. Shin, S. H. Choi, E. Kim, E. Bylykbashi, J. A. Kim, S. Chung, D. Y. Kim, R. D. Kamm, R. E. Tanzi, Advanced Science 2019, 1900962.
[156] K. I. Kane, E. L. Moreno, S. Hachi, M. Walter, J. Jarazo, M. A. Oliveira, T. Hankemeier, P. Vulto, J. C. Schwamborn, M. Thoma, Scientific reports 2019, 9, 1796.
[157] J. T. S. Fernandes, O. Chutna, V. Chu, J. P. Conde, T. F. Outeiro, Front Neurosci 2016, 10, 511.
[158] H. Phatnani, T. Maniatis, Cold Spring Harbor perspectives in biology 2015, 7, a020628.

[159] F. Loria, J. Y. Vargas, L. Bousset, S. Syan, A. Salles, R. Melki, C. Zurzolo, Acta neuropathologica 2017, 134, 789.
[160] E. C. Freundt, N. Maynard, E. K. Clancy, S. Roy, L. Bousset, Y. Sourigues, M. Covert, R. Melki, K. Kirkegaard, M. Brahic, Annals of neurology 2012, 72, 517.
[161] A. Seidi, H. Kaji, N. Annabi, S. Ostrovidov, M. Ramalingam, A. Khademhosseini, Biomicrofluidics 2011, 5, 022214.
[162] H. Mochizuki, K. Goto, H. Mori, Y. Mizuno, J Neurol Sci 1996, 137, 120.
[163] A. Virlogeux, E. Moutaux, W. Christaller, A. Genoux, J. Bruyere, E. Fino, B. Charlot, M. Cazorla, F. Saudou, Cell reports 2018, 22, 110.
[164] B. Deleglise, B. Lassus, V. Soubeyre, M. Doulazmi, B. Brugg, P. Vanhoutte, J.-M. Peyrin, Scientific reports 2018, 8, 11596.
[165] K. Le Cann, A. Foerster, C. Rösseler, A. Erickson, P. Hautvast, S. Giesselmann, D. Pensold, I. Kurth, M. Rothermel, V. B. Mattis, G. Zimmer-Bensch, S. von Hörsten, B. Denecke, T. Clarner, J. Meents, A. Lampert, Scientific reports 2021, 11, 6934.
[166] A. Kunze, S. Lengacher, E. Dirren, P. Aebischer, P. J. Magistretti, P. Renaud, Integrative Biology 2013, 5, 964.
[167] O. Pansarasa, M. Bordoni, L. Diamanti, D. Sproviero, S. Gagliardi, C. Cereda, Int J Mol Sci 2018, 19.
[168] Anonymous, Memorial Sloan Kattering Cencer Center, .
[169] Y. Fan, D. T. Nguyen, Y. Akay, F. Xu, M. Akay, Scientific Reports 2016, 6, 25062.
[170] R. Gu, X. Zhang, G. Zhang, T. Tao, H. Yu, L. Liu, Y. Dou, A. Li, J. Qin, Neurochemical research 2017, 42, 1478.
[171] T. B. Terrell-Hall, A. G. Ammer, J. I. Griffith, P. R. Lockman, Fluids and Barriers of the CNS 2017, 14, 3.
[172] T. D. Brown, M. Nowak, A. V. Bayles, B. Prabhakarpandian, P. Karande, J. Lahann, M. E. Helgeson, S. Mitragotri, Bioengineering & Translational Medicine 2019.
[173] H. Xu, Z. Li, Y. Yu, S. Sizdahkhani, W. S. Ho, F. Yin, L. Wang, G. Zhu, M. Zhang, L. Jiang, Scientific reports 2016, 6, 36670.
[174] M. Ruzycka, M. R. Cimpan, I. Rios-Mondragon, I. P. Grudzinski, Journal of nanobiotechnology 2019, 17, 71.
[175] Z. Xu, E. Li, Z. Guo, R. Yu, H. Hao, Y. Xu, Z. Sun, X. Li, J. Lyu, Q. Wang, ACS applied materials & interfaces 2016, 8, 25840.
[176] W. Liu, J. Song, X. Du, Y. Zhou, Y. Li, R. Li, L. Lyu, Y. He, J. Hao, J. Ben, Acta biomaterialia 2019, 91, 195.
[177] S. Feng, J. Cen, Y. Huang, H. Shen, L. Yao, Y. Wang, Z. Chen, PLOS ONE 2011, 6, e20599.
[178] !!! INVALID CITATION !!! .
[179] D. Milatovic, S. Zaja-Milatovic, R. M. Breyer, M. Aschner, T. J. Montine, in *Reproductive and Developmental Toxicology (Second Edition)*, (Ed: R. C. Gupta), Academic Press, 2017, 1051.
[180] F. Bianco, N. Tonna, R. D. Lovchik, R. Mastrangelo, R. Morini, A. Ruiz, E. Delamarche, M. Matteoli, Analytical chemistry 2012, 84, 9833.
[181] N. J. Abbott, A. A. K. Patabendige, D. E. M. Dolman, S. R. Yusof, D. J. Begley, Neurobiology of Disease 2010, 37, 13.
[182] R. D. Bell, B. V. Zlokovic, Acta Neuropathologica 2009, 118, 103; H. Wolburg, K. Wolburg-Buchholz, J. Kraus, G. Rascher-Eggstein, S. Liebner, S. Hamm, F. Duffner, E.-H. Grote, W. Risau, B. Engelhardt, Acta Neuropathologica 2003, 105, 586.
[183] A. Herland, A. D. van der Meer, E. A. FitzGerald, T.-E. Park, J. J. F. Sleeboom, D. E. Ingber, PloS one 2016, 11, e0150360.
[184] J. J. Lochhead, G. McCaffrey, C. E. Quigley, J. Finch, K. M. DeMarco, N. Nametz, T. P. Davis, Journal of cerebral blood flow and metabolism : official journal of the International

Society of Cerebral Blood Flow and Metabolism 2010, 30, 1625; W. A. Banks, M. A. Erickson, Neurobiology of Disease 2010, 37, 26.
[185] L. Cucullo, N. Marchi, M. Hossain, D. Janigro, Journal of Cerebral Blood Flow & Metabolism 2010, 31, 767.
[186] B. Chen, B. Friedman, Q. Cheng, P. Tsai, E. Schim, D. Kleinfeld, P. D. Lyden, Stroke 2009, 40, e666.
[187] L. Liu, K. Guo, J. Lu, S. S. Venkatraman, D. Luo, K. C. Ng, E.-A. Ling, S. Moochhala, Y.-Y. Yang, Biomaterials 2008, 29, 1509; A. Oliveira Melo, G. Malinger, R. Ximenes, P. Szejnfeld, S. Alves Sampaio, A. Bispo de Filippis, Ultrasound in Obstetrics & Gynecology 2016, 47, 6; R. Y. Shih, K. K. Koeller, Radiographics 2015, 35, 1141.
[188] H. Tang, Y. Abouleila, L. Si, A. M. Ortega-Prieto, C. L. Mummery, D. E. Ingber, A. Mashaghi, Trends in Microbiology 2020, 28, 934; A. Last, M. Maurer, A. S. Mosig, M. S. Gresnigt, B. Hube, FEMS Microbiology Reviews 2021; B. Baddal, P. Marrazzo, Pathogens 2021, 10, 203.
[189] D. L. Heymann, A. Hodgson, A. A. Sall, D. O. Freedman, J. E. Staples, F. Althabe, K. Baruah, G. Mahmud, N. Kandun, P. F. C. Vasconcelos, S. Bino, K. U. Menon, The Lancet 2016, 387, 719.
[190] X. Qian, H. N. Nguyen, M. M. Song, C. Hadiono, S. C. Ogden, C. Hammack, B. Yao, G. R. Hamersky, F. Jacob, C. Zhong, Cell 2016, 165, 1238.
[191] M. M. F Shahabipour, S Satta, A Sun, N R de Barros, S Li, T Hsiai, N Ashammakhi, Biofabrication 2021.
[192] E. Karzbrun, A. Kshirsagar, S. R. Cohen, J. H. Hanna, O. Reiner, Nat Phys 2018, 14, 515.
[193] Y. N. Ertas, M. Mahmoodi, F. Shahabipour, V. Jahed, S. E. Diltemiz, R. Tutar, N. Ashammakhi, Emergent Materials 2021, 4, 35; A. M. Sun, T. Hoffman, B. Q. Luu, N. Ashammakhi, S. Li, Bio-Design and Manufacturing 2021, 4, 757; S. Satta, A. Lai, S. Cavallero, C. Williamson, J. Chen, A. M. Blázquez-Medela, M. Roustaei, B. J. Dillon, N. Ashammakhi, D. D. Carlo, Z. Li, R. Sun, T. K. Hsiai, Advanced Science 2021, 8, 2103266; S. F. Satta S, Gao W, Ashammakhi N, Hsiai T. , Theranostics 2022.
[194] L. Pellegrini, A. Albecka, D. L. Mallery, M. J. Kellner, D. Paul, A. P. Carter, L. C. James, M. A. Lancaster, Cell Stem Cell 2020, 27, 951.
[195] T. P. Buzhdygan, B. J. DeOre, A. Baldwin-Leclair, T. A. Bullock, H. M. McGary, J. A. Khan, R. Razmpour, J. F. Hale, P. A. Galie, R. Potula, A. M. Andrews, S. H. Ramirez, Neurobiology of Disease 2020, 146, 105131.
[196] L. Si, H. Bai, M. Rodas, W. Cao, C. Y. Oh, A. Jiang, R. Moller, D. Hoagland, K. Oishi, S. Horiuchi, S. Uhl, D. Blanco-Melo, R. A. Albrecht, W.-C. Liu, T. Jordan, B. E. Nilsson-Payant, J. Logue, R. Haupt, M. McGrath, S. Weston, A. Nurani, S. M. Kim, D. Y. Zhu, K. H. Benam, G. Goyal, S. E. Gilpin, R. Prantil-Baun, R. K. Powers, K. Carlson, M. Frieman, B. R. tenOever, D. E. Ingber, bioRxiv 2020, 2020.04.13.039917.
[197] A. Ramani, L. Müller, P. N. Ostermann, E. Gabriel, P. Abida-Islam, A. Müller-Schiffmann, A. Mariappan, O. Goureau, H. Gruell, A. Walker, M. Andrée, S. Hauka, T. Houwaart, A. Dilthey, K. Wohlgemuth, H. Omran, F. Klein, D. Wieczorek, O. Adams, J. Timm, C. Korth, H. Schaal, J. Gopalakrishnan, 2020, 39, e106230.
[198] J. Kim, K.-T. Lee, J. S. Lee, J. Shin, B. Cui, K. Yang, Y. S. Choi, N. Choi, S. H. Lee, J.-H. Lee, Y.-S. Bahn, S.-W. Cho, Nature Biomedical Engineering 2021, 5, 830.
[199] S. R. Mehta, C. M. Tom, Y. Wang, C. Bresee, D. Rushton, P. P. Mathkar, J. Tang, V. B. Mattis, Cell reports 2018, 25, 1081.
[200] G. A. Van Norman, JACC: Basic to Translational Science 2016, 1, 170.
[201] C. H. Wong, K. W. Siah, A. W. Lo, Biostatistics 2019, 20, 273.
[202] A. Akhtar, Cambridge Quarterly of Healthcare Ethics 2015, 24, 407; M. Balls, J. Bailey, R. D. Combes, Taylor & Francis, 2019.

[203] G. S. Offeddu, Y. Shin, R. D. Kamm, Current Opinion in Biomedical Engineering 2020, 13, 119.
[204] M. Beatrice, B. Dries, L. Yi-Chen Ethan, Current Pharmaceutical Design 2018, 24, 5419.
[205] E. W. Esch, A. Bahinski, D. Huh, Nature reviews Drug discovery 2015, 14, 248.
[206] L. R. Volpatti, A. K. Yetisen, Trends in biotechnology 2014, 32, 347.
[207] I. Papademetriou, E. Vedula, J. Charest, T. Porter, PloS one 2018, 13, e0205158.
[208] J. H. Yeon, D. Na, K. Choi, S.-W. Ryu, C. Choi, J.-K. Park, Biomedical microdevices 2012, 14, 1141.
[209] D. W. Lee, S.-Y. Lee, I. Doh, G. H. Ryu, D.-H. Nam, BioMed Research International 2017, 2017, 7218707.
[210] N. R. Wevers, D. G. Kasi, T. Gray, K. J. Wilschut, B. Smith, R. van Vught, F. Shimizu, Y. Sano, T. Kanda, G. Marsh, Fluids and Barriers of the CNS 2018, 15, 23.
[211] T.-E. Park, N. Mustafaoglu, A. Herland, R. Hasselkus, R. Mannix, E. A. FitzGerald, R. Prantil-Baun, A. Watters, O. Henry, M. Benz, Nature communications 2019, 10, 2621.
[212] S. Chakraborty, C. G. Filippi, T. Wong, A. Ray, S. Fralin, A. J. Tsiouris, B. Praminick, A. Demopoulos, H. J. McCrea, I. Bodhinayake, Journal of neuro-oncology 2016, 128, 405.
[213] M. Demeule, J. C. Currie, Y. Bertrand, C. Ché, T. Nguyen, A. Régina, R. Gabathuler, J. P. Castaigne, R. Béliveau, Journal of neurochemistry 2008, 106, 1534.
[214] Y. J. Yu, J. K. Atwal, Y. Zhang, R. K. Tong, K. R. Wildsmith, C. Tan, N. Bien-Ly, M. Hersom, J. A. Maloney, W. J. Meilandt, Science translational medicine 2014, 6, 261ra154.
[215] H. G. Yi, Y. H. Jeong, Y. Kim, Y. J. Choi, H. E. Moon, S. H. Park, K. S. Kang, M. Bae, J. Jang, H. Youn, S. H. Paek, D. W. Cho, Nat Biomed Eng 2019, 3, 509.
[216] S. Pasteuning-Vuhman, R. de Jongh, A. Timmers, R. J. Pasterkamp, Trends in Molecular Medicine 2020.
[217] D. Pamies, T. Hartung, H. T. Hogberg, Experimental biology and medicine 2014, 239, 1096.
[218] G. D. Vatine, R. Barrile, M. J. Workman, S. Sances, B. K. Barriga, M. Rahnama, S. Barthakur, M. Kasendra, C. Lucchesi, J. Kerns, Cell stem cell 2019, 24, 995.
[219] S. Au - Jagadeesan, M. J. Au - Workman, A. Au - Herland, C. N. Au - Svendsen, G. D. Au - Vatine, JoVE 2020, e60925.
[220] G. Indiveri, B. Linares-Barranco, T. J. Hamilton, A. Van Schaik, R. Etienne-Cummings, T. Delbruck, S.-C. Liu, P. Dudek, P. Häfliger, S. Renaud, Frontiers in neuroscience 2011, 5, 73.
[221] T. Levi, T. Fujii, Micromachines 2016, 7, 146.
[222] S. Choi, S. H. Tan, Z. Li, Y. Kim, C. Choi, P.-Y. Chen, H. Yeon, S. Yu, J. Kim, Nature materials 2018, 17, 335.
[223] T. Levi, T. Nanami, A. Tange, K. Aihara, T. Kohno, IEEE Transactions on Circuits and Systems II: Express Briefs 2018, 65, 577.
[224] J. Schemmel, D. Briiderle, A. Griibl, M. Hock, K. Meier, S. Millner, "A wafer-scale neuromorphic hardware system for large-scale neural modeling", presented at *Proceedings of 2010 IEEE International Symposium on Circuits and Systems*, 2010; S. B. Furber, F. Galluppi, S. Temple, L. A. Plana, Proceedings of the IEEE 2014, 102, 652.
[225] D. S. Modha, R. Singh, Proceedings of the National Academy of Sciences 2010, 107, 13485; M. Davies, N. Srinivasa, T.-H. Lin, G. Chinya, Y. Cao, S. H. Choday, G. Dimou, P. Joshi, N. Imam, S. Jain, IEEE Micro 2018, 38, 82.
[226] D. Bovard, A. Iskandar, K. Luettich, J. Hoeng, M. C. Peitsch, Toxicology Research and Application 2017, 1, 2397847317726351; Y. Cong, X. Han, Y. Wang, Z. Chen, Y. Lu, T. Liu, Z. Wu, Y. Jin, Y. Luo, X. Zhang, Micromachines 2020, 11, 381.

[227] N. Ashammakhi, M. A. Darabi, B. Çelebi-Saltik, R. Tutar, M. C. Hartel, J. Lee, S. M. Hussein, M. J. Goudie, M. B. Cornelius, M. R. Dokmeci, A. Khademhosseini, Small Methods 2020, 4, 1900589.
[228] L. Vernetti, A. Gough, N. Baetz, S. Blutt, J. R. Broughman, J. A. Brown, J. Foulke-Abel, N. Hasan, J. In, E. Kelly, Scientific reports 2017, 7, 42296.
[229] J. P. Wikswo, E. L. Curtis, Z. E. Eagleton, B. C. Evans, A. Kole, L. H. Hofmeister, W. J. Matloff, Lab on a chip 2013, 13, 3496.
[230] Y. Zhao, R. K. Kankala, S.-B. Wang, A.-Z. Chen, Molecules 2019, 24, 675.
[231] J. P. Wikswo, E. L. Curtis, Z. E. Eagleton, B. C. Evans, A. Kole, L. H. Hofmeister, W. J. Matloff, Lab on a Chip 2013, 13, 3496.
[232] I. Maschmeyer, A. K. Lorenz, K. Schimek, T. Hasenberg, A. P. Ramme, J. Hübner, M. Lindner, C. Drewell, S. Bauer, A. Thomas, N. S. Sambo, F. Sonntag, R. Lauster, U. Marx, Lab on a chip 2015, 15, 2688.
[233] P. G. Miller, M. L. Shuler, Biotechnol Bioeng 2016, 113, 2213; Y. I. Wang, M. L. Shuler, Lab on a chip 2018, 18, 2563.
[234] A. P. Li, C. Bode, Y. Sakai, Chem Biol Interact 2004, 150, 129.
[235] K. Ronaldson-Bouchard, G. Vunjak-Novakovic, Cell Stem Cell 2018, 22, 310.
[236] J. A. Brown, V. Pensabene, D. A. Markov, V. Allwardt, M. D. Neely, M. Shi, C. M. Britt, O. S. Hoilett, Q. Yang, B. M. Brewer, Biomicrofluidics 2015, 9, 054124.
[237] O. Kilic, D. Pamies, E. Lavell, P. Schiapparelli, Y. Feng, T. Hartung, A. Bal-Price, H. T. Hogberg, A. Quinones-Hinojosa, H. Guerrero-Cazares, Lab on a Chip 2016, 16, 4152.
[238] E.-M. Materne, A. P. Ramme, A. P. Terrasso, M. Serra, P. M. Alves, C. Brito, D. A. Sakharov, A. G. Tonevitsky, R. Lauster, U. Marx, Journal of biotechnology 2015, 205, 36.
[239] X. Wang, M. Cirit, J. S. Wishnok, L. G. Griffith, S. R. Tannenbaum, Analytical chemistry 2019.
[240] C. D. Edington, W. L. K. Chen, E. Geishecker, T. Kassis, L. R. Soenksen, B. M. Bhushan, D. Freake, J. Kirschner, C. Maass, N. Tsamandouras, Scientific reports 2018, 8, 4530.
[241] A. Van Den Berg, C. L. Mummery, R. Passier, A. D. Van der Meer, Lab on a Chip 2019, 19, 198.
[242] J.-H. Choi, M. Santhosh, J.-W. Choi, Micromachines 2020, 11, 21.
[243] A. Gokaltun, M. L. Yarmush, A. Asatekin, O. B. Usta, Technology 2017, 5, 1.
[244] J. Lachaux, C. Alcaine, B. Gomez-Escoda, C. M. Perrault, D. O. Duplan, P.-Y. J. Wu, I. Ochoa, L. Fernández, O. Mercier, D. Coudreuse, Lab on a Chip 2017, 17, 2581.
[245] M. A. Darabi, A. Khosrozadeh, Y. Wang, N. Ashammakhi, H. Alem, A. Erdem, Q. Chang, K. Xu, Y. Liu, G. Luo, A. Khademhosseini, M. Xing, Advanced science (Weinheim, Baden-Wurttemberg, Germany) 2020, 7, 1902740.
[246] N. Picollet-D'hahan, A. Zuchowska, I. Lemeunier, S. Le Gac, Trends in Biotechnology 2021, 39, 788.
[247] M. Zhu, Y. Wang, G. Ferracci, J. Zheng, N.-J. Cho, B. H. Lee, Scientific reports 2019, 9, 1.
[248] A.-N. Cho, Y. Jin, Y. An, J. Kim, Y. S. Choi, J. S. Lee, J. Kim, W.-Y. Choi, D.-J. Koo, W. Yu, Nature communications 2021, 12, 1.
[249] K. Fetah, P. Tebon, M. J. Goudie, J. Eichenbaum, L. Ren, N. Barros, R. Nasiri, S. Ahadian, N. Ashammakhi, M. R. Dokmeci, Progress in Biomedical Engineering 2019, 1, 012001; A. K. Miri, E. Mostafavi, D. Khorsandi, S.-K. Hu, M. Malpica, A. Khademhosseini, Biofabrication 2019, 11, 042002.
[250] S. R. A. Kratz, G. Höll, P. Schuller, P. Ertl, M. Rothbauer, Biosensors 2019, 9, 110.
[251] A. G. N Ashammakhi, R Tutar, A Fricker, I Roy, X Chatzistavrou, E Hoque Apu, K-L Nguyen, T Ahsan, I Pountos, E Caterson, Tissue Engineering Part B: Reviews 2021; S. Bang, S. Jeong, N. Choi, H. N. Kim, Biomicrofluidics 2019, 13, 051301; M. A. Mofazzal Jahromi,

A. Abdoli, M. Rahmanian, H. Bardania, M. Bayandori, S. M. Moosavi Basri, A. Kalbasi, A. R. Aref, M. Karimi, M. R. Hamblin, Molecular Neurobiology 2019, 56, 8489.
[252] L. A. Low, D. A. Tagle, Experimental Biology and Medicine 2017, 242, 1573.
[253] J. Rogal, C. Probst, P. Loskill, Future science OA 2017, 3, FSO180.
[254] A. P. Ramme, L. Koenig, T. Hasenberg, C. Schwenk, C. Magauer, D. Faust, A. K. Lorenz, A.-C. Krebs, C. Drewell, K. Schirrmann, Future science OA 2019, 5, FSO413; S. Jagadeesan, M. J. Workman, A. Herland, C. N. Svendsen, G. D. Vatine, JoVE (Journal of Visualized Experiments) 2020, e60925; Y. Wang, L. Wang, Y. Guo, Y. Zhu, J. Qin, RSC advances 2018, 8, 1677.
[255] K. L. Fetah, B. J. DiPardo, E. M. Kongadzem, J. S. Tomlinson, A. Elzagheid, M. Elmusrati, A. Khademhosseini, N. Ashammakhi, Small 2019, 15, 1901985; M. Elmusrati, N. Ashammakhi, Journal of Craniofacial Surgery 2018, 29, 1682; A. Mencattini, F. Mattei, G. Schiavoni, A. Gerardino, L. Businaro, C. Di Natale, E. Martinelli, Frontiers in Pharmacology 2019, 10, 100; E.-M. L. Kongadzem, 2018.
[256] B. Liu, E. Kim, A. Meggo, S. Gandhi, H. Luo, S. Kallakuri, Y. Xu, J. Zhang, Journal of neural engineering 2017, 14, 026008.
[257] J. W. Kamande, T. Nagendran, J. Harris, A. M. Taylor, Frontiers in bioengineering and biotechnology 2019, 7.
[258] T. Nagendran, R. S. Larsen, R. L. Bigler, S. B. Frost, B. D. Philpot, R. J. Nudo, A. M. Taylor, Nature communications 2017, 8, 625.
[259] R. Booth, S. Noh, H. Kim, Lab on a Chip 2014, 14, 1880.
[260] M. Campisi, Y. Shin, T. Osaki, C. Hajal, V. Chiono, R. D. Kamm, Biomaterials 2018, 180, 117.